THE ROLE OF CORTACTIN IN ENDOLYSOSOMAL COMPARTMENT REGULATION

By

NAN HYUNG HONG

Dissertation

Submitted to the Faculty of the

Graduate School of Vanderbilt University

in partial fulfillment of the requirements

for the degree of

DOCTOR OF PHILOSOPHY

in

CANCER BIOLOGY

May, 2015

Nashville, Tennessee

Approved:

Alissa M. Weaver, M.D., Ph.D.

Anne K. Kenworthy, Ph.D.

Matthew J. Tyska, Ph.D.

Rebecca S. Cook, Ph.D.

Vito Quaranta, Ph.D.

To my loving family and friends

who have encouraged and supported me on this journey.

아빠, 엄마 감사하고, 사랑합니다!

ACKNOWLEDGEMENTS

First and foremost, I would like to express my special appreciation and thanks to my advisor Dr. Alissa Weaver, who has provided me with excellent guidance and support, and given me the confidence to develop into an independent scientist. I would also like to thank my committee members: Dr. Vito Quaranta, Dr. Anne Kenworthy, Dr. Rebecca Cook, and Dr. Matthew Tyska for serving as my committee members and for all of the great advice and support that they have given me over the years.

I am very thankful to previous and current members of the Weaver lab: Seema Sinha, Christi French, Kellye Kirkbride, Aron Parekh, Rachel Jerrell, Bong Hwan Sung, Tyne Miller, Kaitlin Costello, Andrew McKenzie, Selma Maacha, Anthony Maldonado, Daisuke Hoshino, Mallory Miles for their scientific inputs, friendship, and all the fun we have had. They made the lab an enjoyable place to work.

I would like to thank the former and present staffs of the Department of Cancer Biology, especially Tracy Tveit and Toni Shepard. I am also thankful to people in Vanderbilt Cores: CarolAnn Bonner of the Vanderbilt Cell Imaging Shared Resource; Dr. Joe Roland of the Epithelial Biology Core Imaging Resources for training me in using microscopes. I specially thank to Dr. Matthew Tyska and Nathan Grega Larson for usage of their total internal reflection microscope.

I am grateful for all my friends; those in and outside of Nashville for helping me stay sane through these difficult years. Their support and care helped me to focus on my study. I greatly value their friendship and I deeply appreciate their belief in me.

Finally, I would like to thank my parents and brother. They were always supporting me and encouraging me with their best wishes. None of this would have been possible without the love and patience of my family.

TABLE OF CONTENTS

LIST OF FIGURES

LIST OF ABBREVIATIONS

ADP	Adenosine diphosphate
AP-2	Adaptor proteins-2
aPKC	atypical proteins kinase C
Arp2/3	Actin related protein 2/3
ATP	Adenosine triphosphate
B2AR	β2 adrenergic receptor
BFA	Brefeldin A
BSA	Bovine serum albumin
Dyn-2	Dynamin-2
ECM	Extracellular matrix
EGFR	Epidermal growth factor
EM	Electron microscopy
ER	Endoplasmic reticulum
F-actin	Filamentous actin
FIG4	Factor-induced gene 4
G-actin	Globular actin
GFP	Green fluorescent protein
HNSCC	Head and Neck Squamous Cell Carcinoma
HRP	Horseradish peroxidase
KD	Knock down
LE/Lys	Late endosomal/lysosomal
LSD	Lysosomal storage disease
M6PR	Mannose-6-phosphate receptor
MMP	Matrix metalloproteinase

MT1-MMP	Membrane type I-matrix metalloproteinase
MVB	Multivesicular body
N-WASP	Neural Wiskott-Aldrich syndrome protein
NPC	Niemann-Pick disease type C
NPF	Nucleation promoting factor
NTA	Amino acid terminal acidic
$PI(3,4,5)P_3$	Phosphatidylinositol 3,4,5-trisphosphate
$PI(3,4)P_2$	Phosphatidylinositol 3,4-bisphosphate
$PI(3,5)P_2$	Phosphatidylinositol 3,5-bisphosphate
PI(3)P	Phosphatidylinositol 3-monophosphate
$PI(4,5)P_2$	Phosphatidylinositol 4,5-bisphosphate
PI(4)P	Phosphatidylinositol 4-monophosphate
PI(5)P	Phosphatidylinositol 5-monophosphate
PI3K	Phosphatidylinositol 3-kinase
PIKfyve	FYVE-containing phosphoinositide kinase
PIP	Phosphatidylinositol phosphate
PIPK III	Type III phosphatidylinositol phosphate kinase
PM	Plasma membrane
RTK	Receptor Tyrosine Kinase
siRNA/shRNA	small interference RNA/small hairpin RNA
TGN	Trans Golgi Network
SNARE	Soluble N-ethylmaleimide-sensitive factor-activating protein receptor
t-SNARE	target SNARE
V-ATPase	Vacuolar H+-ATPase
v-SNARE	vesicle SNARE

VAMP7	Vesicle-associated membrane protein 7
VCA	Verprolin homology, central, and acidic
VSV-G	Vesicular stomatitis virus glycoprotein
WASH	WASP and SCAR Homologue
WASP	Wiskott-Aldrich syndrome Protein
WAVE/SCAR	Wiscott-Aldrich syndrome protein family verprolin-homologous proteins
WHAMM	WASP homologues associated with actin, membrane, and microtubules

CHAPTER I

INTRODUCTION

Intracellular membrane trafficking overview

Eukaryotic cells are highly compartmentalized with membranous organelles, which create enclosed compartments that serve specific functions critical to cell behavior and survival. The functional organization of organelles, including the protein and lipid composition, is required for proper cell function and depends on the accurate and efficient exchange of molecules mediated by vesicular transport. For example, cargo molecules present in endosomes (either newly synthesized or taken up by a cell from the outside) may be directed to the lysosome for degradation, the trans-Golgi network (TGN), or the cell surface.

The accurate delivery of molecules to their appropriate membrane domain contributes to establishment and maintenance of cell polarity and other processes that are crucial for normal cell physiology and tissue homeostasis. Thus, it is expected that disruption of traffic regulation and coordination would result in human diseases. In fact, multiple human disorders including diabetes, cancer, heart disease and degenerative brain disorders are caused directly or indirectly by defects in the regulation of vesicular trafficking (Aridor and Hannan, 2002; Howell et al., 2006).

In cancer, vesicle trafficking plays an important role in cancer development and progression in various aspects including invasion, metastasis, angiogenesis, tumor immune privilege, and multidrug resistance (Fletcher and Rappoport, 2009; Roberts and Kurre, 2013; Tsai et al., 2014). For example, the epidermal growth factor receptor (EGFR) plays key roles in essential cellular functions including proliferation and migration. Sorting of activated EGFR for lysosomal degradation serves as a mechanism

for signaling down-regulation, which in turn controls signaling duration and amplitude. Trafficking defects resulting in mislocalization and poor down regulation of the EGFR are associated with enhanced signaling (Sorkin and Zastrow, 2009), which can lead to development of cancer (Roepstorff et al., 2008). Matrix metalloproteinase (MMP) trafficking is another good example. MMPs are key enzymes in tumor invasion that remodel and breach extracellular matrix (ECM). Recycling of transmembrane MT1-MMP from endosomes has been proposed as a means of regenerating the active enzyme at the surface (Itoh and Seiki, 2006; Li et al., 2008). Indeed, recent studies have revealed that endosomal trafficking is critical for targeted delivery of MT1-MMP to promote cancer cell invasion (Castro-Castro et al., 2012; Clark et al., 2007; Monteiro et al., 2013; Rossé et al., 2014a). Therefore, a better understanding of how proper intracellular trafficking is achieved is important for human health. Ultimately, one could envision drug intervention in multiple diseases that are caused by malfunctioning of trafficking.

The spatial organization of membrane trafficking requires coordination of a series of proteins including the actin cytoskeleton. In this study, I focus on the actin cytoskeleton and its role in the regulation of intracellular trafficking.

Actin cytoskeleton and its function in mammalian cells

The actin cytoskeleton is a dynamic structure that plays a vital role in numerous cellular activities, including motility, cytokinesis, vesicular trafficking, and signaling (Pollard and Cooper, 2009). During cell migration, coordinated polymerization of actin filaments drives the extension of flat membrane protrusions called lamellipodia and finger-like protrusions called filopodia. These protrusions organize cell-matrix adhesion and probe the environment for cues at the leading edge (Rotty et al., 2013) (Figure 1). During endocytosis, the actin cytoskeleton provides the force for generating membrane invagination and for the scission of endocytic vesicles from the plasma membrane

(Kaksonen et al., 2006). In addition, actin filaments together with myosin motors form contractile structures in cells. These include myofibrils of muscle cells and stress fibers found in many nonmuscle cell types (Tojkander et al., 2012).

In cells, actin exists in two states, the monomeric globular (G)-actin and filamentous (F)-actin. F-actin is a polymer that grows at the barbed (or plus (+)) end by the spontaneous addition of adenosine triphosphate (ATP)-bound G-actin and shortens (depolymerizes) by dissociation of adenosine diphosphate (ADP)-bound monomers from the pointed (or minus (-)) end. This process is tightly regulated in time and space by signaling regulation of a number of actin-binding proteins including nucleation factors (e.g., Arp2/3 complex, formins), actin monomer-binding proteins, capping proteins, and stabilizing/destabilizing factors (Chesarone and Goode, 2009; Cooper and Sept, 2008; Ono, 2007; Paavilainen et al., 2004). Nucleation factors such as formins and the actin-related protein 2/3 (Arp2/3) complex are crucial to initiate the formation of new filaments. Formins mediate actin nucleation of unbranched filaments, such as those in stress fibers (Figure 1). The Arp2/3 complex nucleates and organizes branched filament networks in lamellipodia and other structures as shown in Figure 1. By itself Arp2/3 has weak nucleation activity, thus Arp2/3 is activated by actin nucleation promoting factors (NPFs). Most mammalian NPFs are members of the Wiskott-Aldrich syndrome protein (WASP) family (Class I), including WASP, neural WASP (N-WASP), WASP family verprolin homologue (WAVE/SCAR), WASP homologues associated with actin, membrane, and microtubules (WHAMM), and WASP and SCAR homologue (WASH). Class I NPFs possess a verprolin homology, cofilin homology, and acidic (VCA) domain that allows for the binding of G-actin (through V motif) and Arp2/3 (CA motif). Class II NPFs, exemplified by cortactin, contain an Arp2/3-interacting acidic region but bind actin filaments instead of monomers. This leads to much weaker activation activity which may not be physiologically relevant in the absence of a Class I NPF. Instead the function

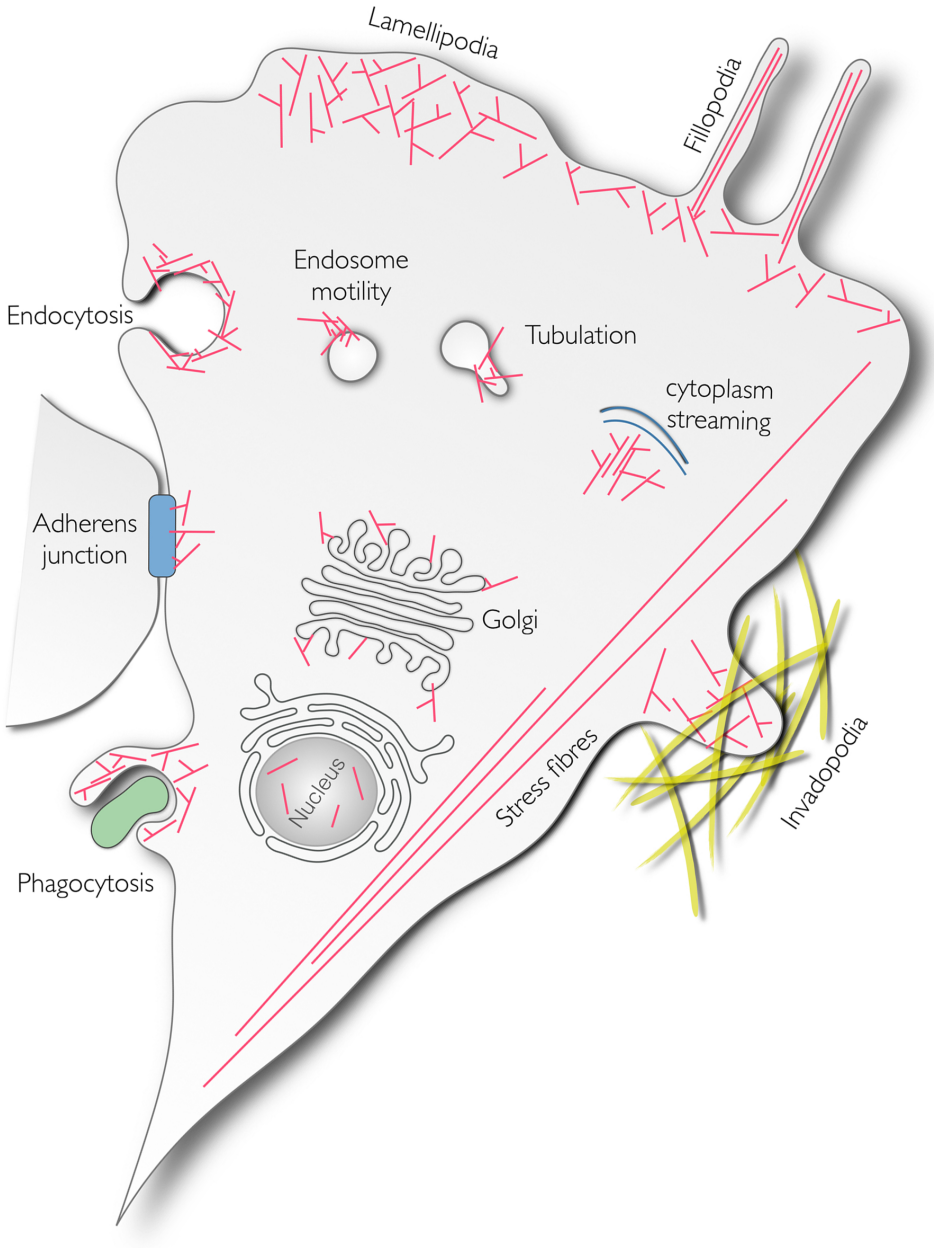

Figure 1. Cellular function of the actin cytoskeleton.

The dynamic actin polymerization is involved in different processes. These processes include endocytic uptake at the plasma membrane, phagocytosis. At the leading edge actin provides the protrusive force that is required to generate and extend the broad sheet-like or finger-like protrusions known as lamellipodia and filopodia, respectively. In addition, actin assembly has a role in Golgi and vesicular membrane dynamics, and stress fiber formation. It also contributes to cytoplasmic streaming (represented by blue lines) and cell junction assembly.

of Class II NPF is likely to be synergistic activation of Arp2/3 complex together with Class I NPFs. WASP family proteins initiate actin polymerization in different subcellular locations. SCAR/WAVEs are responsible for activating the Arp2/3 complex in lamellipodia (Oikawa et al., 2004), whereas N-WASP usually regulates endocytosis at the plasma membrane and the formation of specialized invasive structures such as podosomes and invadopodia. WHAMM is important for Golgi function (Campellone et al., 2008) and WASH is essential for endosomal sorting (Derivery et al., 2009; Gomez and Billadeau, 2009).

Actin cytoskeletal control of intracellular vesicular trafficking

The actin cytoskeleton is a critical regulator of membrane trafficking. Dynamic remodeling of the actin cytoskeleton at the surface of intracellular organelles has been shown to control endosomal motility, fission and fusion, and sorting (Anitei and Hoflack, 2012; Lanzetti, 2007). The involvement of actin polymerization in the motility of intracellular organelles was initially suggested by the observation that certain intracellular bacterial and viral pathogens such as *Listeria, Shigella*, and *Vaccinia* exploit the host actin polymerization machinery to assemble an actin tail, also called as "comet-tail", that serves as propulsive force required for movement (Cudmore et al., 1995; Theriot et al., 1992). Subsequently, Merrifield et al. and others demonstrated that intracellular organelles such as endosomes and lysosomes also induce actin-rich tails at their surface, enabling movement through the cytoplasm (Merrifield et al., 1999; Taunton et al., 2000).

In addition to controlling endosome motility, branched actin networks at the surface of endosomes play a role in cargo sorting by regulating membrane tubulation and fission. Thus, silencing of the Arp2/3 complex or inhibiting actin polymerization using inhibitory drugs result in enlarged endosomes with no tubules (Derivery et al., 2012).

The branched actin networks have been shown to stabilize membrane tubule while it clusters cargos such as β2 adrenergic receptor (B2AR), whereas perturbation of actin assembly leads to a defective accumulation of B2AR in endosomes (Puthenveedu et al., 2010). Recently WASH was identified as a major Arp2/3 NPF on endosomes that controls cargo sorting. Upon WASH knockdown, endosomes form exaggerated tubules, as if their fission was impaired (Derivery et al., 2009; Gomez and Billadeau, 2009). The exaggerated tubule phenotype in WASH knockdown cells is associated with defects in various cargo transport, including transferrin receptor, integrins, mannose-6-phosphate receptor, and EGFR (Derivery et al., 2009; Duleh and Welch, 2010; Gomez and Billadeau, 2009; Zech et al., 2011).

Actin polymerization at Golgi membranes also controls protein transport. Overexpression and depletion studies on the Golgi localized Arp2/3 NPF, WHAMM, indicate that branched actin assembly facilitates anterograde membrane transport by promoting tubule elongation (Campellone et al., 2008). In addition, Arp2/3-mediated actin nucleation is linked to dynamin-mediated fission of transport vesicles at the *trans*-Golgi network (TGN). Interference with dynamin2/cortactin or dynamin2/syndapin2/cortactin blocks post-Golgi protein transport (Cao et al., 2005; Kessels and Qualmann, 2004; Salvarezza et al., 2009).

Another possible role of endosomal actin is to prevent clustering of endosome (Drengk et al., 2003). Indeed, in WASH knockout cells, endosomes and lysosomes are aggregated (Gomez et al., 2012). Actin assembly on endosome surface aids in concentrating membrane proteins into microdomains and actin remodeling may provide spatial constraints that restrict the fusion machinery to sites of membrane fusion. This suggests that endosomal actin structures form a positive shell that surrounds the organelles and prevents their membranes from uncontrolled vesicle fusion.

General features of cortactin

Cortactin was first identified as an F-actin binding protein and a substrate of the Src tyrosine kinase (Kanner et al., 1990; Wu et al., 1991). Subsequently, it was discovered to be a binding partner of the Arp2/3 complex which facilitates *de novo* F-actin nucleation and actin branch assembly (Uruno et al., 2001; Weaver et al., 2001). *In vitro*, cortactin is weaker activator of actin assembly than N-WASP (Weaver et al., 2001; Weed et al., 2000), yet it has a unique property. The Arp2/3 complex binds to the sides of pre-existing actin filament, in a step which contributes to its activation (Higgs and Pollard, 2001; Mullins et al., 1998). By binding to F-actin and Arp2/3 complex simultaneously, cortactin can promote the association of Arp2/3 complex with actin filament and also stabilizes the newly formed branches (Weaver et al., 2001). These unique features are important for the function of cortactin in numerous actin-dependent cellular processes. For example, cells expressing high levels of cortactin have enhanced cell motility (Bryce et al., 2005; Kowalski et al., 2005; Patel et al., 1998; Schuuring et al., 1993). Our laboratory, in previous has shown that interaction of cortactin with Arp2/3 complex and actin filament is required for resecretion of ECM from LE/Lys compartment to promote cell migration (Sung et al., 2011).

Cortactin is comprised of four major domains (Figure 2): N-terminal acidic (NTA), tandem repeats, proline-rich, and Src homology 3 (SH3). The NTA domain of cortactin is important for cortactin localization to the cell periphery (Uruno et al., 2001; Weaver et al., 2001; Weed et al., 2000). It binds to the Arp3 subunit of the Arp2/3 complex via a DDW motif and can synergize Arp2/3 complex activation in the presence of N-WASP *in vitro* to promote actin polymerization (Uruno et al., 2001; Weaver et al., 2001; 2002; Weed et al., 2000). The NTA domain is followed by six and a half repeats that are each made up of a stretch of 37 amino acids, of which the fourth is the most important for F-actin binding (Weed et al., 2000). These interactions with Arp2/3 and F-actin are both necessary and

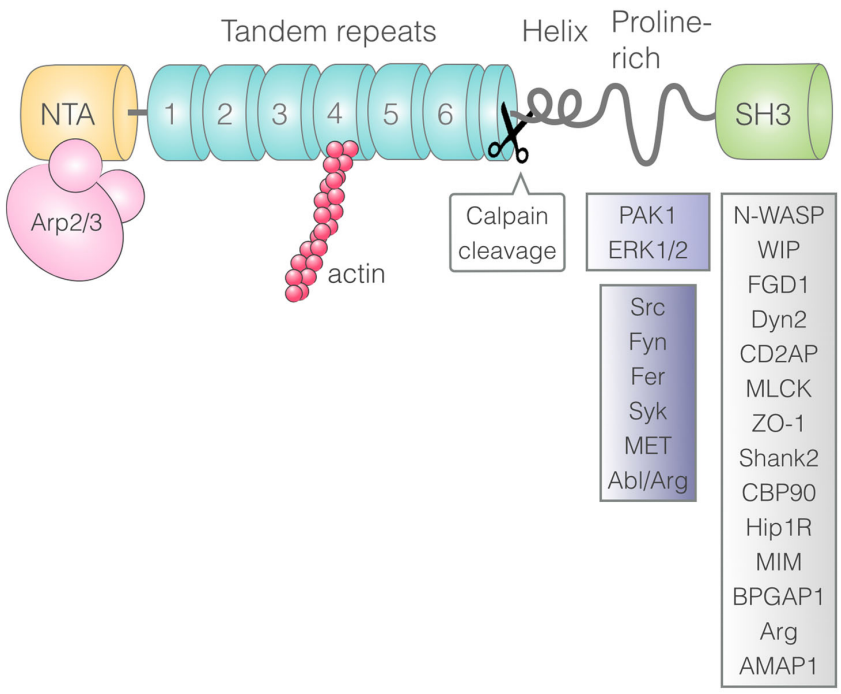

Figure 2. Cortactin domain structure and its interacting partners.

Schematic diagram of cortactin domains. Specific cortactin domains are described in the text. N-terminus of cortactin directs activation of Arp2/3 complex and actin branch stabilization through direct interaction with branched actin nucleator Arp2/3 complex and actin filaments. C-terminus Proteins in light purple box represent kinases known to phosphorylate cortactin. Proteins in grey box represent SH3 binding partners.

sufficient for direct regulation of Arp2/3 complex mediated branched actin assembly (Uruno et al., 2001; Weaver et al., 2001). In addition to being important for regulation of branched actin assembly, localization of cortactin to sites of dynamic actin assembly in cells typically requires the Arp2/3 complex and F-actin binding sites (Bryce et al., 2005; Katsube et al., 2004; Uruno et al., 2001; Weed et al., 2000). Following the repeats region is an α-helical domain which is a site of calpain cleavage (Huang et al., 1997; Perrin et al., 2006)) and a proline-rich region that contains multiple phosphorylation sites. At the carboxy terminus is an SH3 domain that binds to a number of additional proteins. SH3-binding partners include the Arp2/3 NPF N-WASP (Weaver et al., 2002), the WASP-interacting protein WIP (Kinley et al., 2003), the membrane trafficking regulatory GTPase dynamin 2 (McNiven et al., 2000), the tight junction protein ZO-1 (Katsube et al., 1998), synaptic adaptor protein Shank2 (Du et al., 1998), the membrane scaffold protein CD2AP (Lynch et al., 2003), the contractility-enhancing myosin light chain kinase (Dudek et al., 2002), and Cdc42 activator guanine nucleotide exchange factor facio dysplasia 1 (FGD1) (Hou et al., 2003). All these interactions suggest that cortactin may function as a central element connecting actin branches to cytoskeletal, membrane trafficking and signaling machineries.

Cortactin in cancer invasiveness

The human cortactin gene (CTTN) is encoded in a segment 11q13 on chromosome 11, a region that is amplified in various cancers, including head and neck squamous cell carcinoma (HNSCC), breast, ovary, lung, and liver cancer (Akervall et al., 1995; Buday and Downward, 2007; Chuma et al., 2004; Ormandy et al., 2003; Patel et al., 1996; Schuuring, 1995; Schuuring et al., 1993). Amplification of CTTN and the resulting overexpression of cortactin protein in tumors is significantly associated with poor patient prognosis, including decreased survival and increased tumor metastasis.

Many studies have thus focused on the role of cortactin in tumor invasion and metastasis. Studies using siRNA/or shRNA against cortactin or inhibitory cortactin antibodies to antagonize cortactin have shown that cortactin promotes both the formation and maturation of invadopodia, which are branched actin-rich protrusive structures formed by invasive cancer cells that degrade the extracellular matrix (ECM) (Weaver, 2008; Yamaguchi and Condeelis, 2007). One of proposed mechanisms by which cortactin regulates invadopodia is regulation of Arp2/3 activity at plasma membrane signaling sites (Ayala et al., 2008; Oser et al., 2009). Cortactin also regulates invadopodia-mediated ECM degradation through the regulation of MMP secretion at invadopodia. (Clark and Weaver, 2008; Clark et al., 2007). However, the underlying mechanism was unclear when my study began.

Cortactin in membrane trafficking

Increasing evidence indicates that actin associated with endosomes plays an important role in post-internalization events along the endocytic pathway in both yeast and mammals. Dynamic actin assembly has been reported to regulate tubulation and generation of vesicles, transport, docking and fusion of vesicles, and motility of endosomes (Anitei and Hoflack, 2012; Lanzetti, 2007). It is not surprising that cortactin has been found to regulate many of these same events (Figure 3) since almost all of the cellular activities of cortactin require binding to the Arp2/3 complex and actin filaments. For instance, overexpression of cortactin inhibited the ubiquitylation and subsequent degradation of the EGF receptor, an effect that might contribute to the invasive phenotype of cortactin-overexpressing tumor cells (Timpson et al., 2005). Cao et al. showed cortactin-Dyn-2 interaction at the Golgi mediates vesicle scission and regulates cargo transport from the TGN (Cao et al., 2005). Puthenveedu et al. also showed that the depletion of cortactin leads to defective accumulation of β2 adrenergic receptor in

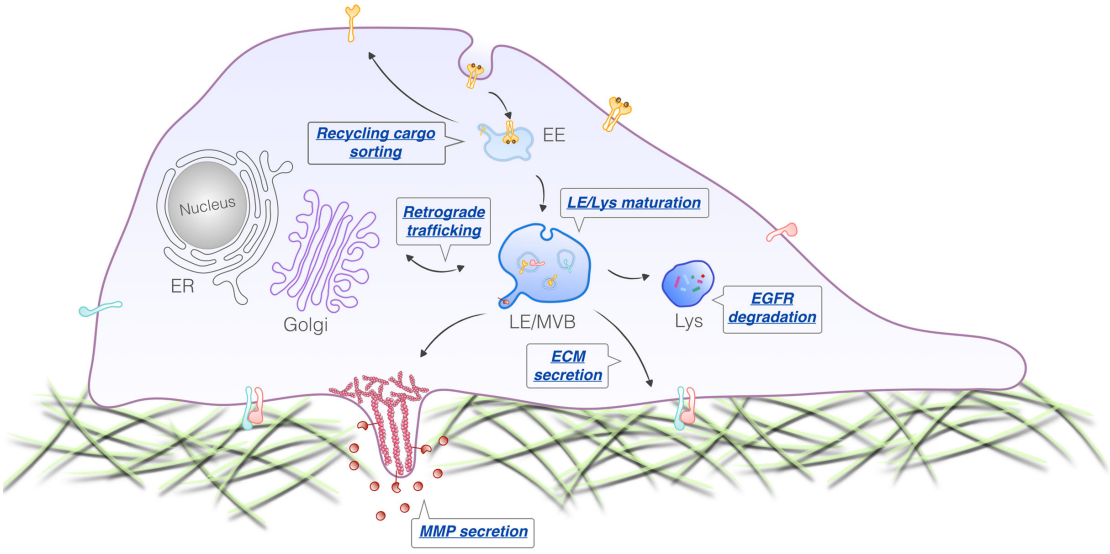

Figure 3. Cortactin function in membrane trafficking.

endosomes (Puthenveedu et al., 2010). Furthermore, aPKC-mediated phosphorylation of cortactin has been shown to regulate MT1-MMP recycling to plasma membrane from late endocytic compartment by recruiting the membrane scission protein, Dyn-2 (Monteiro et al., 2013; Rossé et al., 2014b). All of these studies implicate the importance of cortactin function in determining the fate of the endocytosed proteins.

Cortactin has been detected on organelles in the endolysosomal system together with the Arp2/3 activator WASH (Derivery et al., 2009; Gomez and Billadeau, 2009; Monteiro et al., 2013). They may cooperatively regulate endosomal tubule formation and elongation through the regulation of actin dynamics. Silencing of the Arp2/3 complex or inhibiting actin polymerization using drug results in enlarged endosomes with no tubules (Derivery et al., 2012; Ohashi et al., 2011). Depletion of cortactin or WASH also results in endosome enlargement (Duleh and Welch, 2010; Kirkbride et al., 2012), but with opposite effects on endosome morphology, endosomes with no tubules at all or exaggerated tubulation, respectively (Derivery et al., 2009; Gomez and Billadeau, 2009; Puthenveedu et al., 2010). However, it has been also reported that complete loss of the WASH leads to enlarged endosomes with no tubules at all (Gomez et al., 2012). Even with opposite phenotypes, it is clear that they act in same pathway of endosomal sorting, as suggested by the enlargement of endosomes, which reflects the accumulation of endosomal material.

Phosphoinositides overview

Phosphatidylinositol (PI) and its phosphorylated derivatives, phosphoinositides (PIPs), are minor components quantitatively of membranes but serve essential membrane associated signaling roles in eukaryotic cells (Di Paolo and De Camilli, 2006; Lemmon, 2008; Roth, 2004). PI is composed of an inositol headgroup, a glycerol moiety and two fatty acid chains that enable insertion into lipid membranes (Figure 4 A). The

inositol headgroup, a glycerol moiety and two fatty acid chains that enable insertion into lipid membranes (Figure 4 A). The inositol headgroup can be reversibly phosphorylated at 3-, 4-, and/or 5-hydroxy positions, generating 7 different phosphoinositide species: PI(3)P, PI(4)P, PI(5)P, PI(4,5)P_2, PI(3,5)P_2, PI(3,4)P_2, and PI(3,4,5)P_3. A wide range of phosphoinositide kinases and phosphatases that are differentially localized within a cell mediate turnover of their target substrate (Figure 4 A). Therefore, different phosphoinositide species are enriched in particular subcellular compartments, and specify organelle identity that may provide the mechanism for fine-tuning the membrane trafficking flow (Figure 4 B). For example, PI(4,5)P_2 and PI(3,4,5)P_3 predominate on the plasma membrane, whereas PI(4)P is abundant at the Golgi complex and on post-Golgi vesicles (Panaretou and Tooze, 2002; Wang et al., 2003). PI(3)P and its derivative PI(3,5)P_2 confer identity to endosomal membranes, marking respectively early and late endosomes (Di Paolo and De Camilli, 2006; van Meer et al., 2008). Various human diseases, including cancer, bipolar disorder, metabolic syndrome, are caused by genetic mutations in phosphoinositides metabolizing enzymes (McCrea and De Camilli, 2009), indicating that phosphoinositide metabolism has a vital role in physiological and pathological conditions. Phosphoinositides play a central role in regulating actin dynamics at the membrane by directing subcellular localization and in many cases regulating activity of actin-binding proteins. For instance, PI(4,5)P_2 binds to profilin, gelsolin, vinculin, α-actinin, and N-WASP and regulates their activities (Burn et al., 1985; Fraley et al., 2005; Janmey and Stossel, 1987; Miki et al., 1996; Papayannopoulos et al., 2005; Saarikangas et al., 2010; van Rheenen et al., 2007; Yonezawa et al., 1991). In addition, PI(3,4,5)P_3, which is produced by PI3K from PI(4,5)P_2, recruits WAVE2 to the polarized membrane and this recruitment is essential for lamellipodia formation at the leading edge as it activates Arp2/3 to induce actin polymerization (Oikawa et al., 2004). During endocytosis PI(4,5)P_2 promotes Arp2/3-mediated actin polymerization that

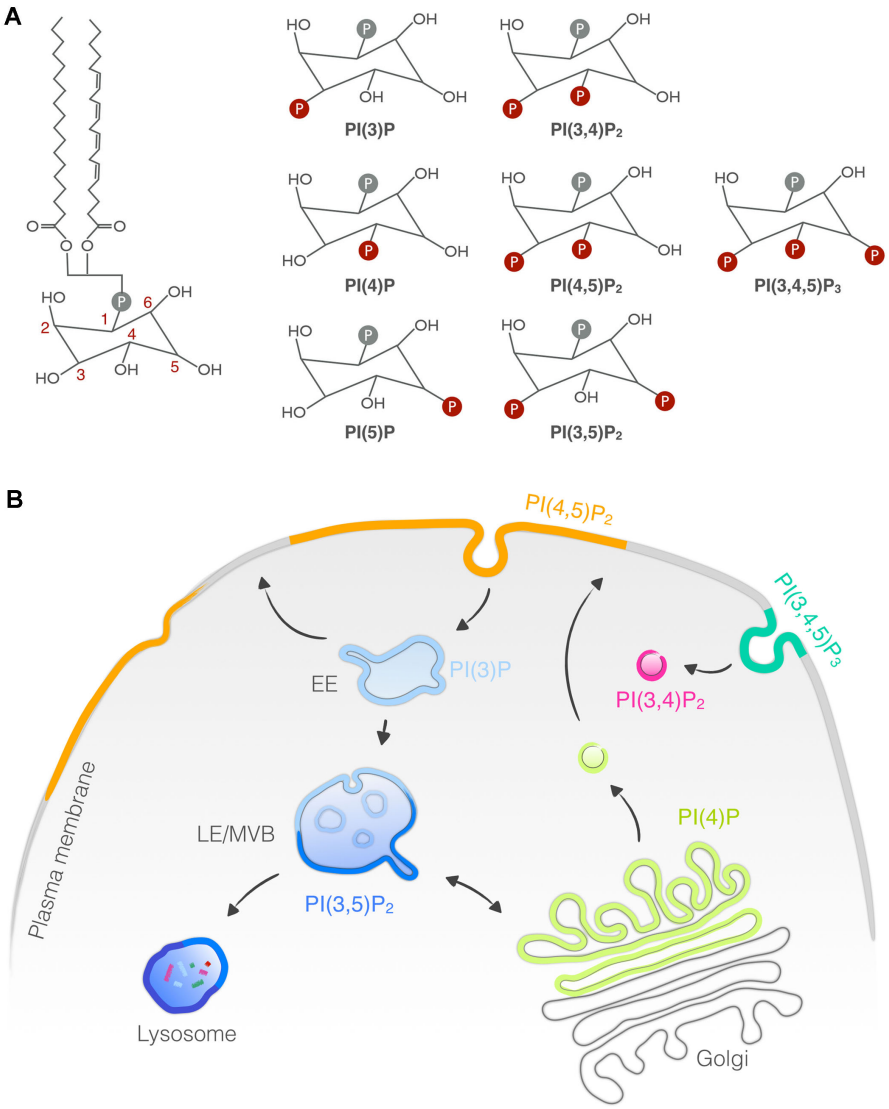

Figure 4. Structure, metabolism, and subcellular localization of phosphoinositides. (A) Phosphatidylinositol can be phosphorylated by phosphoinositide kinases or dephosphorylated by phosphoinositide phosphatase, generating the indicated phosphoinositide derivatives. The metabolic pathways shown in dotted lines indicate the uncertainty of physiological relevance in vivo. (B) Subcellular localization of phosphoinositides. Only predominant phosphoinositides are shown for simplicity. The majority of $PI(4,5)P_2$ is located in the plasma membrane, and that is where it is converted to $PI(3,4,5)P_3$. PI(4)P is highly enriched in the Golgi and in some endosomes that are part of the TGN. PI(3)P is formed on endosomes such as early endosomes (EE) and and is converted to $PI(3,5)P_2$ at the level of sorting endosomes and regions that form the invaginating membranes destined to become luminal in late endosome/mutivesicular bodies (LE/MVB).

In addition, $PI(3,4,5)P_3$, which is produced by PI3K from $PI(4,5)P_2$, recruits WAVE2 to the polarized membrane and this recruitment is essential for lamellipodia formation at the leading edge as it activates Arp2/3 to induce actin polymerization (Oikawa et al., 2004). During endocytosis $PI(4,5)P_2$ promotes Arp2/3-mediated actin polymerization that provides the force for generating invagination from the plasma membrane by recruitment of dynamin interacting with actin binding protein such as cortactin and syndapin (Merrifield et al., 2005; 2004). PI(4)P also implicated in connecting actin cytoskeleton to Golgi membrane. A recent study has shown that GOLPH3, which is a PI(4)P effector at the Golgi, interacts with an unconventional myosin MYO18A that binds to F-actin, and this maintains a tensile force on Golgi required for vesicle budding for anterograde trafficking (Dippold et al., 2009). Together, these data implicate the importance of interplay between phosphoinositide and actin dynamics in the regulation of various cellular processes.

$PI(3,5)P_2$ and its function in membrane trafficking

$PI(3,5)P_2$ is much less abundant than most phosphoinositides, respectively present at about 0.1 and 0.04% of total PIs in yeast and mammals. $PI(3,5)P_2$ is proposed to be mainly localized to late endosomes and lysosomes (Figure 4 B (Dove et al., 2009)) based on the location of its synthesizing enzyme complex. This enzyme complex in mammalian cells consists of the type III phosphatidylinositol phosphate kinase (PIPKIII) PIKfyve which phosphorylates the 5 position of the inositol ring of PI(3)P, the scaffold protein Vac14, and the opposing phosphatase FIG4 (Ikonomov et al., 2009b; Jin et al., 2008; Sbrissa et al., 2008; Shisheva, 2008) (Figure 5). Genetic disruption of any of these components lead to decreases in cellular $PI(3,5)P_2$ levels (Chow et al., 2007; Ikonomov et al., 2011; Zhang et al., 2007; Zolov et al., 2012). Many studies to elucidate the cellular function of $PI(3,5)P_2$ have employed genetic and pharmacologic manipulation of its

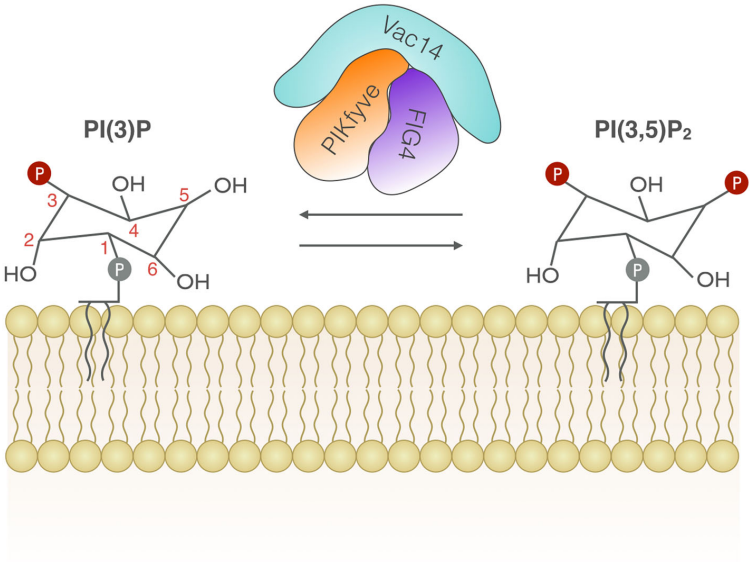

Figure 5. The PI(3,5)P_2 metabolizing enzyme complex. The dynamic and rapid changes in PI(3,5)P_2 is tightly regulated by its synthesizing enzyme complex, which consists of the phosphoinositide kinase, FYVE finger-containing (PIKfyve) the phosphatase FIG4 and the scaffold protein Vac14.

metabolizing enzymes. Physiological functions of $PI(3,5)P_2$ in yeast were originally discovered by studying the phenotype of mutants lacking Fab1 (known as PIKfyve in mammalian cell), the yeast orthologue of PIPKIII. Fab1-deficient yeast cells contain grossly enlarged vacuoles which are poorly acidified and show a defect in the ubiquitin-dependent sorting of proteins into multivesicular bodies (Gary et al., 1998). In mammalian cells, studies using either dominant negative mutants, siRNA knockdown or pharmacological antagonists of PIKfyve, Vac14, or Fig 4 (Chow et al., 2007; de Lartigue et al., 2009; Ikonomov et al., 2001; 2009b; 2006; 2009a; Jin et al., 2008; Rutherford et al., 2006; Sbrissa et al., 2007; Zhang et al., 2007) have likewise found a significant defect in membrane dynamics that leads to enlarged endosomes.

Through such studies, $PI(3,5)P_2$ is now known to play an essential role in endo-lysosomal transport. Knockdown of PIKfyve inhibits retrograde traffic of proteins from endosomes to the TGN (Rutherford et al., 2006), including sorting receptors (e.g., CI-M6PR; cation independent mannose-6-phosphate receptor) and Soluble N-ethylmaleimide-sensitive factor-activating protein receptor (SNARE) membrane fusion proteins (Bonifacino and Rojas, 2006). Retrograde trafficking is coordinately regulated by the endosomal Rab family GTPase Rab9, the retromer protein complex that mediates cargo recognition and budding of endosomal membranes, and WASH-mediated actin nucleation (Dong et al., 2013). Interestingly, PIKfyve binds and promotes membrane association of p40, a Rab9 GTPase effector. Although p40 does not seem to bind $PI(3,5)P_2$, interaction with PIKfyve may serve to coordinate $PI(3,5)P_2$-dependent functions like membrane fission that is mediated by the $PI(3,5)P_2$ effector Atg18 (Dove et al., 2004).

$PI(3,5)P_2$ controls the lysosome-dependent degradative pathway, autophagy. In *C. elegans*, mutations in Fab1 causes an increase in autophagosomes (Nicot et al., 2006), suggesting decreased degradation. Similarly, pharmacological inhibition of

PIKfyve in mammalian cells causes an accumulation of autophagosomes and the autophagic marker microtubule-associated protein light chain 3 II (LC3-II) (Jefferies et al., 2008; Martin et al., 2013). Autophagic protein degradation occurs after fusion of autophagosome with lysosomes and requires functional lysosomes with low pH. Thus, the accumulation of autophagosomes could occur as a consequence of impaired capability of autophagosome to fuse with lysosome. In deed, it has been proposed that $PI(3,5)P_2$ regulates Ca2+ release from vacuoles thereby triggering membrane fusion(Dong et al., 2010; Li et al., 2013). In addition, fab1 deficient yeast vacuoles and endolysosomes in mutant *Drosophila* and *C. elegans* are all poorly acidified (Nicot et al., 2006; Rusten et al., 2006; Gary et al., 1998), suggesting that defective acidification may also contribute to autophagy failure in $PI(3,5)P_2$ deficient cells. However, underlying mechanism how $PI(3,5)P_2$ mediates endolysosome acidification is a complete mystery due to the lack of effector involved in acidification.

$PI(3,5)P_2$ is also implicated in membrane traffic to the plasma membrane. Impaired insulin-stimulated translocation of glucose transporter to the plasma membrane was observed in muscle-specific PIKfyve knock-out mice (Ikonomov et al., 2013). In addition, it has been shown that the formation of $PI(3,5)P_2$ facilitates endosome transport to the plasma membrane leading to an increased abundance of AMPA-type glutamate receptor GluA1 protein in the plasma membrane (Seebohm et al., 2012).

Despite its importance in endolysosomal membrane trafficking, the underlying mechanism by which $PI(3,5)P_2$ regulates these processes are still unclear, largely due to the lack of effectors. Therefore, identification of the new effector proteins that interact with $PI(3,5)P_2$ is critical to unravel the mechanism.

Purpose of this study

The branched actin regulator cortactin is a central protein connecting signaling pathways with the actin cytoskeleton and plays a role in diverse cellular processes, including cell motility, membrane trafficking, invasion, and cell morphogenesis. Previously, our laboratory demonstrated a role of cortactin-mediated actin assembly in the aggressiveness of cancer cells, including motility, invasiveness and tumor growth (Bryce et al., 2005; Clark et al., 2009; Sung et al., 2011). Mechanistically, we have found that most of those phenotypes are highly tied to the ability of cells to secrete molecules such as extracellular matrix, proteinases, and growth factors (Clark et al., 2009; 2007; Sung et al., 2011). These data are consistent with other recent studies demonstrating the importance of cortactin and the actin cytoskeleton in membrane trafficking (Cao et al., 2005; Kjeken et al., 2004; Lanzetti, 2007; Salvarezza et al., 2009). When this study began, it was unclear at intracellular membrane compartment was the source for secretion of proteinases and other factors that might promote cancer aggressiveness. It was also unclear what activities of cortactin were important and how they might be coordinated on secretory organelles. I first focused on identifying which trafficking organelles were most affected by the loss of cortactin expression. I found that cortactin-mediated branched actin assembly regulates LE/Lys compartment maturation and subsequent retrograde transport to the Golgi complex. This finding then leads me to ask the question of what is the upstream regulatory input is that might regulate cortactin activity on LE/Lys compartment. My study focusing on the interaction between $PI(3,5)P_2$ and cortactin should identify a key part of the mechanism by which $PI(3,5)P_2$ controls membrane trafficking and reveal cortactin and branched actin as novel effector of $PI(3,5)P_2$. The main objective of this work is to understand basic molecular mechanism underlying protein secretion that promotes cancer invasiveness. By understanding the underlying molecular mechanism that promotes secretion by aggressive cancer cells,

this study will point towards future novel approaches to managing cancer invasiveness and metastasis.

CHAPTER II

MATERIALS AND METHODS

Constructs, antibodies, and reagents

The construct encoding HRP-TGN38 was a gift from Dan Cutler (UCL) and the temperature-sensitive VSV-G (ts045-VSV-G-GFP) was a gift from Jennifer Lippincott-Schwartz (NIH). Cortactin mutant cDNAs were obtained from Dr. J Thomas Parsons and subcloned into LZRS retroviral vector, as previously described (Bryce et al., 2005). The construct encoding human Vac14 was a gift from Dr. Lois Weisman (University of Michigan) and subcloned into pEGFP-N1 using BglII and Sal I site.

Antibodies were as follows: Goat anti-HRP (123-005-021; Jackson Immunoresearch Labs), mouse anti-cortactin (clone 4F11; Millipore), rabbit anti-GST antibody (#2622; Cell Signaling), Rhodamine-phalloidin (Molecular probes). Calreticulin (ab2907) and mannosidaseII (ab12277) antibodies were from abcam. Rabbit anti-cortactin (H-191), GRASP65 (sc-30093), ERGIC-53 (sc-32442), and mouse anti PIK5KIII (sc-100408) were from Santa Cruz Biotechnology. The GM130, p230^{trans} (611280), rabbit anti-Rab7 (9367) antibodies were from BD Biosecience. The conformation-specific mouse monoclonal anti-VSV-G antibody (I14) was provided by Anne K. Kenworthy (Vanderbilt University, Nashville, TN). Rabbit anti-WASH was a gift from Daniel Billadeau (Mayo Clinic; (Gomez and Billadeau, 2009)). GCC185 was a generous gift from Irina Kaverina (Vanderbilt).

PIP strips and polyPIPosomes were from Echelon Biosciences (Y-P003, Y-P005, and Y-P035). All liposome experiments in chapter IV used polyPIPosomes. Cycloheximide (Calbiochem Co.) was stored as 1 mg/ml stock solution in methanol.

Latrunculin A was purchased from Sigma. YM201636 (Selleckchem) and CK-666 (Millipore) were stored as 10 mM and 100 mM, respectively, stock solutions in DMSO.

Cell culture and generation of stable cell lines

SCC61 cells were maintained in DMEM supplemented with 20% fetal bovine serum (FBS), 0.4 µg/mL hydrocortisone, and 4 µg/mL puromycin (for stable cell lines) and 600 µg/mL G418 (for stable cortactin rescue cell lines). HeLa cells were maintained in RPMI 1640 supplemented with 10% bovine growth serum (BGS) and 4 µg/ml puromycin. MCF10A cells were maintained in DMEM/F12 supplemented with 5% horse serum, cholera toxin (0.1 µg/mL), insulin (1 mg/mL), hydrocortisone (0.5 µg/mL) and EGF (20 ng/mL). MDA-MB-231 cells were maintained in DMEM supplemented with 10% FBS. All cells were maintained at 37°C in 5% CO_2. Stable cell lines used in CHAPTER III were generated as previously described (Bryce et al., 2005; Clark et al., 2007). Stable knockdown of cortactin or stable expression of mRFP-Rab7 in MDA-MB-231 cells was achieved using BLOCK-it Lentiviral RNAi expression system and ViralPower Lentiviral expression system (Invitrogen) according to manufacturer's protocol.

Transfection and Drug treatments

For all assays, cells were plated on uncoated (HeLa and MDA-MB-231) or fibronectin-coated (50 µg/mL;SCC61) glass coverslips. For TGN-HRP, FLAG-tagged cortactin and GFP-Rab7 transfection, cells were transfected with 0.5 µg/well of cDNA using Lipofectamine2000. For mRFP-Rab7, mEGFP-F-tractin, and EGFP-Vac14 transient transfections, MDA-MB-231 cells were transfected with 0.5 µg/well of cDNA with Lipofectamine 3000. For inhibition of PIKfyve and/or Arp2/3 activity, cells grown on coverslips were serum-starved (complete growth media lacking FBS) for 3 h before treating with YM201636 or CK-666, as previously described (Ikonomov et al., 2009a).

YM201636 and CK-666 dissolved in DMSO were diluted with DMEM and added to cells at a final concentration of 800 nM and 100 μM, respectively for 2 h.

For siRNA assays of Golgi morphology, control (D-001210-02-05), cortactin (M-010508-00-005), Rab7a (M-010388-00-0005), and Rab9 (M-004177-01) siGENOME SMARTpool siRNA constructs were obtained from Thermo Scientific. Control, cortactin (200 nM, 72h), Rab9 (200 nM, 96 h) or Rab7a (100 nM, 48 h) siRNA were transfected with SCC61 and HeLa cells using Oligofectamine (Life Technologies). For Rab9 analysies, only cells with obvious loss of Rab9 expression determined by immunofluorescence were used in the quantification. PIKfyve knockdown was performed with an ON-TARGETplus siRNA SMARTpool (L-005058-00-0005; GE Dharmacon) using Lipofectamine RNAiMAX (Life Technologies). As a control for the knockdown, a non-targeting control pool was used (D-001810-10-05; GE Dharmacon). Cells were seeded in six-well plates at a density of 2.0 x 10^5 cells/well prior to transfection using Lipofectamine RNAiMAX (Life Technologies) and 40 nM of siRNAs. After a 48 h incubation, cells were reseeded onto six-well plates at the same density or onto coverslips at a density of 3.5 x 10^4 cells/well and retransfected with 40 nM oligos for 24 h. Cells were then processed for western blotting and immunofluorescence.

Protein purification

To purify GST-tagged proteins, *E. Coli* BL21DE3 were transformed with the appropriate plasmid. After growth to approximately OD_{600}=0.8 expression was induced with IPTG (1 mM) for 20 h at 20°C. Cells were pelleted and resuspended in preparation buffer (300mM NaCl, 0.5mM EDTA, 50mM Tris, pH8.0) supplemented with 2mg/ml lysozyme and protease inhibitors, and lysed with sonication. The lysate was then centrifuged at 96,000 x g at 4 °C for 30 min. The supernatant was incubated overnight with glutathione-Sepharose at 4°C before elution with 25 mM glutathione, 150 mM NaCl,

50 mM Tris, pH 8.0. Purified proteins were aliquoted, snap frozen in liquid nitrogen, and stored at -80 °C. Actin was purified from chicken pectoralis skeletal muscle and gel filtered as described in (Bryce et al., 2005).

Lipid overlay assay

PIP strips were blocked in PBST (0.1% Tween 20(v/v)) supplemented with 3% fatty acid-free BSA (Sigma) for overnight at 4°C and then incubated with 0.5 µg/ml GST fusion proteins for 1 h at room temperature. After washes with PBST-BSA, the membranes were blotted with Rabbit anti-GST for 1 h at room temperature followed by IRDye 800 Goat anti-Rabbit secondary antibody for 1 h.

Liposome binding assay

70 nM of purified GST fusion protein was incubated with 3 µM liposomes in 20 mM HEPES, 120 mM NaCl, 1 mM EGTA, 0.2 mM $CaCl_2$, 1 mM $MgCl_2$, 5 mM KCl, 1 mg/ml fatty acid-free BSA, pH 7.4 for 15 min at room temperature. Liposome-protein complexes were then further incubated with streptavidin-conjugated magnetic beads (Invitrogen) for 30 min at room temperature. After washing with binding buffer and isolation with a magnet, liposome-bound protein was analyzed by SDS-PAGE. The intensity of bands was quantified by ImageJ software. K_d was calculated using a one-site binding hyperbola nonlinear regression analysis (Graphpad).

PI(3,5)P_2-F-actin competition assay

3 µM F-actin was prepared from monomers by polymerization in 80 mM KCl, 2 mM $MgCl_2$, 20 mM HEPES, pH 7.4 for 1 h at room temperature. Then, various concentrations of actin filaments (0-1.5 uM) prepared by dilution with polymerization buffer were incubated with 250 nM PI(3,5)P_2-containing liposomes and 70 nM cortactin and then processed as for the liposome binding assay. Graphpad software was used for

nonlinear regression analysis of data sets and K_i was calculated using one-phase exponential decay equation.

Actin assembly TIRF assay

Glass flow chambers were constructed from glass coverslips (24 x 40 mm and 22 x 22 mm; no. 1.5) using doubled sided tape (3M). Coverslips were cleaned for 10 min with plasma cleaner and 30 min bath in 0.1 M KOH, and then coated with methoxy-polyethylene glycol-silane (mPEG-Silane-5K, Creative PEGworks; 0.1% in 95% ethanol, 0.1% HCl) for overnight at room temperature. The mPEG-Silane coating was used to minimize filament binding to the chamber surface. The chambers were washed twice each with high then low salt buffer solutions (1 % (w/v) BSA, 50 mM Tris, pH 7.5, and 600/150 mM NaCl, respectively), followed by two washes with 1 X TIRF buffer. The 1x TIRF buffer contained MKEI (100 mM KCl, 2 mM $MgCl_2$, 2 mM EGTA, 20 mM imidazole pH 7.0), 15 mM Glucose, 100 mM DTT, 0.2 mM ATP, 0.5 % 4000 cP methylcellulose, 20 µg/ml catalase, 0.1 mg/ml glucose oxidase, and 0.1 % BSA. Glucose oxidase, catalase, and BSA were added just before use. Actin polymerization reactions were initiated by adding a protein solution containing the proteins (Arp2/3 complex, GST-VCA, cortactin, or PI(3,5)P_2-liposome) in 1 x TIRF buffer to a solution of 4.5 µM 33% Oregon-Green actin mixed with 50 µM $MgCl_2$ and 200 µM EGTA to give a final reaction solution of 0.75 µM 33% Oregon-Green actin. Images were collected on a Nikon TiE inverted microscope equipped with a Nikon 100x/1.49NA TIRF objective, and Photometrics Evolve EM-CCD camera (Photometrics, Tucson, AZ). The 1.5x optivar was used for all images to increase magnification. 488-nm laser was used to excite Oregon-Green. Images were acquired with Nikon Elements software.

Debranching assay

Polymerization reactions were initiated by mixing 3 μM G-actin with 100 nM Arp2/3 complex and 600 nM GST-VCA in polymerization buffer, and incubated for 8 min to form fully polymerized actin branches. At this time, rhodamine-phalloidin (0 min sample), 500 nM cortactin, 500 nM cortactin plus 500 nM PI(3,5)P_2-liposome, or buffer was added, then further incubated for 5, 10, 15, 20, or 30 min before adding equimolar (3 μM final concentration) rhodamine-phalloidin (from a 200 μM stock in methanol) to stop filament debranching and stain the actin filaments. After 4 min of incubation with rhodamine-phalloidin, filaments were diluted into fluorescence buffer containing MKEI, 100 mM dithiothreitol, 20 μg/ml catalase, 100 μg/ml glucose oxidase, 3 mg/ml glucose, and 0.5% methylcellulose, 4000cp. 4 μl was applied to glass coverslips (Fisherbrand, 22 x 22 mm, # 1.5). Image were acquired with an Eclipse TE2000-E widefield fluorescent microscope (Nikon) equipped with a Plan Apo 100x/1.4NA, oil immersion lens (used in combination with x1.5 optivar), and a cooled charge-coupled device camera (HAMAMATSU) by use of MetaMorph software. Branching was analyzed by manually counting unbranched filaments and number of branching of filaments with one or more branches. Percent branching was then calculated by the following equation: % branched filaments = (number of branched filaments per field/ number of total filaments) x 100.

Immunofluorescence and Image analysis

Cells were fixed in either 4% paraformaldehyde or methanol (Mannosidase II), permeabilized with TritonX100 or saponin ($p230^{trans}$), incubated with primary and secondary antibodies for 1 h each at room temperature. Hoechst was added on the last wash for 5 min and the coverslips were then mounted using Aqua Poly/Mount (Polysciences, Inc). Secondary antibodies used were: goat anti-mouse Alexa Fluor 488 (GM130, cortactin (4F11), ERGIC-53, p230trans); goat anti-mouse Dylight 633 (for

p230trans); goat anti-rat Alexa Fluor 546 (for LAMP2); goat anti-rabbit Alexa 488 (for M6PR, calreticulin (Golgi area)); goat anti-mouse Alexa Fluor 594 (LAMP1); goat anti-rabbit Alexa Fluor 594 (for FLAG, Mannosidase II, GRASP65, calreticulin (colocalization); cortactin (colocalization; H-191)); donkey anti-guinea pig 488 (GCC185); donkey anti-goat Alexa Fluro 488 (HRP). For Rab7 staining, cells were fixed for 15 min in 4% paraformaldehyde at 37°C and blocked and permeabilized with 5% normal goat serum containing 0.3% Triton X-100 for 1 hr at room temperature. Primary antibodies diluted in PBS containing 1% BSA and 0.3% Triton X-100 were added to cells for staining overnight at 4°C followed by secondary antibody incubation for 1 h at room temperature. For filipin staining, cells were plated on coverslips for 24 hours, fixed in 3% PFA for 1 hour, quenched with glycine (1.5 mg/mL) and stained with filipin (0.05 mg/mL) for 2 hours at room temperature and imaged under UV light.

Images for quantification of Golgi area were acquired with an Eclipse TE2000-E wide-field fluorescent microscope (Nikon) equipped with a Plan Apo VC 60x, 1.4NA, oil immersion lens and a cooled charge-coupled device (CCD) camera (HAMAMATSU, C4742-80-12AG) by the use of *Metamorph* software. Golgi area was quantitated by thresholding the images based on GM130 and a goat anti-mouse Alexa Fluor 488 staining. Cell area was determined manually by tracing the cell perimeter in rhodamine-phalloidin stained images (not shown in most figures), and the ratio of Golgi to Cell area was calculated based on the thresholded area using *Metamorph* software. For colocalization experiments, images were acquired on a confocal laser scanning microscope (model LSM 510; Carl Zeiss, Inc.), using a Plan-APOCHROMAT 63x/1.4 oil DIC objective and either a Argon/2, HeNe1 and/or HeNe2 laser. Z-axis sectioning was at 0.2 µm intervals. Colocalization and intensity were quantitated using *MetaMorph* software after thresholding images to remove background. Colocalization Image J plugin

was used to show colocalized pixels between two images for M6PR localization analysis. Colocalized pixels were displayed as white on RGB overlay images.

VSV-G Trafficking Assay

SCC61 and HeLa cells were transiently transfected (0.75 mg/well in a 6-well dish containing glass coverslips) with a construct encoding ts045 VSV-G-GFP cDNA, and incubated for 16 h at 40℃. Cells were then treated with 100 μg/ml of cycloheximide for 30 min to stop protein synthesis and then shifted to 32℃ for 0, 30, 45, 60, 120, or 180 min prior to fixation to allow transport of the nascent VSV-G through the secretory pathway. For determination of surface VSV-G, live cells were incubated with an antibody (I14) directed against the luminal domain of VSV-G for 10 min at 4℃, washed extensively, fixed, and stained with an Alexa 594 secondary antibody. Average fluorescence intensity of cell surface VSV-G protein was used to calculate the extent of VSV-G transport

Live cell imaging

For visualization of the dynamic effect of YM201636 on endosomes, MDA-MB-231 cells stably expressing mRFP-Rab7 were cultured on poly-D-Lysine-coated MatTek dishes overnight. Before imaging they were serum starved for 3 h and then 800 nM YM201636 was added. 20 min after drug treatment, images were captured every 10 sec for 90 min on a confocal microscope (model LSM 710; Carl Zeiss, Inc.), using a 63x/1.40 Plan-APOCHROMAT oil objective and Argon-488 and HeNe-561 laser under 5% CO_2 at 37°C. For the analysis the stability of actin on endosomes, MDA-MB-231 cells stably expressing mRFP-Rab7 were transfected with mEGFP-F-tractin. Then, cells were cultured on 35mm glass bottom dishes (In Vitro Scientific, no.1.5) overnight. After 2 h incubation of cells with DMSO or YM201636, 10 μM latrunculin A was added and images

were captured every 2 sec on a DeltaVision deconvolution microscope (Applied Precision) equipped with a CoolSNAP HQ2 camera (Photometrics), and a UPSLAPO 100x/1.4 oil immersion objective. Individual raw files were deconvoluted using Applied Precision Softwork deconvolution package. Actin fluorescence intensity was manually tracked using manual tracking plugin of Fiji software.

Electron Microscopy (Stable shRNA KD cells; Conventional TEM)

Cells ($1x10^6$) were plated on 10 cm dishes and 24 h later were fixed in 2.5% glutaraldehyde in 0.1 M Cacodylate buffer with 1% CaCl for 1 h at room temperature. The fixation buffer was then replaced with fresh buffer and incubated overnight at 4℃. The samples were scraped and transferred to conical tubes and washed extensively followed by osmications for 1 h in 1% aqueous osmium tetroxide. The samples were then washed extensively followed by en bloc stained in ethanolic uranyl acetate for 10 min. The cells were dehydrated by passage through a graded series of increasing concentrations of ethanol. Dehydration was continued through increasing concentrations of ethanol. After the samples were embedded in epon resin and polymerized, cells were thin sectioned (50 nm) and imaged using a CM12 transmission EM (Philips) equipped with an AMT 542 camera.

Morphometry analysis of organelle areas

Point counting stereology was used to quantitate relative volume of cytoplasm occupied by Golgi or LE/Lys elements (Jerome et al. 1998; Weibel et al. 1969). Thin sections from two independent blocks per cell line were randomly imaged for analysis. Additionally, one of the blocks was analyzed using two different sections. The magnification of images was optimized such that a point of the grid would fall on identifiable organelle structures. All micrographs used for stereology were 40,000x. A grid of intersecting lines (squares = 0.25 um^2) was superimposed using ImageJ Grid

Plugin on each micrograph and the number of intersection points that fell on cytoplasm and organelles of interest were counted. From each section ≥30 micrographs/cell line/section were collected in an unbiased manner and counted. The ratio: # points (organelle)/# points cytoplasm (minus the nucleus) was used to calculate a fractional cell cytoplasmic volume occupied by Golgi or LE/Lys. Student's t-test was used to determine the significance of the data.

Data presentation and statistical analysis

Graphs were generated using Prism Graphpad version 5. Statistical analysis was performed using SPSS version 18 and 22. All data were tested for normality using a Kolmogorov-Smirnov normality test. Data with a normal distribution were analyzed using a student t-test and plotted using mean +/ standard error bar graphs. Data with a non-normal (non-parametric) distribution were analyzed using a Mann-Whitney U test (Mann-Whitney U test with Bonferroni correction was used for Golgi area/cell area analysis). Data are presented as box and whiskers plots with the box indicating the 25^{th} and 75^{th} percentiles, solid line indicating the median, and the whiskers indicating the 95% confidence intervals.

CHAPTER III

REGULATION OF LATE ENDOSOMAL/LYSOSOMAL MATURATION AND TRAFFICKING BY CORTACTIN AFFECTS GOLGI MORPHOLOGY

Introduction

Actin assembly is increasingly recognized to play an integral role in membrane trafficking events, including vesicle formation, fission, transport, and fusion (Lanzetti, 2007). The branched actin regulator and tumor-overexpressed protein, cortactin, is thought to be a key coordinator of membrane trafficking since it decorates branched actin networks throughout the cell and binds to a variety of membrane trafficking, signaling, and cytoskeletal proteins (Clark and Weaver, 2008; Kirkbride et al., 2011; Lanzetti, 2007). Indeed, a number of studies have shown that cortactin can regulate endocytic trafficking, including initial endocytosis from the plasma membrane (Cao et al., 2010; 2003; Engqvist-Goldstein et al., 2004; Grassart et al., 2010; Merrifield et al., 2005; Sauvonnet et al., 2005; Zhu et al., 2007; 2005) and recycling (Puthenveedu et al., 2010; Sung et al., 2011). Cortactin has also been shown to regulate secretion of several proteins that promote aggressive tumor phenotypes (Clark et al., 2009; 2007; Sung et al., 2011) and might utilize either Golgi (Cao et al., 2005; Salvarezza et al., 2009) or endocytic (Steffen et al., 2008; Sung et al., 2011) trafficking pathways. Two studies have shown that expression of a dominant-negative cortactin molecule that lacks the SH3 domain blocks exit of model cargo-containing vesicles from the *trans*-Golgi network (TGN) (Cao et al., 2005; Salvarezza et al., 2009), suggesting an important role for cortactin in actin assembly and trafficking at the Golgi. However, the overall role of cortactin in Golgi structure and function is poorly understood.

Perturbation of either actin assembly or actin binding to Golgi membranes leads to either compaction or fragmentation of the Golgi (Campellone et al., 2008; Dippold et al., 2009; Egea et al., 2006; Hayes and Pfeffer, 2008; Lanzetti, 2007; Lázaro-Diéguez et al., 2006; Valderrama et al., 1998); however, the underlying mechanisms are unclear. Although treatment with actin-targeting drugs typically leads to compaction of the Golgi by light microscopy, there is variation in the effects on cisternal ultrastructure including cisternal fragmentation or bloating depending on the drug (Lázaro-Diéguez et al., 2006; Valderrama et al., 1998). A variety of mechanisms have been proposed for these effects on the Golgi, including an essential role for actin in maintaining cisternal structure, intralumenal pH, and vesicular trafficking (Egea et al., 2006; Lázaro-Diéguez et al., 2006; Matas et al., 2004; Valderrama et al., 1998; 2001; 2000). Vesicular trafficking in particular seems a likely mechanism by which actin regulators control Golgi homeostasis, since a growing number of actin-associated molecules and actin regulators have been shown to affect both trafficking to or from the Golgi concomitant with Golgi morphology changes (Campellone et al., 2008; Hehnly et al., 2010; Warner et al., 2003).

The endocytic system communicates with the Golgi apparatus at multiple points (Pfeffer, 2009). In addition to receiving essential cargo from the Golgi, a number of lipid and protein cargoes are returned to the Golgi from early and late endosomes. Indeed, proper homeostasis of the Golgi depends on intact function of endocytic trafficking. For example, in certain lysosomal storage diseases (LSD) such as Niemann-Pick disease type C (NPC), accumulation of cholesterol and other cargo in immature late endosomal/lysosomal (LE/Lys) hybrid organelles can lead to defective retrograde trafficking of mannose-6-phosphate receptor (M6PR) and other cargo to the Golgi apparatus (Choudhury et al., 2002; Ganley and Pfeffer, 2006). A potential mechanism for the disturbance of LE trafficking by LSD is aberrant accumulation of assembled

SNARE complexes that accompanies defective breakdown of cholesterol-rich lipid rafts (Fraldi et al., 2010).

In this chapter, we investigated the role of cortactin in regulating Golgi morphology, size and trafficking. We found that knockdown (KD) of cortactin in several cell types leads to a substantial alteration in Golgi organization by light and electron microscopy; however stereology quantification indicated little alteration in Golgi apparatus size. In addition, trafficking of the model protein ts045-VSV-G (VSV-G) from the endoplasmic reticulum (ER) through the Golgi to the plasma membrane was unaffected, as was Brefeldin A (BFA)-induced assembly or disassembly of the Golgi in cortactin-KD cells. By contrast, EM studies revealed that cortactin-KD cells contained many enlarged LE/Lys hybrid organelles, suggesting a defect in LE/Lys maturation and trafficking. Likewise, cortactin-KD cells accumulated the retrograde LE-to-Golgi cargo M6PR as well as free cholesterol in LE. Inhibition of LE/Lys maturation by siRNA-depletion of the GTPase Rab7 or treatment with the lysosomotropic agent chloroquine induced a Golgi morphology phenotype that was identical to that of cortactin-KD cells. Furthermore, Golgi morphology defects of cortactin-KD cells were partially rescued by removing the LE/Lys cargo cholesterol from the culture media. Reexpression of cortactin mutants in cortactin-KD cells revealed that cortactin binding to the actin-nucleating Arp2/3 complex is essential for rescue of Golgi morphology defects. These data are consistent with a model in which cortactin indirectly regulates Golgi homeostasis by controlling LE/Lys maturation and trafficking.

Results

Cortactin regulates Golgi morphology

To examine how cortactin regulates the Golgi, we began by immunostaining SCC61 head and neck squamous cell carcinoma (HNSCC) cells stably expressing either

human cortactin-specific shRNA (cortactin-KD1 or –KD2), a scrambled oligo shRNA (scrambled) or a cortactin-specific shRNA along with an shRNA-insensitive mouse cortactin gene (KD1/rescue) (Figure 6 A) (Bryce et al., 2005; Clark et al., 2007). By light microscopy, the Golgi in scrambled control SCC61 cells was dispersed around the nucleus, consistent with the reported Golgi morphology in aggressive cancer cells (Ayala et al., 1999). By contrast, loss of cortactin expression resulted in a dramatic change in Golgi morphology to a more compact perinuclear cluster, which was rescued by reexpression of shRNA-insensitive cortactin. Quantification of the ratio of total Golgi area to total cell area (Burman et al., 2010) showed that the Golgi occupies significantly less area within cortactin-KD SCC61 cells compared to scrambled oligo control cells and KD1/rescue cells (Figure 6 B).

Analysis of *cis*- (GM130, GRASP65), *medial*- (Mannosidase II) and *trans*-Golgi ($p230^{trans}$, GCC185) markers revealed that the morphology of the entire Golgi apparatus is altered in cortactin-KD cells. The ER-Golgi intermediate compartment (ERGIC; ERGIC-53 as a marker) was also more compact in KD cells. There were no obvious changes in ER morphology, as assessed by immunostaining of calreticulin (Figure 7 A). We confirmed that our TGN antibodies mark the appropriate secretory compartment by low level transient expression of the TGN marker, TGN38–HRP (Connolly et al., 1994; Egorov et al., 2009), in both control and cortactin-KD cells. The localization of TGN38-HRP resembled that of $p230^{trans}$ and GCC185, and further confirmed the compact TGN morphology in cortactin-KD cells (Figure 7).

Stable expression of cortactin shRNA in both HeLa cervical cancer and MCF10A breast epithelial cells also led to a more compact Golgi morphology, indicating that the effect of cortactin-KD was not unique to SCC61 or HNSCC cells (Figure 6 B). We also tested the effect of transient expression of cortactin-specific siRNA on Golgi morphology

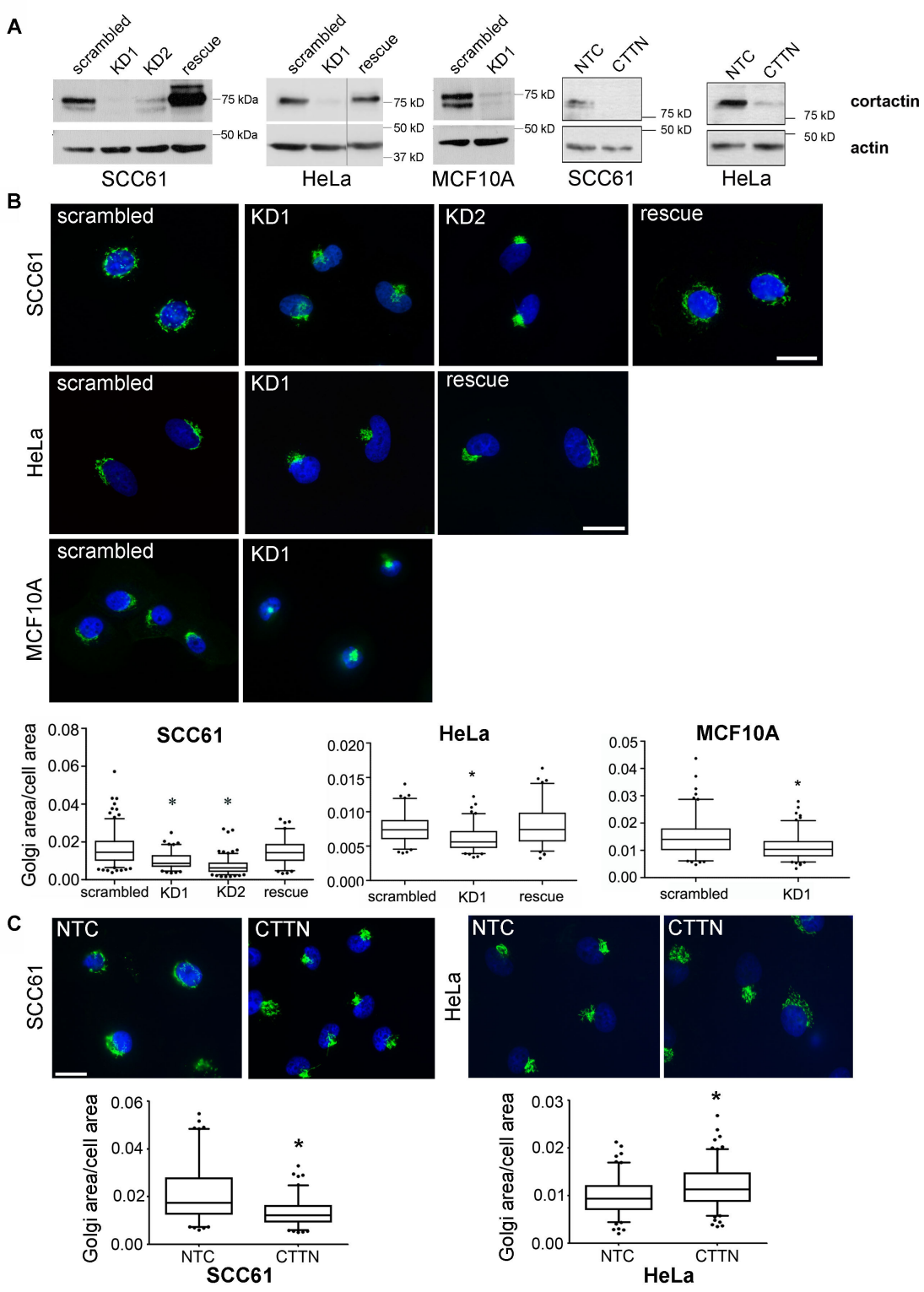

Figure 6. Figure legend on next page.

Figure 6. Cortactin regulates Golgi morphology. (A) Immunoblot of cortactin expression (top panels) and β-actin loading control (bottom panels) in SCC61m Hela and MCF10A stable (3 left panels) or transient (2 right panels) KD cell lines. For the transient siRNA experiments NTC indicates nontargeting control and CTTN indicates cortactin-specific siRNA. (B) Representative images of SCC61 cells (top), HeLa cells (middle) and MCF10A cells (bottom) stably expressing control shRNA (scrambled), human cortactin-specific shRNA (KD1, KD2), or cortactin-KD1 plus shRNA-resistant wild-type mouse cortactin (rescue) and immunostained for the Golgi marker marker, GM130 (green), actin filaments (rhodamine-phalloidin, not shown) and the nucleus (Hoechst, blue). Graphs show quantification of the ratio of Golgi area to total cell area of individual cells. (C) Representative images and analyses of transient control (NTC) or cortactin-KD (CTTN) SCC61 or HeLa cells. Scale bar = 25 mm. For each condition, n ≥20 cells from each of 3 independent experiments. *$p<0.05$.

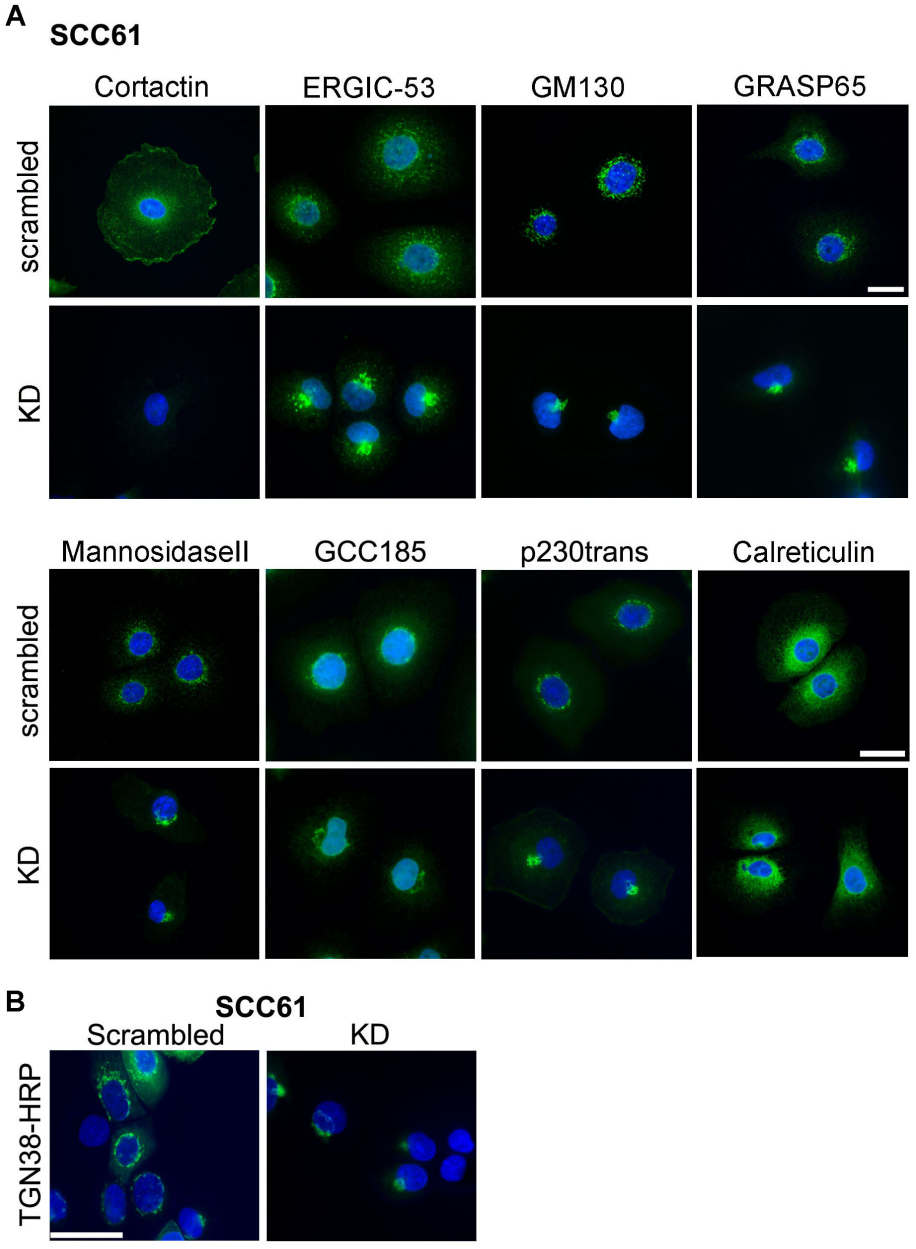

Figure 7. Cortactin affects the size of the Golgi, ERGIC, and TGN compartments. (A) SCC61 control (scrambled) and cortactin-knockdown (KD) cells were immunostained for cortactin or the indicated markers of the secretory pathway (green). Nuclei are stained with Hoechst (blue). (B) Control and KD cells were transiently transfected with TGN38-HRP for 24 hours followed by immunostaining against-HRP (green) and Hoechst (blue). n = 2 independent experiments.

(Figure 6 C). In SCC61 cells transfected with cortactin-specific siRNA for 72 h, the phenotype was identical to that of stable cortactin shRNA expression with a decrease in Golgi area. By contrast, in HeLa cells, which under normal conditions have a more response to transient versus stable KD of cortactin. However, we can conclude from these data that loss of cortactin affects Golgi homeostasis over both a short-term (Figure 6 C) and long-term (Figure 6 B) timescale.

Cortactin is not essential for Golgi assembly from ER membranes or VSV-G transport to the plasma membrane.

One possible explanation for the altered Golgi morphology of cortactin-KD cells is that cortactin affects membrane flow and/or Golgi assembly from ER membranes (Guo and Linstedt, 2006; Lowe, 2002), leading to a net decrease in the size of the Golgi compartment over time. To test the possibility of altered membrane flow from the ER to the Golgi, we performed a BFA washout assay in which control and stable cortactin-KD cells were incubated with 5 μg/ml BFA to disassemble the Golgi and allow fusion with the ER (Klausner et al., 1992). After 30 min, the BFA was washed out and cells were fixed and immunostained for the Golgi marker GM130 (Figure 8) at various timepoints. In both control and cortactin-KD cells, the Golgi was effectively dispersed by treatment with BFA (compare “control” to “+BFA” images). Likewise, the Golgi in both scrambled and cortactin-KD HeLa and SCC61 cells reassembled after BFA washout (compare “120 min” to “+BFA” images). Note that the Golgi morphology of cortactin-KD cells is more compact after BFA washout, indicating a return to steady state morphology by 120 min (compare “120 min” to “control” images). Overall, these data indicate that cortactin is not essential for BFA-induced Golgi disassembly or for reassembly from ER membranes.

To further test whether trafficking from the ER to the Golgi and forward to the plasma membrane (PM) was impaired in cortactin-KD cells, we analyzed synchronized

trafficking of the model constitutive cargo protein ts045-VSV-G-GFP (VSV-G) in stable KD and control SCC61 and HeLa cells. As previously described (Hirschberg et al., 1998; Presley et al., 1997), cells were transiently transfected with temperature-sensitive VSV-G plasmid and incubated at the restrictive temperature (40^{o}C) to induce retention of expressed VSV-G in the ER (Figure 9). A temperature shift to the permissive temperature (32^{o}C) allows proper folding of the extracellular domain and subsequent transport of VSV-G to the Golgi and then to the PM (Hirschberg et al., 1998; Presley et al., 1997). At various time points after the temperature shift, live unpermeabilized cells were incubated for 10 min with a monoclonal antibody that recognizes the extracellular domain of VSV-G (I14, (Feinstein and Linstedt, 2008) and then fixed and processed for immunofluorescence. This method allows specifically detection of only the PM-localized pool of VSV-G (Feinstein and Linstedt, 2008) by I14 staining as well as intracellular localization using the GFP tag. At the 0 min time point, VSV-G on the PM was minimal as determined by I14 staining and retained in the ER in both SCC61 and HeLa cells (Figure 9 A). However, over time in both cell types, there was movement of GFP-VSV-G from the ER to the Golgi (compare localization patterns of VSV-G-GFP at 0 min and 60 min) and an increase in PM VSV-G staining (Figure 9, A and B; I14 staining). Surprisingly, there was no difference between control and cortactin-KD cells in the rate of appearance of VSV-G at the PM as quantitated from I14 staining (Figure 9 C) (Cao et al., 2005)**.** These data indicate that cortactin is not an essential regulator of ER-to-Golgi or Golgi-to-PM trafficking, at least for the major anterograde transport route utilized by VSV-G (Ponnambalam and Baldwin, 2003).

EM analysis reveals minimal changes in Golgi ultrastructure or volume, and an abundance of immature LE/Lys hybrid organelles.

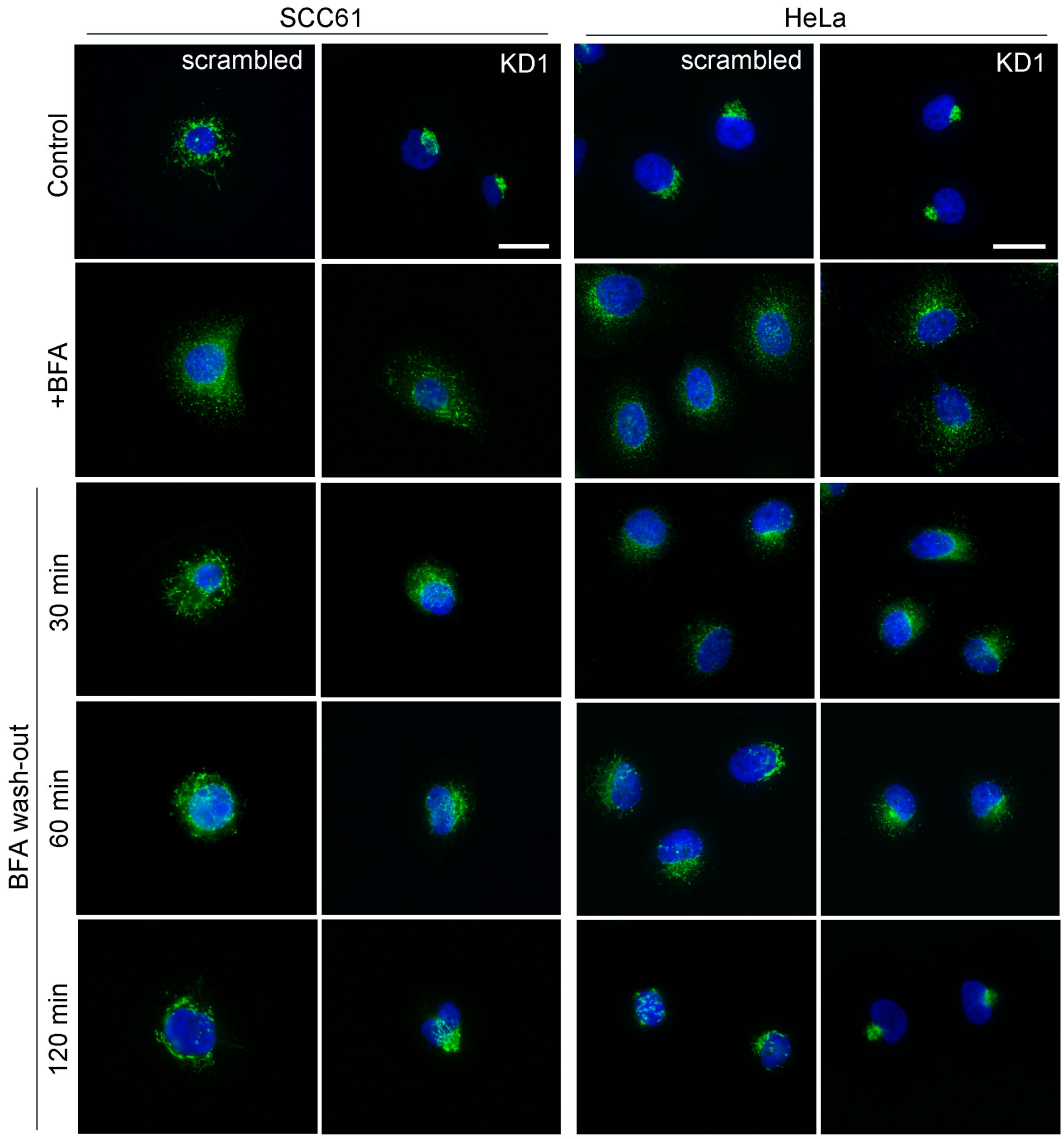

Figure 8. Loss of cortactin does not distrupt Golgi disassembly or reassembly. SCC61 (left panels) and HeLa (right panels) scrambled and KD1 cells were treated with Brefeldin A (5 µg/ml, "+BFA") for 30 minutes, followed by replacing the media with serum-containing media ("wash-out") for the indicated times. The cells were fixed and the Golgi and nuclei were stained using GM130 (green) and Hoechst (blue), respectively. Representative images are shown. Compare 120 min timepoint to vehicle-treated cells ("Control"). n = 2 independent experiments. Scale bars = 25 μm.

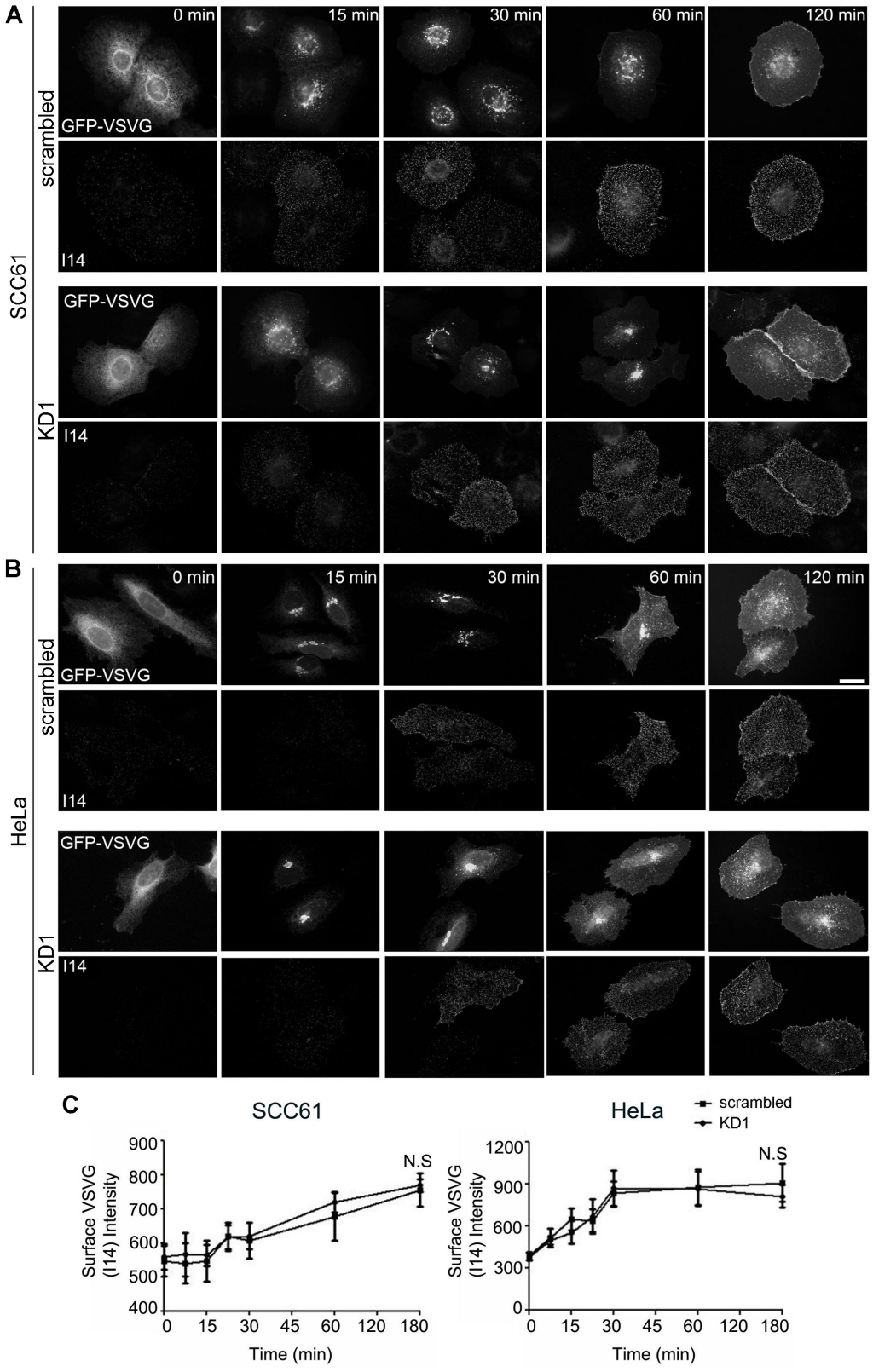

Figure 9. Figure legend on next page.

Figure 9. Cortactin-KD does not affect transport of VSV-G to the plasma membrane. (A, B)Transport of ts045-VSV-G-GFP (VSV-G) to the plasma membrane was assessed over a 3-h period following a shift of the cells to the permissive temperature of 32^{o}C in SCC61 or HeLa cells expressing either control (scrambled) or cortactin-specific shRNA (KD1). Representative images showing total expressed VSV-G (green) and cell surface I14-detected VSV-G (red) in SCC61 cells (A) and HeLa cells (B). (C) Analysis of the average surface intensity of I14 VSV-G staining at each time point after the shift to 32^{o}C for SCC61 (left) or HeLa (right) cells. n=3; >20 cells per independent experiment at each time point. N.S. = Not significant. Scale bar = 25 μm.

The changes in Golgi morphology identified in cortactin-KD cells by light microscopy could represent a variety of organizational, size, or structural changes in the Golgi apparatus. In order to determine whether cortactin affects Golgi structure or size, we performed transmission EM on 50 nm sections obtained from control and cortactin-KD SCC61 and HeLa cells (Figure 10). Surprisingly, loss of cortactin did not dramatically alter the structure of the Golgi stacks, although there was a subtle increase in *cis*- and *trans*-Golgi-associated coated and non-coated vesicles in KD cells (Figure 10, A and B, zoom shows TGN-associated traffic). To determine whether Golgi size was altered in cortactin-KD cells, we performed point counting morphometryanalysis on random thin sections (Jerome et al., 1998; Weibel et al., 1969) and quantitated the percent volume of the cytoplasm occupied by Golgi elements. For both SCC61 and HeLa cells, there was a small decrease in the Golgi volume; however this difference was only statistically significant in SCC61 cells, possibly due to variability in Golgi volume between HeLa samples. A more obvious change in both SCC61 and HeLa cortactin-KD cells was a large and statistically significant expansion in the number and size of LE/Lys hybrid organelles (asterisks in images in Figure 10) containing excess membrane and undigested cellular elements. This morphological phenotype is reminiscent of lysosomal storage diseases such as Niemann-Pick C, in which lamellar bodies, autophagolysosomes, and other immature LE/Lys hybrid organelles fill the cytoplasm. Consistent with our morphological identification of LE/Lys, by light microscopy cortactin-KD cells contain enlarged Rab7/LAMP1-double positive LE/Lys compartments (Figure 11 (Sung et al., 2011). Interestingly, when challenged by a dextran pulse, the large LE/Lys compartments in cortactin-KD cells are studded with small vesicles containing dextran, but do not contain dextran themselves (Figure 11), suggesting a storage-disease-like fusion defect (Heard et al., 2010; Vitry et al., 2010). Overall, these data suggest that cortactin-KD cells exhibit a profound perturbation in LE/Lys maturation and/

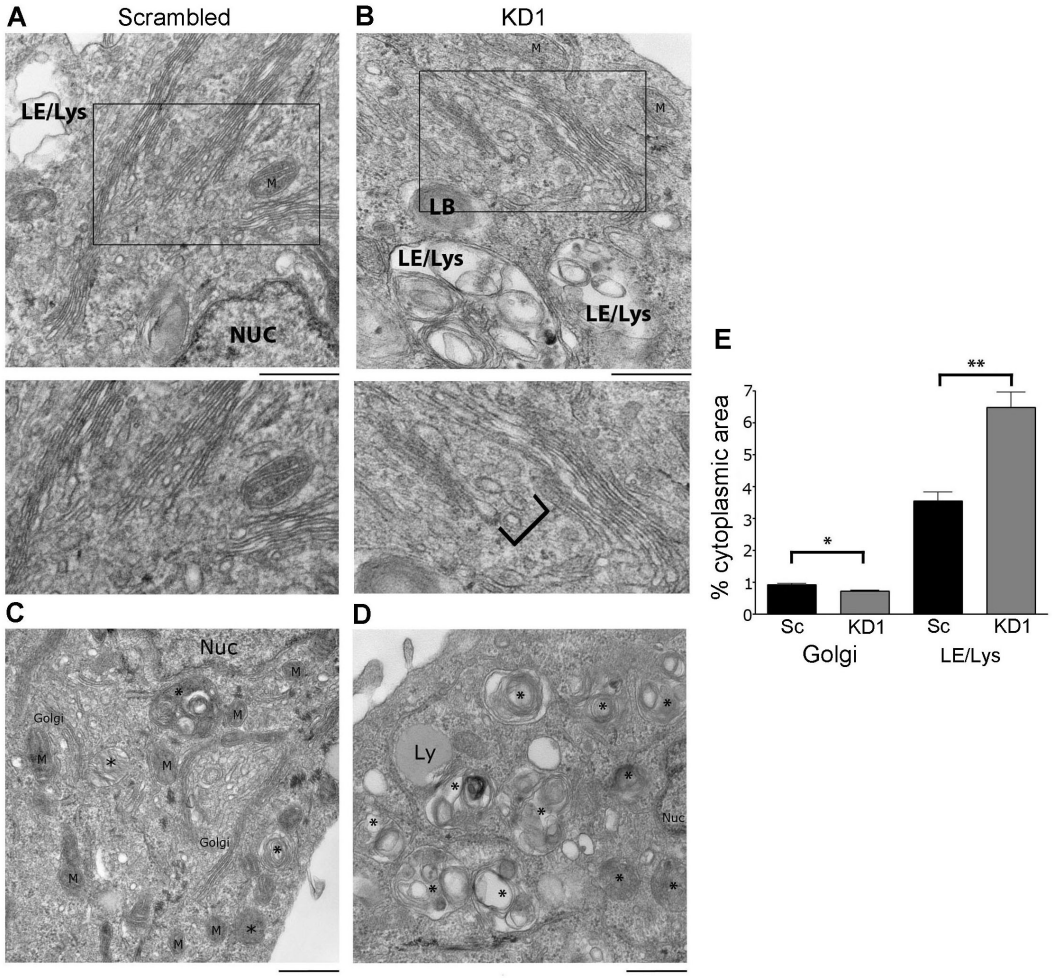

Figure 10. Figure legend on next page.

Figure 10 continued

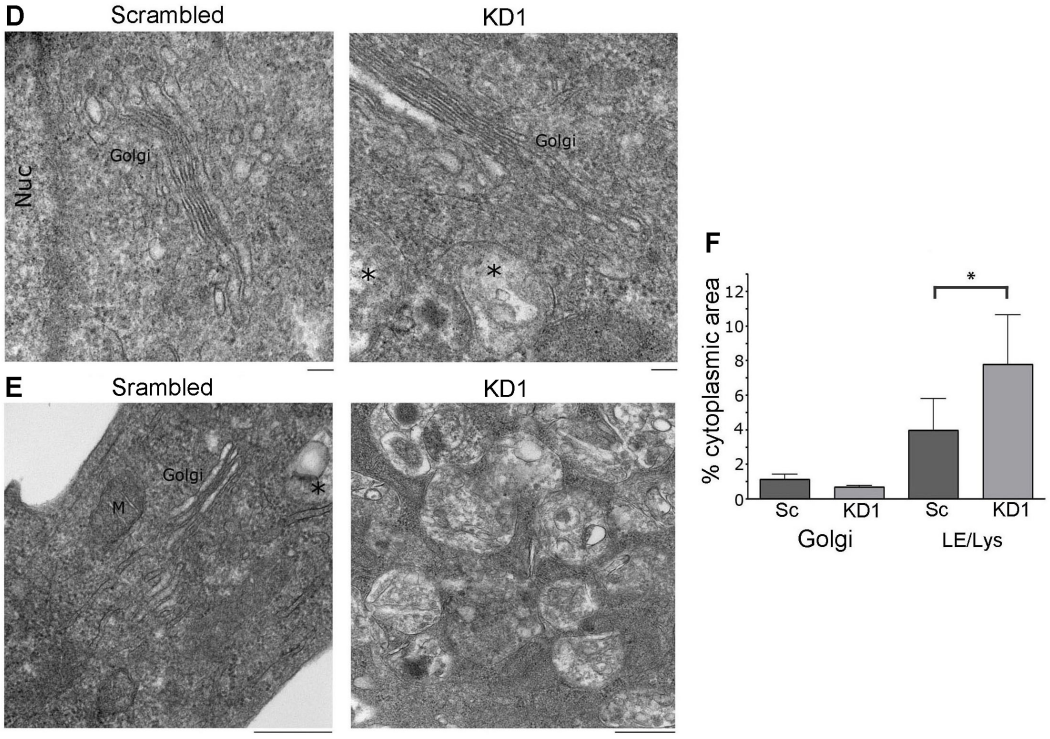

Figure 10. Cortactin-KD cells contain many LE/Lys hybrid organelles and have little perturbation in Golgi structure or volume. Transmission electron microscopy was performed on 50 nm thick cellular sections. (A, D) Representative images of the overall Golgi morphology in SCC61-scrambled and SCC61 cortactin-KD1 cells (A) and HeLa cells (D). Note the increase in LE/Lys and lamellar bodies (LB) within KD cells. NUC = nucleus. Zooms of the Golgi shown below A. An increase in *trans*-Golgi-associated vesicles in KD cells is indicated with a bracket. (B, E) Representative images of the cytoplasmic contents of control and cortactin-knockdown SCC61 (B) and HeLa cells (E). Note the large number of LE/Lys hybrid organelles filling the cytoplasm. LE/Lys and LB are indicated by *, M indicates mitochondria. Scale bar = 500 nm. (C, F) % Cytoplasmic volume occupied by Golgi or LE/Lys was analyzed by point counting stereology of random thin sections and plotted. N = 3 sections, from 2 independent blocks. Mean+/-SE shown. *p<0.05, **p<0.01.

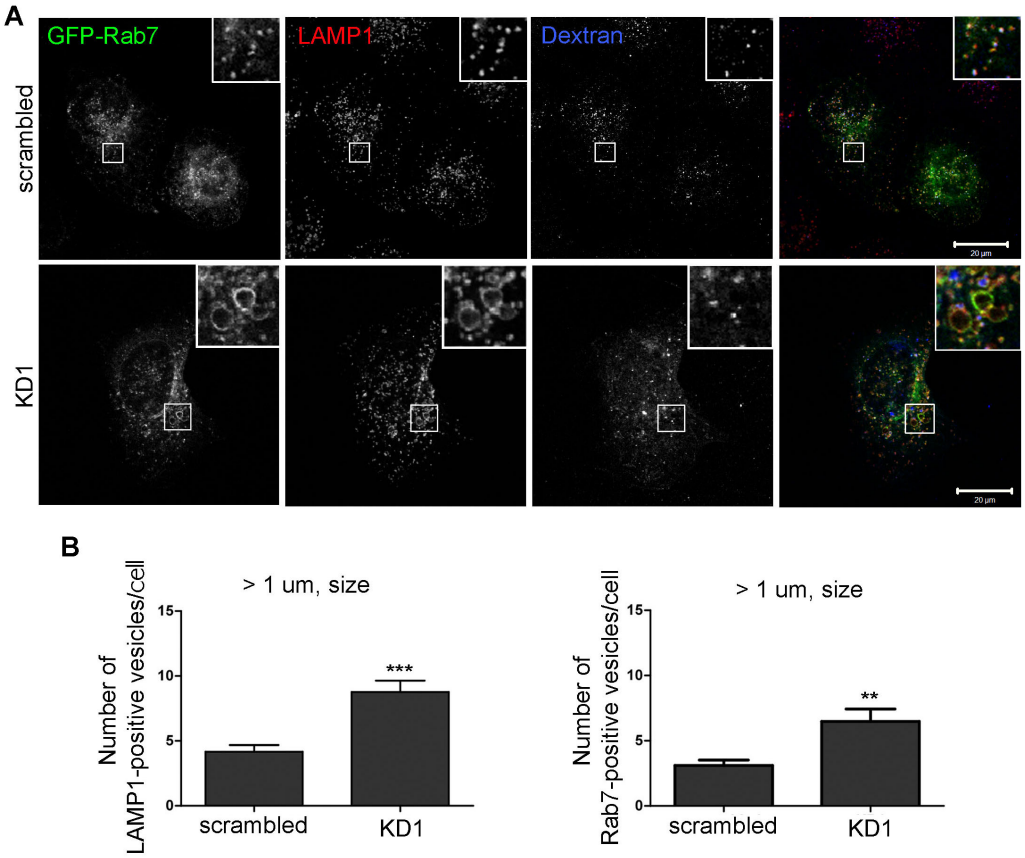

Figure 11. Enlarged hybrid compartments containing late LE/Lys markers are increased in cortactin-KD cells and these compartments are inaccessible to a fluid-phase marker. Control (scrambled) and cortactin-KD (KD1) SCC61 cells were transiently transfected with a GFP-Rab7 construct, then incubated for 15 minutes at 37°C in serum free medium containing 1 mg/ml Alexa Fluor 546-conjugated Dextran 10,000 followed by a 4 hour chase period in medium lacking dextran. Then, cells were fixed and immunostained for LAMP1 to label lysosome. (A) Representative images showing enlarged Rab7 (green) and LAMP1 (red) double positive compartments in KD1 cells. Boxed areas are zoomed to show dextran (blue) at the LE/Lys compartments in control cells (top right) and to show Rab7 and LAMP1 double positive enlarged vesicles that are inaccessible for dextran in KD cells (bottom right). (B) Quantitation of the number of enlarged LAMP1-positive and Rab7-positive vesicles per cell with size > 1 μm. n=20 from 2 independent experiments. Mean +/-SE shown. ** p<0.01, *** p< 0.001. Scale bar = 20 μm.

or trafficking and more minor changes in Golgi size and organization.

Cortactin colocalizes with a subset of late endosomal markers.

Since loss of cortactin did not have a major effect on anterograde trafficking or Golgi ultrastructure, we hypothesized that cortactin may not act directly on the Golgi to regulate its morphology (the major Golgi phenotype that we observed). Instead, the compact Golgi morphology that we observed in cortactin-KD cells might be the consequence of altered retrograde membrane flow back to the Golgi, potentially from LE/Lys. To determine which compartments cortactin is associated with and thus might be regulating, parental SCC61 cells were fixed and immunostained for cortactin and a variety of markers, including Golgi, ER, LE and Lysosomes. Single confocal images were then analyzed for colocalization. Consistent with previous reports, cortactin localizes to the cell periphery as well as to perinuclear puncta (Weed and Parsons, 2001). There was no apparent overlap between cortactin staining and ER (calreticulin), ERGIC (ERGIC53), or *cis/medial*-Golgi (GM130, Mannosidase II) compartments (Figure 12). For the TGN, there was a small amount of cortactin colocalization with GCC185 but not with p230^{trans} (Figure 13 A; and Figure 12, respectively). In addition, we found that cortactin colocalizes with and is adjacent to a subset of Rab7-positive and LAMP1-positive (Figure 13, B and C) vesicles. Since retrograde trafficking to the Golgi from LE/Lys compartments involves docking with GCC185 at the TGN (Derby et al., 2007; Reddy et al., 2006), these colocalization data suggest that cortactin might be involved in LE/Lys-to-Golgi trafficking.

Cortactin regulates localization of mannose-6-phosphate receptor (M6PR).

To directly test whether cortactin promotes LE-to-Golgi trafficking, we analyzed in cortactin-manipulated cells the localization of a canonical marker of that pathway:

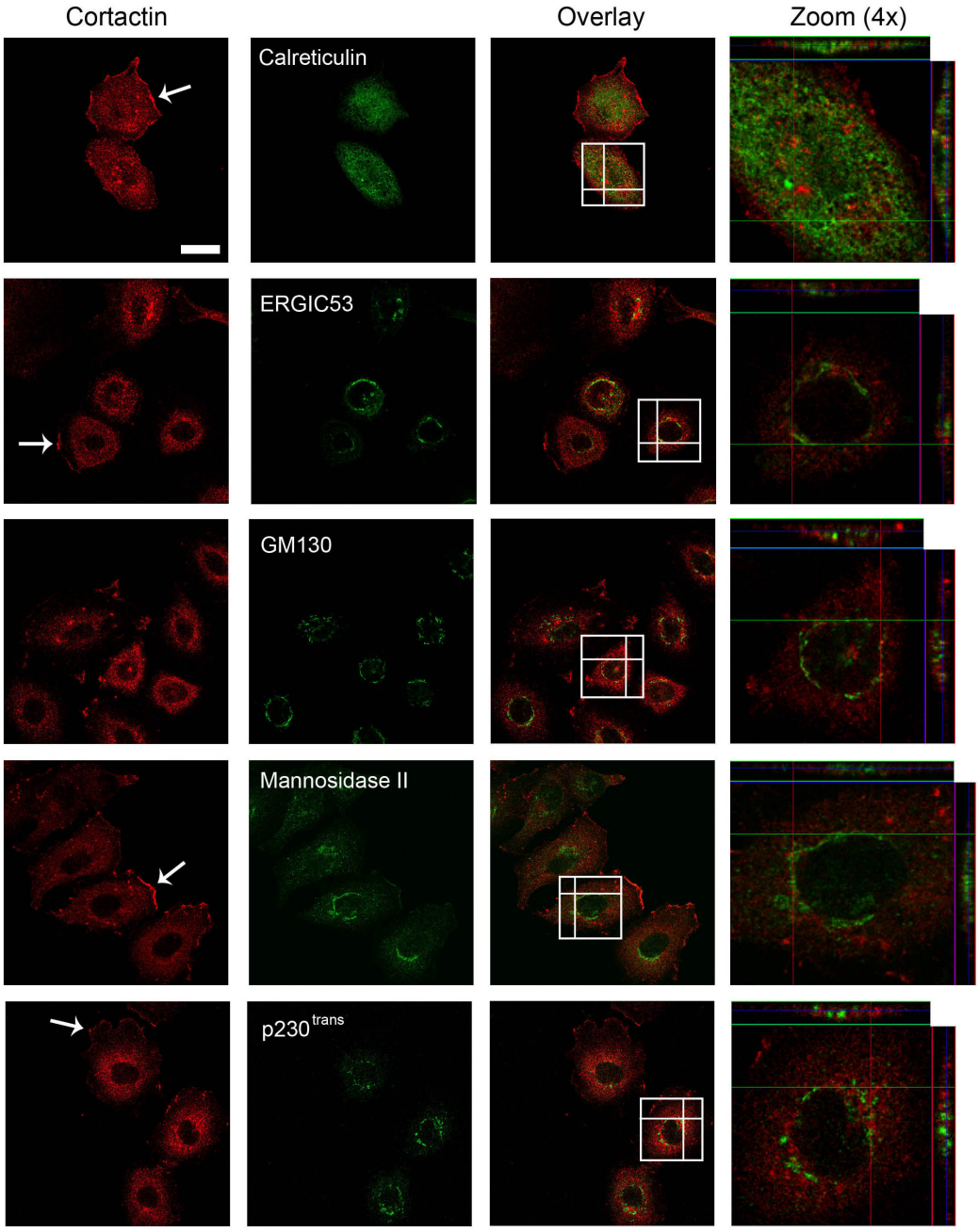

Figure 12. Cortactin does not localize with most ER or Golgi markers. SCC61 parental cells were fixed and stained for both cortactin (left panel, red) and the indicated markers of ER (Calreticulin), ERGIC (ERGIC53) or Golgi (GM130, Mannosidase II, p230^{trans}) (green). Images are overlaid and zoomed at 4x (white boxes indicate zoomed area, far right panel) to show subcellular localization of cortactin and the indicated markers. Z-slices of specific lines through the cell (indicated by the white lines) are shown along the top and right side of the zoomed images. Arrows indicate cortactin staining in lamellipodia. Scale bar = 25 μm.

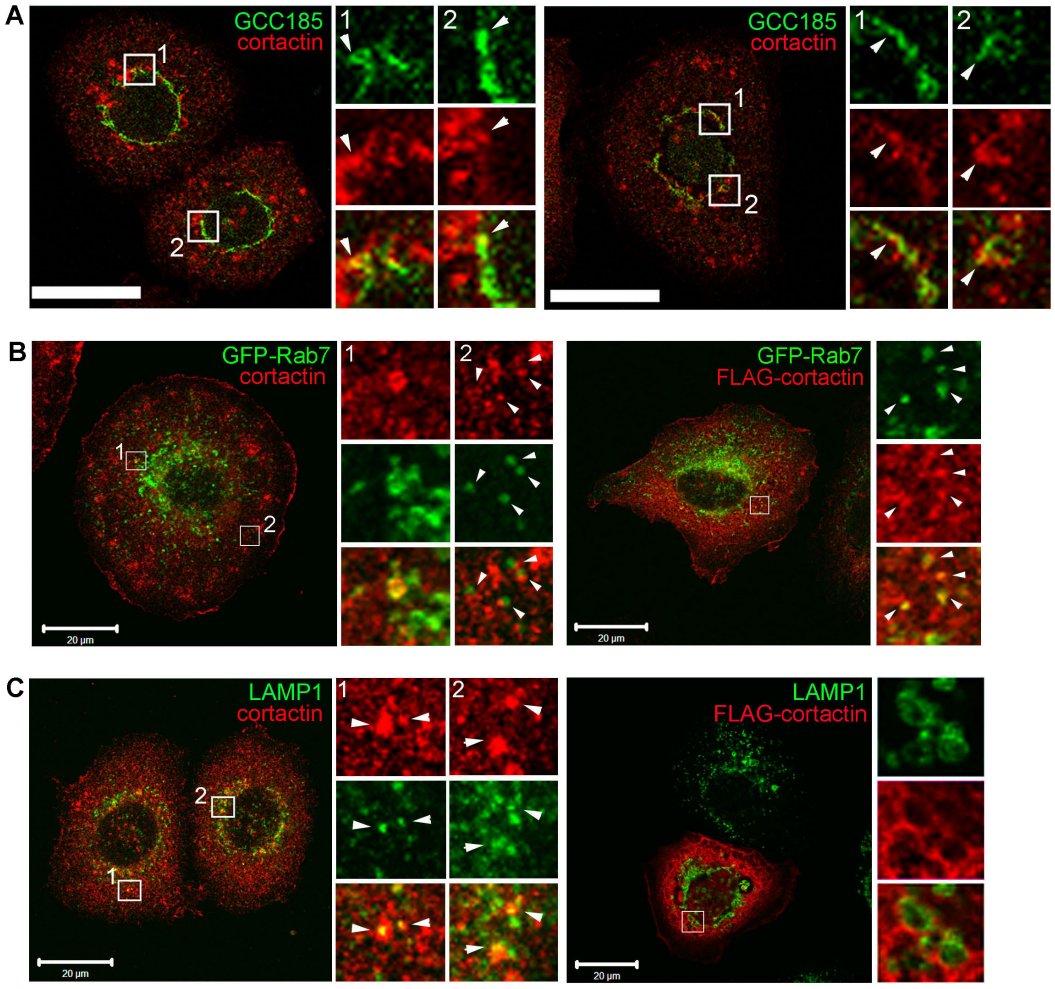

Figure 13. Cortactin colocalizes with a subset of GCC185, Rab7 and LAMP1-positive vesicles. (A) SCC61 parental cells were fixed and stained for cortactin (red) and the TGN marker GCC185 (green). Scale bar = 25 µm. (B, C) Representative images of endogenous (left) or exogenously expressed (Flag-tagged, right) cortactin (red) localization at GFP-Rab7- (B, green) or LAMP1-positive (C, green) late endosomal and lysosomal compartments in parental SCC61 cells. Scale bar = 20 µm. Boxed areas are zoomed to show colocalization (arrowheads) of cortactin with GCC185, Rab7 or LAMP1.

mannose-6-phosphate receptor (M6PR). M6PR molecules are required for transport of lysosomal hydrolases from the TGN and are returned to the TGN from LE (Pfeffer, 2009). Consistent with the hypothesis that cortactin is critical for trafficking from LE to the TGN, there was a significant increase in M6PR localization to LE (marked by Rab7) in cortactin-KD cells compared to control cells (Figure 14). Likewise, M6PR localization to the TGN (marked by Giantin) was significantly reduced in cortactin-KD cells compared to control cells (Figure 14). These data suggest that cortactin plays a role in trafficking of M6PR back to the Golgi from LE/Lys.

Inhibition of LE/Lys maturation leads to a similar compact Golgi morphology as that of cortactin-KD cells

To formally test whether inhibition of LE/Lys maturation and trafficking could affect Golgi morphology, we treated SCC61 cells with siRNA targeting the late endosomal GTPase Rab7. Rab7 is essential for maturation and trafficking from LE (Vanlandingham and Ceresa, 2009; Zhang et al., 2009) and a dominant negative mutant of Rab7 causes the accumulation of M6PR in early endosomes (Press et al., 1998). Similar to the effects of cortactin-KD, Rab7 siRNA transfection led to a compact Golgi morphology in SCC61 cells (Figure 15, A and B). We also tested whether inhibition of LE/Lys maturation with the lysosomotropic agent chloroquine (Blok et al., 1981a; 1981b; Brown et al., 1984; Kokkonen et al., 2004) could affect Golgi morphology. Indeed, 12 h treatment of SCC61 cells with 60 μM chloroquine led to an overall decrease in the Golgi area to cell area ratio measured by GM130 staining (Figure 15 C) that phenocopied the Golgi morphologies of cortactin-KD and Rab7 siRNA-treated cells (Figures 6 and 15 B).

To further test whether LE maturation and trafficking regulates Golgi morphology, we determined the effect of Rab7 transient siRNA treatment in HeLa cells. Whereas stable KD of cortactin in SCC61, HeLa, and MCF10A cells (Figure 6 B) and transient KD

of cortactin in SCC61 cells (Figure 6 C) all cause a compact Golgi morphology by light microscopy, transient cortactin-KD in HeLa cells instead causes an increase in the Golgi area to cell area ratio (Figure 6 C). Thus, we reasoned that a robust test of whether LE maturation and trafficking regulates Golgi morphology would be to determine whether transient KD of Rab7 in HeLa cells mimics the paradoxical increase in Golgi area/cell area seen with transient cortactin-KD. Indeed, transient Rab7-KD in HeLa cells (Figure 15 A) did phenocopy transient cortactin-KD, causing an increase in the Golgi area/cell area ratio and greater distribution of the Golgi around the nucleus by light microscopy (Figure 15 D).

Finally, we also tested the effect of Rab9 siRNA on Golgi morphology. Whereas Rab7 is critical for LE maturation, which is essential for subsequent LE trafficking, Rab9 is critical for retrograde trafficking of M6PR and other cargo from Rab7-positive LE to the Golgi (Pfeffer, 2009; Vanlandingham and Ceresa, 2009). Therefore, we also tested the effect of Rab9 siRNA on Golgi morphology. Interestingly, transient KD of Rab9 in SCC61 cells had no effect on Golgi morphology (Figure 16). In HeLa cells, Rab9 siRNA treatment did lead to an increase in Golgi area/cell area, but the organization of the Golgi was distinct from that of HeLa cells treated with siRNA to Rab7 or cortactin (Figure 16 B compared to Figure 6 C and B). These data suggest that cortactin functions upstream of Rab9-mediated trafficking, at the level of LE maturation similarly or alongside Rab7. Consistent with that model, our EM analysis revealed the presence of many enlarged immature LE/Lys in cortactin-KD cells (Figure 10).

Regulation of cholesterol homeostasis by cortactin is linked to Golgi morphology changes.

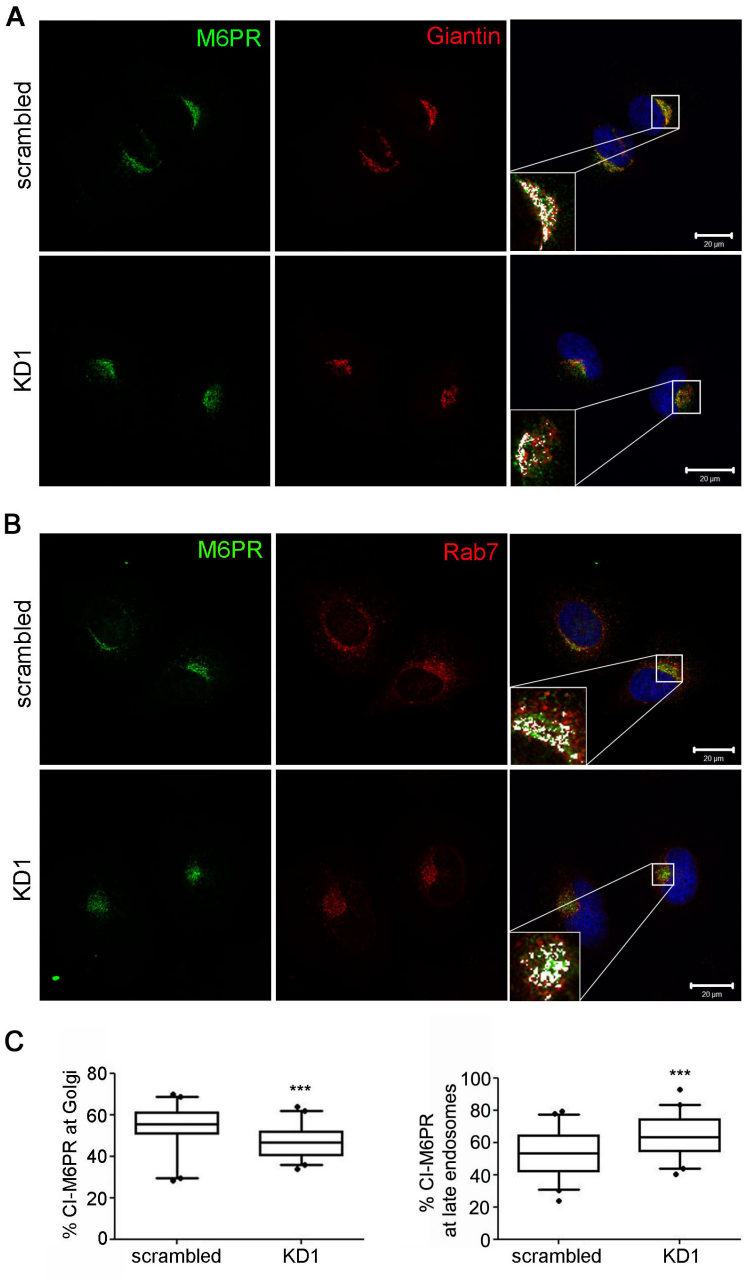

Figure 14. Depletion of cortactin leads to accumulation of Mannose-6-Phosphate Receptor (M6PR) in a late endosomal compartment and depletion from the Golgi. HeLa cells were stained for M6PR (CI-M6PR) and either Golgi marker Giantin (A) or late endosomal marker Rab7 (B). Boxed areas are zoomed to show colocalization of M6PR with Giantin or Rab7. Colocalized single pixels (white) were visualized using colocalization ImageJ plugin. Scale bars = 20 µm. (C) Images were analyzed for % colocalization of M6PR with Giantin or Rab7. n=3; >15 cells per independent experiments. ***p<0.001.

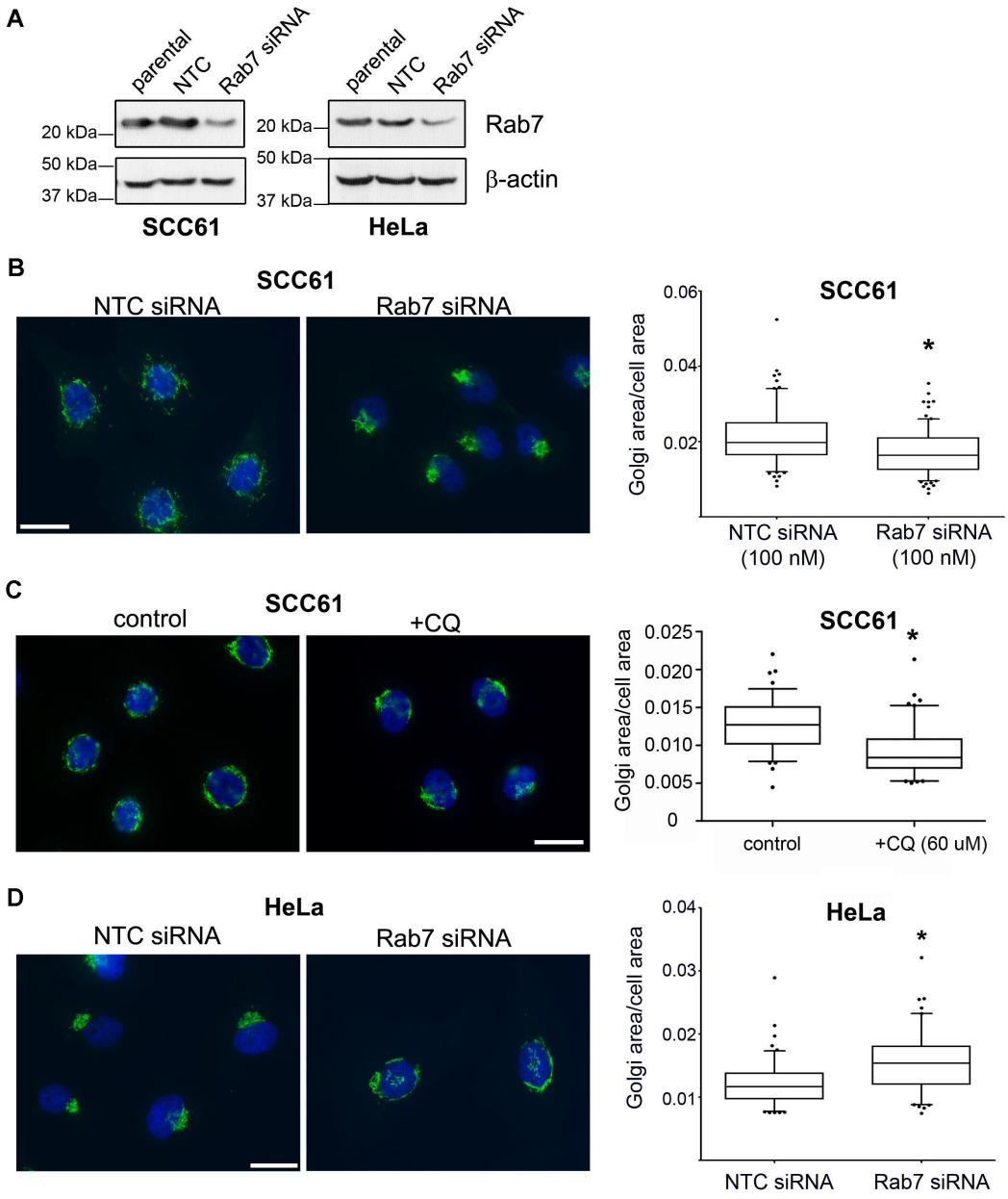

Figure 15. Inhibition of late LE/Lys trafficking leads to a compact Golgi morphology. (A) Representative immunoblot of Rab7 expression levels (top panels) in SCC61 parental cells and those transiently transfected with non-targeting control siRNA (NTC) or Rab7a-specific siRNA, along with a β-actin control. (B) Rab7-KD reduces Golgi size in SCC61 cells. Representative images (green=GM130, blue=Hoechst) and analysis. (C) Chloroquine treatment in SCC61 cells reduces Golgi size. Representative images and analysis of SCC61 parental cells treated with either vehicle (water, "control") or chloroquine (60 μM, "CQ") for 12 hours. (D) Rab7-KD causes an increase in Golgi size in HeLa cells. Representative images and corresponding analysis. Scale bar= 25 μm. n=3, with >30 cells per independent experiment.*p<0.05.

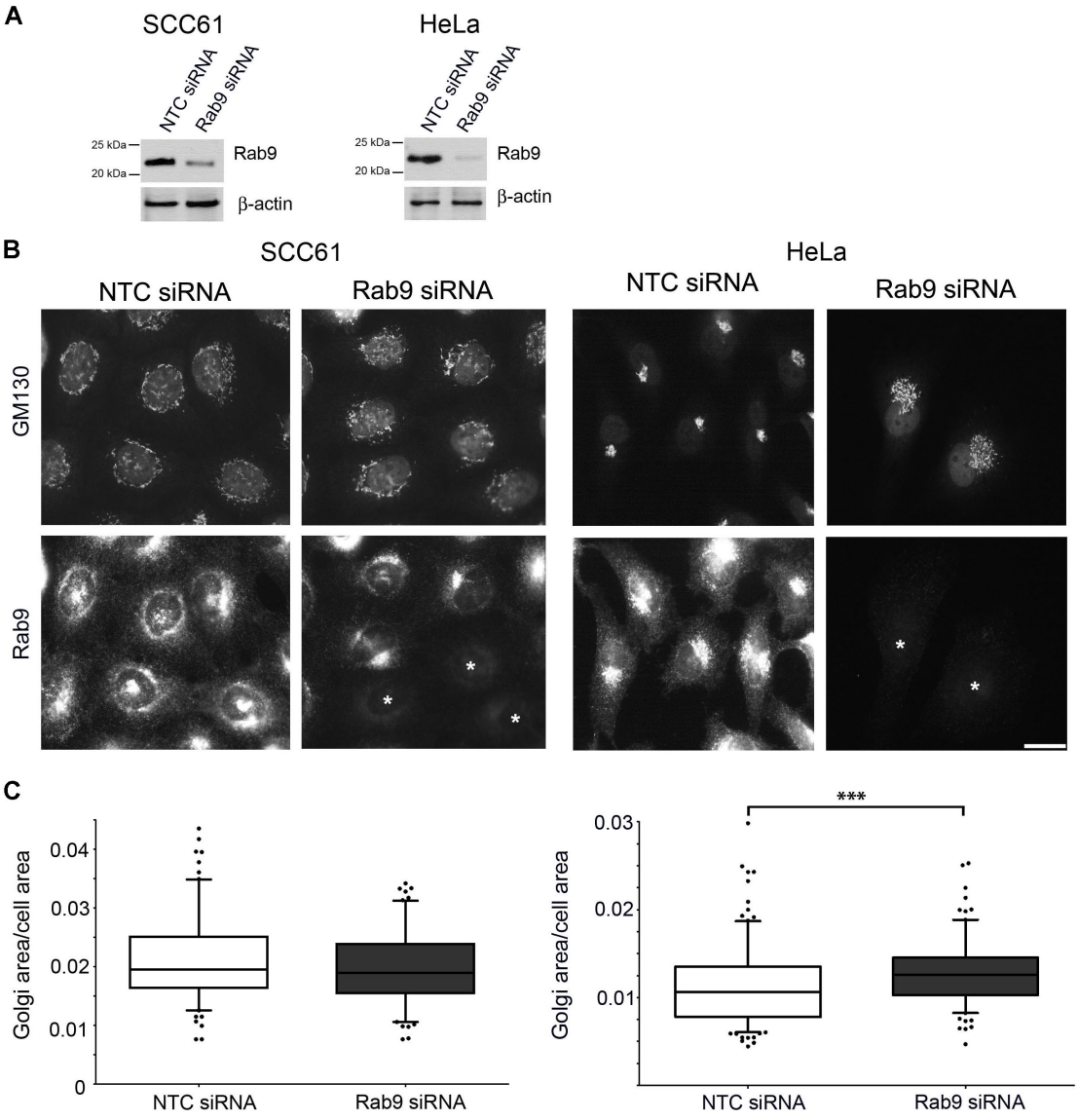

Figure 16. Loss of Rab9 does not phenocopy cortactin-KD. (A) Western blot analysis of Rab9 (top) and b-actin (bottom) from total cell lysates of SCC61 (left) or HeLa (right) cells transfected with the Rab9 siRNA. (B) Representative immunofluorescence images of GM130 staining (top panels) and Rab9 (bottom panels) in transfected cells. Asterisk (*) indicates cells with Rab9 knockdown. (C) Ratio of Golgi area to total cell area including all the data (>130 cells) from 3 independent experiments (>38 cells per independent experiment). Scale bar = 25 μm. ***p<0.001.

A key function of LE is metabolism and trafficking of cholesterol-rich membranes. In lysosomal storage diseases, a buildup of free cholesterol in LE/Lys hybrid organellesbeen shown to affect endosomal dynamics, homeostasis of glycosphingolipids and retrograde trafficking to the Golgi (Choudhury et al., 2002; Ganley and Pfeffer, 2006; Kobayashi et al., 1999). To determine whether cortactin affects cholesterol homeostasis, we stained control and cortactin-KD cells for free cholesterol using filipin. In both cell types, filipin stained intracellular vesicles as well as the plasma membrane (Figure 17). Interestingly, compared with controls, SCC61 cortactin-KD cells contained enlarged and bright intracellular filipin-positive vesicles (arrows, Figure 17 A), suggesting a defect in cholesterol metabolism or trafficking. In HeLa cells, the pattern of filipin staining was altered by cortactin-KD, with increased clustering of the filipin-positive vesicular pattern.

To determine whether the buildup of cholesterol in cortactin-KD cells was connected to the Golgi morphology changes, we performed a rescue experiment in which exogenous cholesterol was removed from the cellular environment. Control and cortactin-KD cells were cultured in media containing lipid-depleted or full serum for 96 h and Golgi area/cell area was analyzed. In control SCC61 and HeLa cells, there was no significant effect on Golgi morphology of culturing in lipid-depleted serum (Figure 17, B and C). By contrast, culturing cortactin-KD cells in lipid-depleted serum led to either a complete (SCC61 KD2, HeLa KD1) or partial (SCC61 KD1) rescue in Golgi morphology, as quantitated by Golgi area/cell area. These data suggest that defective cholesterol homeostasis in cortactin-KD cells is responsible for Golgi morphology changes.

Cortactin binding to the Arp2/3 complex is essential to regulate Golgi morphology.

Cortactin is a well-known regulator of branched actin assembly and also binds a number of membrane trafficking and signaling proteins (Kirkbride et al., 2011). Several

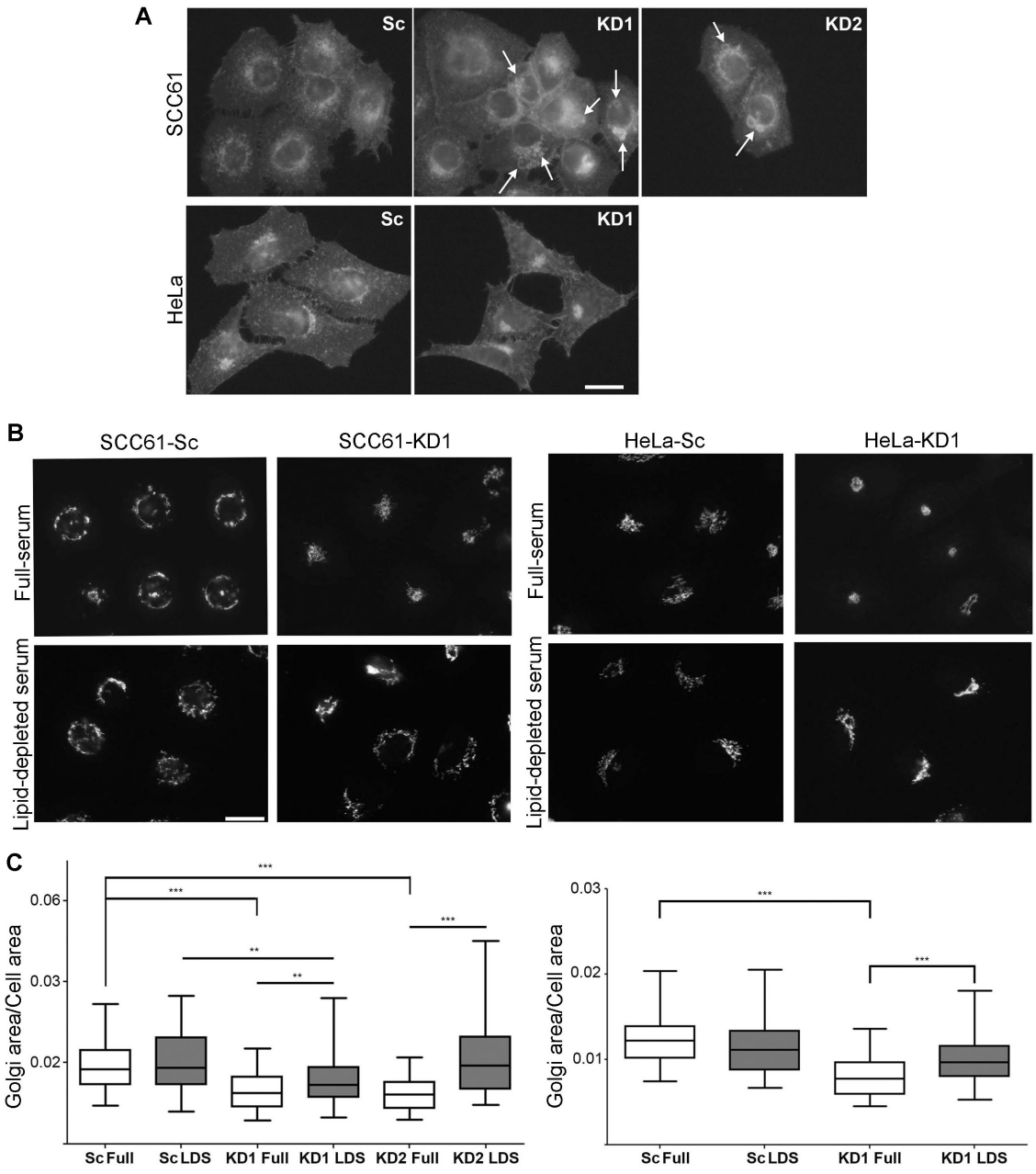

Figure 17. Lipid-depletion rescues Golgi morphology defects in cortactin-KD cells. (A) Representative images of SCC61 (top panels) and HeLa (lower panels) control (Scr) and cortactin-KD (KD1, KD2) cells stained for free cholesterol with filipin. Arrows point to large filipin-positive vacuoles and vesicular compartments. (B) Representative images of GM130 immunofluorescence in cells cultured in full serum (top panels) and lipid-depleted serum (LDS, bottom panels). (C) Ratio of Golgi area to total cell area for SCC61 cells (left) and HeLa cells (right) in full serum or LDS. n = 3, with >22 cells per independent experiment; all data plotted (>85 cells per cell line). Scale bar = 25 μm. **p<0.01; ***p<0.001.

proteins known to interact with cortactin have also been shown to regulate Golgi morphology, including src family kinases , actin and Dynamin-2 (Bard et al., 2003; Valderrama et al., 1998; Weller et al., 2010). Both loss of expression of src family kinases (Bard et al., 2003) and treatment of cells with actin depolymerizing drugs (Valderrama et al., 1998) result in a compact Golgi morphology similar to that seen in cortactin-KD cells. To identify which binding interactions are required for regulation of Golgi morphology by cortactin, we re-expressed shRNA-resistant mouse cortactin constructs with point mutations or small deletions at key binding sites (Bryce et al., 2005; Kinley et al., 2003; Weed et al., 2000) in cortactin-KD SCC61 cells (Figure 18, A and B). Re-expression of either wild-type cortactin or the src phosphorylation (3Y) mutant rescued the knockdown phenotype, with a redistribution of the Golgi around the periphery of the nucleus and an increase in Golgi area/cell area (Figure 18, C and D). In contrast, the Arp2/3-binding (W22A) mutant was unable to rescue the phenotype and retained the compact perinuclear cluster phenotype of cortactin-KD cells (Figure 18, C and D). The SH3 domain (W525K) and actin-binding (Δ4RP) cortactin mutants had intermediate phenotypes that were difficult to classify as either rescued or not. We suspect that there may be a dominant negative effect of these two mutants that leads to a large amount of cell-to-cell variability in terms of both cell and Golgi areas (Figure 18 C). Taken together, these data indicate that cortactin regulates Golgi morphology via interaction with the branched actin nucleator Arp2/3 complex. Although src kinase may indeed be involved generally in regulation of Golgi morphology (Bard et al., 2003; Weller et al., 2010), phosphorylation of cortactin at the canonical src sites does not appear to be essential.

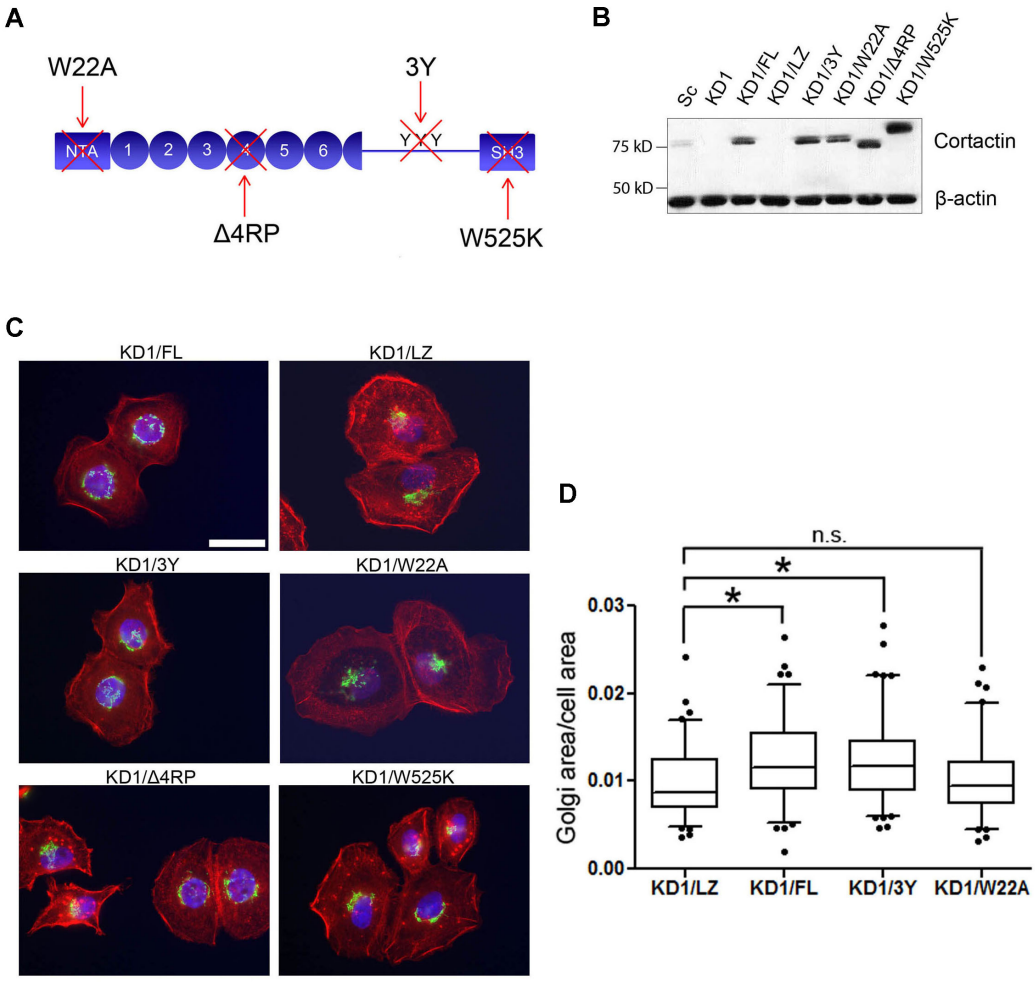

Figure 18. Cortactin binding to the Arp2/3 complex is critical for regulation of Golgi size. (A) Schematic of cortactin with mutant sites indicated: W22A (Arp2/3 binding mutant); 3Y (Src phosphorylation mutant); Δ4RP (F-actin binding mutant); and W525K (SH3 binding mutant). NTA represents the N-terminal acidic domain, YYY represents Src phosphorylation sites, and circles represent cortactin repeat domains. For B-D: FL = wild-type cortactin, LZ = empty vector, Sc = scrambled oligo. Others as indicated in A. (B) Western blot analysis of cortactin mutant expression (top panel) and actin as a loading control (bottom panel) in stable SCC61 cells. (C) Representative widefield images of the Golgi (GM130, green), actin (rhodamine-phalloidin, red) and Hoechst (blue) in the cortactin mutants. (D) Quantitation of Golgi area to cell area ratio from n=3; >20 cells per independent experiment. Scale bar = 25 μm. *p<0.05

Discussion

Cortactin is an actin regulatory protein that has recently been implicated in promoting of secretion of proteases, ECM and growth factors (Clark et al., 2009; 2007; Sung et al., 2011). Since a likely mechanism was control of Golgi-mediated secretion (Cao et al., 2005; Salvarezza et al., 2009), we examined the consequence of cortactin loss on Golgi function and homeostasis. To our surprise, we found that cortactin-KD in two different cell types did not affect the anterograde constitutive transport pathway utilized by VSV-G through the Golgi en route to the PM. Cortactin-KD also had no apparent effect on Brefeldin A-induced Golgi disassembly or reassembly from ER membranes and little effect on the structure of Golgi stacks. Instead, we found that a consistent and major effect of cortactin loss on the Golgi was to alter its light microscopy morphology, most likely by an indirect mechanism involving defective cholesterol trafficking at LE/Lys compartments. Consistent with a block in LE/Lys maturation and/or trafficking, cortactin-KD cells contained enlarged LE/Lys and cholesterol-containing compartments and accumulation of the endosome-to-Golgi retrograde cargo M6PR in LE. Furthermore, removal of cholesterol from the culture media rescued the Golgi morphology defects of cortactin-KD cells. Altogether these data suggest a model in which cortactin regulates LE/Lys cholesterol trafficking, which subsequently impacts Golgi homeostasis.

The phenotype that we noted in cortactin-KD cells, with enlargement of an immature membrane-filled LE/Lys compartment, intracellular accumulation of free cholesterol, and alteration in Golgi homeostasis is reminiscent of that seen in cells with lysosomal storage diseases (Mukherjee and Maxfield, 2004). For example, Niemann-Pick C disease occurs due to a specific defect in cholesterol transport out of LE/Lys that results in defective transport of retrograde cargo to the Golgi, including glycosphingolipids and M6PR (Choudhury et al., 2002; Ganley and Pfeffer, 2006;

Kobayashi et al., 1999). Indeed we find that removal of cholesterol from the endocytic system by culturing cortactin-KD cells in lipoprotein-deficient serum led to a partial rescue of Golgi morphology defects. Interestingly, recent data shows that accumulation of cholesterol occurs in cells with diverse lysosomal storage diseases and leads to accumulation of aberrant assembled SNARE complexes on LE/Lys (Fraldi et al., 2010), which may explain how gross changes in retrograde trafficking (Choudhury et al., 2002; Ganley and Pfeffer, 2006; Kobayashi et al., 1999; Mukherjee and Maxfield, 2004) and Golgi morphology could occur. Since cortactin is an actin regulator that is known to regulate endosomal tubulation and trafficking (Ohashi et al., 2011; Puthenveedu et al., 2010), it seems likely that cholesterol accumulation in cortactin-KD cells occurs secondary to LE/Lys maturation and/or trafficking defects rather than by direct regulation of cholesterol transport. Consistent with that idea, inhibition of LE/Lys maturation with Rab7 siRNA or chloroquine treatment (Huotari and Helenius, 2011; Vanlandingham and Ceresa, 2009; Zhang et al., 2009) led to a similar Golgi morphology change as cortactin-KD. However, it will be important in the future to determine exactly how actin dynamics, regulated by cortactin, controls cholesterol homeostasis and trafficking at LE.

To understand the morphological changes we observed by light microscopy in cortactin-KD cells, we performed point counting morphometry analysis of EM images. Although there was a small change in Golgi volume measured by this method, it was insufficient to fully account for the large changes in Golgi area/cell area that was observed by light microscopy. One possible reason for the discrepancy between the two methods is that light microscopy is detecting primarily changes in Golgi distribution (spread out versus compact). Since EM has higher resolution, it is a more accurate method for determining volume than light microscopy (Quinn et al., 1983; Weibel, 1979). Another possibility, which is not mutually exclusive, is that some of the Golgi marker staining is actually labeling the LE/Lys compartment because membrane flow is

altered. Indeed, a compartment that includes both Golgi and LE/Lys components was first identified as the 'GERL' (Golgi–ER–lysosomal compartment) described by Alex Novikoff in 1964 (Novikoff et al., 1964) and may become expanded in certain situations, such as neuronal storage diseases (Vitry et al., 2010) and Ras-transformation (Narita et al., 2011). Additional future studies are required to distinguish between these two possibilities; however our data indicate that either way LE/Lys dysfunction is responsible for the light microscopy Golgi morphology changes.

Molecules that directly regulate the actin cytoskeleton have been previously shown to significantly affect Golgi morphology. In particular, studies by several different groups have shown that treatment with toxins that affect actin dynamics/stability or siRNA-mediated KD of actin-associated proteins leads to compaction of the Golgi in a similar manner to that described here in cortactin-KD and Rab7-KD cells (di Campli et al., 1999; Dippold et al., 2009; Egea et al., 2006; Lázaro-Diéguez et al., 2006; Valderrama et al., 1998). While it is certainly likely that some of the reported phenotypes are due to direct regulation of Golgi actin, we speculate that in some cases the common "compacted" morphology may be a secondary consequence of disturbed lipid trafficking secondary to LE/Lys maturation defects. The cortactin-KD phenotype depended on interactions with Arp2/3 complex, suggesting that regulation of branched actin networks is critical. Interestingly, both the Arp2/3 complex and actin filaments have been shown to regulate late endosomal size, shape and maturation (Duleh and Welch, 2010; Hölttä-Vuori et al., 2005), all phenotypes that are consistent with the expansion of LE/Lys in cortactin-KD cells and the reported role of cortactin in autophagosome-lysosome fusion (Lee et al., 2010). Such alterations in late endosome maturation would necessarily affect trafficking to other sites, including the Golgi. Indeed, Rab7-KD is known to block late endosomal maturation and trafficking (Vanlandingham and Ceresa, 2009) and in this study phenocopied the effect of cortactin-KD on Golgi morphology. Based on our data,

we speculate that LE/Lys maturation and trafficking may be particularly sensitive to actin dynamics.

An unexpected finding of this study was that cortactin did not affect trafficking of VSV-G to the PM or, in our system, colocalize with most Golgi markers. Interestingly, the one TGN marker for which we did observe cortactin colocalization is GCC185, a Golgin tether that binds M6PR-containing vesicles returning from late endosomes (Derby et al., 2007; Reddy et al., 2006). Our VSV-G transport data were unexpected since two previous studies found that expression of a dominant mutant of cortactin that lacks 50 amino acids of the SH3 domain leads to a block in the exit of VSV-G (Cao et al. 2005) or p75-GFP cargo (Salvarezza et al., 2009) from the TGN. Expression of the same mutant also led to bloated TGN cisternae, consistent with a Golgi exit block (Cao et al., 2005; Salvarezza et al., 2009). By contrast, despite a >95% knockdown of cortactin levels in stable HeLa and SCC61 cells, we observed no difference in the rate of VSV-G arrival at the PM and Golgi ultrastructure was relatively normal (Figure 10), albeit with some accumulation of vesicles at the cis- and trans-Golgi. Our data suggest that in the absence of cortactin, molecular trafficking components regulating anterograde bulk transport remain functional. The most probable explanation for the difference in our findings from those of previous studies is the use of dominant negative mutants versus knockdown of endogenous proteins. We speculate that the dominant-negative cortactin mutant decreases TGN exit by either sequestering critical factors (such as Arp2/3 complex or Src kinase) or masking Golgi-associated branched actin networks that function as recruitment platforms for Dynamin-2 or other critical proteins (Cao et al., 2005; Salvarezza et al., 2009). Additionally, it is certainly possible that cortactin regulates the transport of other cargo from the Golgi, similar to the cargo sorting role reported for cofilin (Blume et al., 2009). Finally, it is possible that cortactin functions at the Golgi are redundant with another similar protein, such as mAbp1 that can link actin

filaments to dynamins (Kessels et al., 2001; Onabajo et al., 2008) and is recruited to dynamic actin at the Golgi (Fucini et al., 2002; Xu and Stamnes, 2006). Indeed, the fact that we found little colocalization of cortactin with any Golgi marker in our squamous carcinoma (SCC61, HeLa) and basal mammary epithelial (MCF10A) cells suggests that other actin-binding proteins may be utilized for recruitment of the fission machinery to the Golgi. Further studies will be required to distinguish between these possibilities.

Cortactin is a prominent Src kinase substrate and is frequently involved in Src-regulated cellular processes (Kirkbride et al., 2011; Wu et al., 1991). Similar to cortactin-KD cells, fibroblasts lacking the src family kinases Src, Yes, and Fyn exhibit a compact Golgi morphology (Bard et al., 2003). Likewise, expression of a constitutively active Src kinase was recently shown to lead to Golgi fragmentation (Weller et al., 2010). Therefore, we were surprised that a cortactin mutant that cannot be phosphorylated by Src kinase (Kinley et al., 2003) fully rescued the Golgi morphology defect of cortactin-KD cells. One possibility is that both proteins still act in concert but that Src phosphorylation of cortactin is not necessary for cortactin regulation of Golgi morphology (Martinez-Quiles et al., 2004). Consistent with that possibility, a large pool of Src kinase is associated with late endosomes (Sandilands and Frame, 2008) and may regulate movement and distribution of lysosomes (Nakayama et al., 1994; Vincent et al., 2007). Alternatively, Src kinase may directly regulate intra-Golgi and Golgi-to-ER trafficking (Bard et al., 2003; Pulvirenti et al., 2008).

Cortactin is well-studied as a regulator of cancer aggressiveness and invasiveness (Kirkbride et al., 2011). One particular focus of the field has been the role of cortactin as a regulator of invadopodia, specialized actin-rich structures with associated extracellular matrix (ECM)-degrading activity (Weaver, 2006). Our interest in the role of cortactin in exocytosis stemmed from our finding that cortactin is essential for secretion of the invadopodia-localized proteinases, MMP2, MMP9, and MT1-MMP (Clark

and Weaver, 2008; Clark et al., 2009; 2007). Thus, it was initially surprising that cortactin is not an essential regulator of Golgi exit, at least not for VSV-G. However, MT1-MMP trafficking to invadopodia was recently shown to depend on the LE/Lys SNARE VAMP7 (Steffen et al., 2008). In addition, both MT1-MMP and MMP9 have been localized to a LE/Lys compartment (Sbai et al., 2010; Steffen et al., 2008). Furthermore, we recently found that the extracellular matrix component fibronectin (FN) can be endocytosed and resecreted from a LE/Lys compartment to promote cell motility, dependent on cortactin (Sung et al., 2011). Therefore, it seems likely that regulation of LE/Lys trafficking is a major function of cortactin that is important not only for Golgi homeostasis but also for cellular motility and invasiveness.

Acknowledgements

Thanks to Paul Miller, Irina Kaverina, and members of the Weaver laboratory for advice. Funding was provided by NIH grants 1R01GM075126, 1R21DE018244 and ACS grant RSG-118085 to A.M.W., the Vanderbilt International Scholars Award Program (N-H.H.), training grants 5T32 CA009592-23 (K.C.K.) and 1F31DE021619 (L.C.L.). EM image acquisition and analysis at Vanderbilt utilized the VUMC Cell Imaging Shared Resource (supported by NIH grants CA68485, DK20593, DK58404, HD15052, DK59637 and EY08126) and was supported in part by UL1 RR024975 from NCRR/NIH.

CHAPTER IV

PI(3,5)P_2 CONTROLS BRANCHED ACTIN DYNAMICS AT LATE ENDOSOMES BY REGULATING CORTACTIN-ACTIN INTERACTIONS

Introduction

Dynamic branched actin assembly occurs at cellular membranes and is nucleated by the Arp2/3 complex upon activation by a member of the Wiskott-Aldrich Syndrome protein (WASP) family (Goley and Welch, 2006). Diverse WASP family members are recruited to distinct membranes in the cell by membrane-associated signaling complexes that function both as localization and activation factors. A contributing factor to dynamic actin assembly is the molecule cortactin that localizes to all sites of branched actin assembly and both promotes WASP-induced actin polymerization and stabilizes actin branches after their formation (Goley and Welch, 2006; Uruno et al., 2001; Weaver et al., 2001; 2002). Most branched actin assemblies have lifetimes in the seconds-minutes scale and are much more dynamic than other forms of actin in the cell (Lai et al., 2008; Puthenveedu et al., 2010). The dynamic nature of branched actin is likely critical for its functions in controlling dynamic protrusions and other membrane-based events.

Increasing evidence indicates that actin plays an important role in post-internalization events along the endocytic pathway, including endosomal tubulation, vesicle fusion and fission, and endosome motility (Derivery et al., 2009; Duleh and Welch, 2010; Monteiro et al., 2013; Ohashi et al., 2011; Puthenveedu et al., 2010; Tanabe et al., 2011). Consistent with its integral role in Arp2/3 complex-mediated branched actin assembly, cortactin has been shown to regulate many of these processes. Our previous studies showed that cortactin controls late

endosomal/lysosomal (LE/Lys) maturation and subsequent retrograde transport to the Golgi apparatus (Kirkbride et al., 2012). In addition, cortactin was also shown to regulate dynamic actin assembly on endosomes in coordination with Arp2/3 complex and Wiskott-Aldrich syndrome protein and Scar homologue (WASH) that is required for cargo sorting (Monteiro et al., 2013; Ohashi et al., 2011; Puthenveedu et al., 2010). Furthermore, it was reported that cortactin is essential for actin-mediated fusion of autophagosomes with lysosomes (Lee et al., 2010). Taken together, these data indicate that cortactin is a key regulator of actin-dependent endosomal processes. However, how cortactin itself is controlled on endosomes is poorly understood.

Phosphoinositides (PIs) are membrane phospholipids that are generated in small amounts at specific cellular membranes by distinct PI kinases. PIs decorate a given organelle with molecular identity and recruit specific effector proteins to confer a distinct set of functions (Behnia and Munro, 2005; Di Paolo and De Camilli, 2006; Kutateladze, 2010), including regulation of the actin cytoskeleton (Janmey and Lindberg, 2004; Saarikangas et al., 2010). Among different PIs, $PI(4,5)P_2$ is the best-characterized regulator of actin organization. $PI(4,5)P_2$ binding to N-WASP is a key step in N-WASP activation by inducing a conformational change that releases the Arp2/3-binding VCA domain (Papayannopoulos et al., 2005; Rohatgi et al., 2000). $PI(4,5)P_2$ also controls actin filament severing, capping, crosslinking and actin-membrane binding interactions, through interactions with actin-binding proteins such as cofilin, gelsolin, capZ, filamin, alpha-actinin, vinculin, and talin (Janmey and Lindberg, 2004; Yin and Janmey, 2003). In addition, $PI(3,4,5)P_3$ regulates activation of the WASP family member WAVE2 to control lamellipodial protrusion (Suetsugu et al., 2006). However, since $PI(4,5)P_2$ and $PI(3,4,5)P_3$ primarily mark the plasma membrane, the role of PIs in controlling actin dynamics at other membrane compartments is less well understood.

$PI(3,5)P_2$ is a low-abundance PI that mainly localizes to late endosomes and lysosomes in higher eukaryotes (Ikonomov et al., 2006; Michell et al., 2006) and in the yeast vacuole (Rudge et al., 2004). $PI(3,5)P_2$ directs trafficking of cargo vesicles along the endosome-lysosome axis, and governs a plethora of associated cellular functions including endolysosome morphology, acidification, autophagy, stress-induced signaling and ion channel activity (de Lartigue et al., 2009; Dove et al., 2009; Shisheva, 2008; Yin and Janmey, 2003). Defects in the regulation of $PI(3,5)P_2$ are linked to several human diseases including Charcot-Marie-Tooth Type 4 and Amyotrophic Lateral Sclerosis, which are thought to be caused by defective autophagy (Bolino et al., 2000; Chow et al., 2007; Ferguson et al., 2009; Kotoulas et al., 2011; Otomo et al., 2012). Despite the well-characterized roles of $PI(3,5)P_2$ in endolysosomal trafficking and disease, few molecular effector proteins of $PI(3,5)P_2$ have been identified.

In this study, we report and characterize a novel and direct binding interaction of cortactin with $PI(3,5)P_2$. We show that purified cortactin interacts with $PI(3,5)P_2$ through its filamentous actin (F-actin) binding domain. Furthermore, $PI(3,5)P_2$ competes with F-actin for binding to cortactin, leading to inhibition of cortactin-mediated branched actin nucleation and stabilization. Inhibition of $PI(3,5)P_2$ synthesis in cells resulted in actin stabilization on late endosomes which is abolished by cortactin depletion. Based on these findings, we propose a model in which $PI(3,5)P_2$ removes cortactin from nascent membrane-associated actin, limiting overall assembly of branched actin at late endosomes. Cycles of conversion between PI(3)P and $PI(3,5)P_2$ may allow fast actin dynamics on endosomal membranes and consequent membrane trafficking events.

Results

Cortactin directly binds to PI(3,5)P_2

Cortactin regulates branched actin assembly at cellular membranes throughout the cell. Since cortactin has a putative PI binding site in its N-terminus (He et al., 1998), we hypothesized that PIs might regulate its recruitment or activity at specific membrane sites. To test this hypothesis and identify candidate PI binding partners, we performed a lipid overlay assay with glutathione S-transferase (GST)-tagged full-length cortactin. GST-fusion proteins (Figure 19 A, Coomassie staining) were incubated with phospholipids immobilized on a nitrocellulose membrane (PIP strip). Full-length cortactin interacted most strongly with PI(3,5)P_2 (Figure 19 B), and to a lesser extent with PI(3)P, PI(4)P, PI(5)P, and PI(3,4)P_2. Hrs-FYVE and PLC-PH lipid binding domains were used as respective positive controls for PI(3)P and PI(4,5)P_2 binding.

PI(3,5)P_2 is found with highest abundance on late endosomes (Di Paolo and De Camilli, 2006; Michell et al., 2006) where cortactin also has been shown to localize (Kirkbride et al., 2012; Rossé et al., 2014b; Sung et al., 2011). To further validate the interaction and determine whether cortactin interacts directly with PI(3,5)P_2 in more physiologically relevant conditions, we performed a liposome pull-down assay. Commercial PolyPIPosome liposomes containing 5% PI (PI(3,5)P_2, PI(3)P, or PI(5)P) and 1% biotin-phosphatidylethanolamine in a mixture of phosphatidylcholine and phosphatidylethanolamine were incubated with GST-cortactin and then isolated with streptavidin-coated magnetic beads. GST alone and the PI(3)P-binding protein GST-2xFYVE were used as respective negative and positive controls. Western blot analysis of the pull-downs revealed that full-length cortactin specifically co-sediments with liposomes containing PI(3,5)P_2, but not with PI(3)P or PI(5)P (Figure 19, C and D). Analysis of binding isotherms with varying lipid input revealed an apparent equilibrium

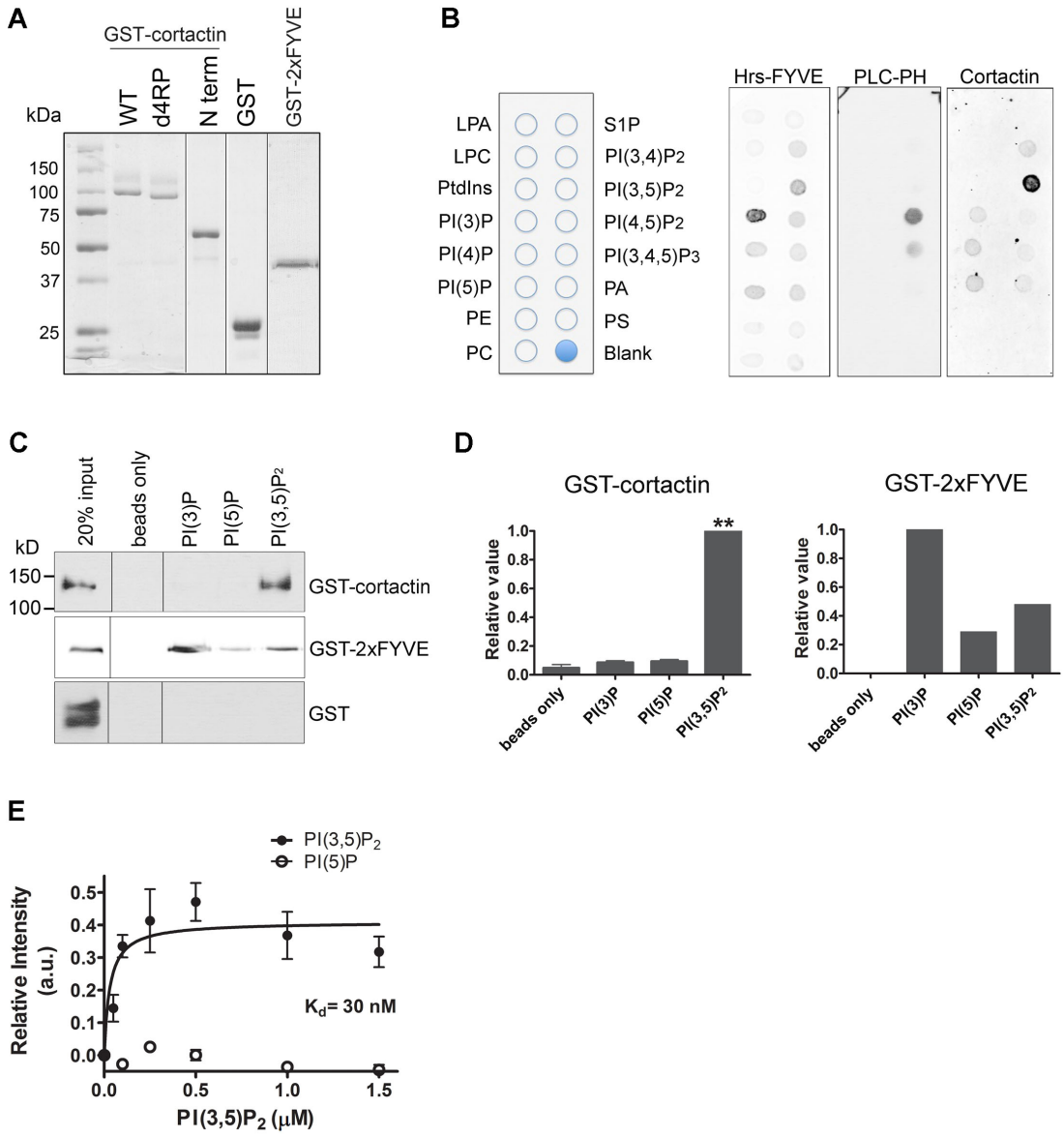

Figure 19. Figure legend on next page.

Figure 19. Cortactin directly interacts with PI(3,5)P_2. (A) Coomassie stained gels of purified GST-tagged proteins. (B)The affinity of the full-length cortactin was examined using a protein-lipid overlay assay. The left panel indicates the identity of lipid species on the PIP strip. Cortactin binds most strongly to PI(3,5)P_2. Binding of the FYVE domain of Hrs and PH domain of PLC-δ1 to PI(3)P and PI(4,5)P_2, respectively, served as positive controls. (C) Pull-down of GST-tagged cortactin by liposomes bearing the indicated PIPs. GST-2x-FYVE, and GST alone is also shown as a positive and negative control. Western blots were probed with anti-GST antibody. (D) The relative binding of the GST-fusion proteins to liposomes containing different PIPs was quantified by densitometric analysis of the GST immunoblots from three independent experiments, except for positive control GST-FYVE that was tested once for pulldown by PI(3)P. Mean+/-SE plotted. **P<0.01* (E) Cortactin binding to liposomes containing PI(3,5)P_2 or PI(5)P as a function of lipid concentration. 70 nM cortactin was incubated with various concentrations of biotinylated liposomes composed of 5% PIP lipids before isolation with streptavidin-beads. Western blots of bound complexes were probed with anti-GST antibody and relative intensity are plotted as a function of PIP concentration. Data points in the PI(3,5)P_2 and negative control PI(5)P binding curves represent means calculated from data points of five and two different experiments, respectively. The K_d for cortactin-PI(3,5)P_2 interaction obtained from nonlinear regression of the data is 30 nM.

dissociation constant (K_d) of 30 nM for cortactin-PI(3,5)P_2 interactions (Figure 19 E). Taken together, these results indicate that cortactin directly and specifically binds to PI(3,5)P_2.

Inhibition of PI(3,5)P_2 synthesis leads to accumulation of cortactin on late endosomes

The enzyme complex that synthesizes PI(3,5)P_2 localizes to both early and late endosomes and consists of the scaffold protein Vac14, the lipid kinase PIKfyve (which converts PI(3)P to PI(3,5)P_2), and the counteracting lipid phosphatase Fig4 (Ikonomov et al., 2006; Nicot et al., 2006; Rudge et al., 2004; Rusten et al., 2006; Rutherford et al., 2006). To determine whether cortactin and PI(3,5)P_2 are likely to be present in the same compartment, we immunolocalized cortactin with the scaffold protein Vac14. This localization method was chosen due to lack of available antibodies that directly recognize PI(3,5)P_2. Immunostaining of SCC61 and HeLa cells transiently expressing hVac14-EGFP (Jin et al., 2008) with antibodies against cortactin revealed that cortactin is indeed present on Vac14-positive vesicular structures (Figure 20 A).

A central function of PIs on membranes is recruitment of cytosolic proteins, including cytoskeletal proteins (Janmey and Lindberg, 2004). To investigate whether PI(3,5)P_2 recruits cortactin to endosomes, we prevented cellular PI(3,5)P_2 synthesis by knocking down PIKfyve expression with siRNA in MDA-MB-231 cancer cells (Figure 20 B). Consistent with previous reports, inhibition of PIKfyve led to enlargement of late endosomes marked by Rab7 (Figure 20 C) (Nicot et al., 2006). Surprisingly, silencing of PIKfyve led to a marked increase in cortactin localization to Rab7-positive late endosomes rather than the expected decrease (Figure 20, C and D). Likewise, treatment of MDA-MB-231 or SCC61 cells with the specific PIKfyve inhibitor drug YM201636 (de Lartigue et al., 2009; Ikonomov et al., 2006; Jefferies et al., 2008),

phenocopied the effect of PIKfyve siRNA (Figure 21 A and C; Figure 22 A and B; and Video 1). Immunofluorescence of YM201636-treated cells using early (EEA1) and late endosomal (Rab7) markers confirmed that the majority of the enlarged vesicular compartments were Rab7-positive only with some endosomes positive for both EEA1 and Rab7, reflecting perturbation in late endosomal maturation and trafficking (Figure 22 C) (Rutherford et al., 2006). These data indicate that $PI(3,5)P_2$ does not function to recruit cortactin to late endosomes but may instead regulate its activity by removing it from the late endosome.

Inhibition of $PI(3,5)P_2$ synthesis leads to cortactin-dependent actin accumulation on Rab7-positive endosomes

Cortactin has a unique role as a regulator of Arp2/3 complex by promoting both assembly and stability of branched actin networks (Uruno et al., 2001; Weaver et al., 2001). Along with cortactin, inhibition of $PI(3,5)P_2$ synthesis by MDA-MB-231 and SCC61 cells with YM201636 or knockdown of PIKfyve caused a striking enrichment of actin on Rab7-positive endosomes (Figure 20 C; and Figure 21 A). Quantitative analysis of the imaging data demonstrated that actin intensity and the number of actin dots on Rab7-positive endosomes were significantly increased in YM201636-treated cells (Figure 21, E and F). Colocalization of actin with Rab7 was also increased in YM201636-treated and PIKfyve-KD cells (Figure 20 D, right; also Figures 21 D and 22 B, right: compare YM201636 and DMSO treatments in control cells;). The drug-induced accumulation of actin on late endosomes was reversed in cortactin-knockdown cells (Figure 21 D and Figure 22 B, right). These data indicate that $PI(3,5)P_2$ synthesis on late endosomes attenuates actin accumulation. Furthermore, in the absence of $PI(3,5)P_2$, actin accumulates in a cortactin-dependent manner.

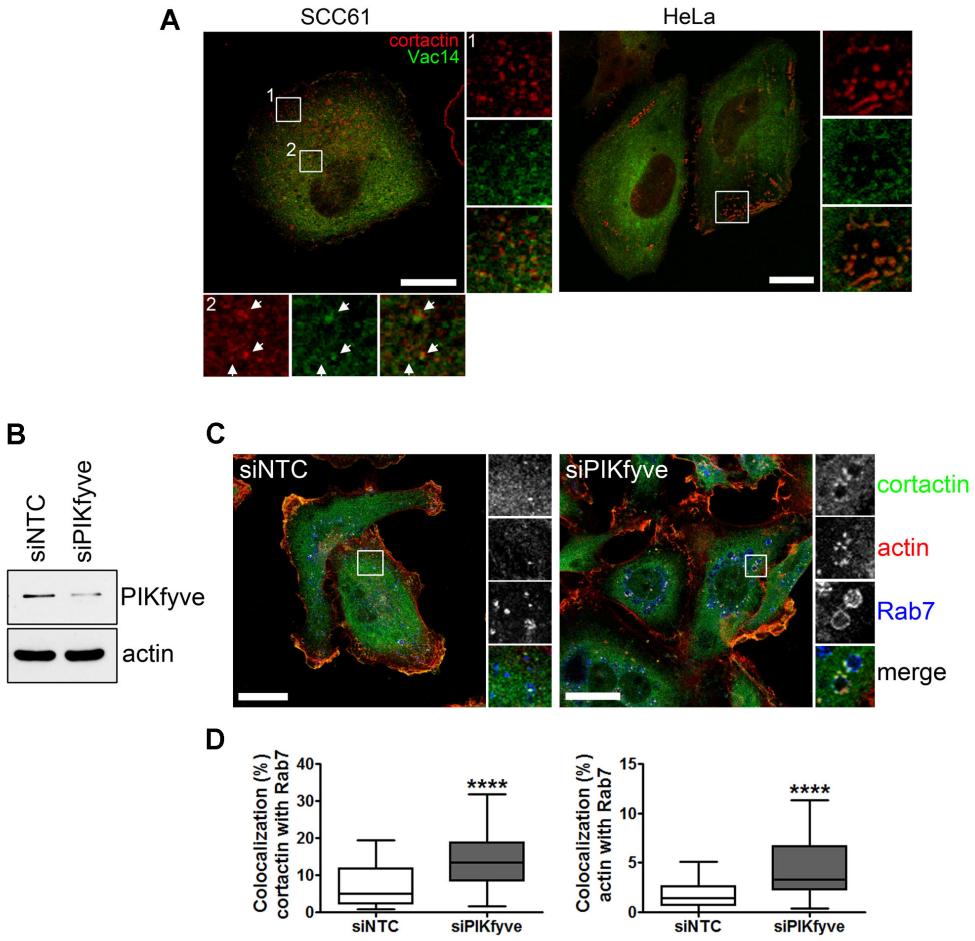

Figure 20. Knockdown of PIKfyve expression leads to accumulation of cortactin and actin at LE membranes. (A) Representative images of endogenous cortactin (red) localized at discrete subdomains of hVac14-EGFP (green)-positive vesicular structures in SCC61 (left) and HeLa (right) cells. Scale bars indicate 20 μm. Representative images of 3 independent experiments for each cell line. (B) Immunoblot of PIKfyve expression in transient knockdown MDA-MB-231 cells. NTC indicates non-targeting control. (C) siRNA against PIKfyve treated cells were processed for immunofluorescence using antibodies recognizing cortactin (green), actin (red), and Rab7 (blue). Scale bars = 20 μm. (D) Quantification of % colocalization of cortactin or actin with Rab7. 3 independent experiments, n≥ 61 cells in each condition. **** *P<0.0001*.

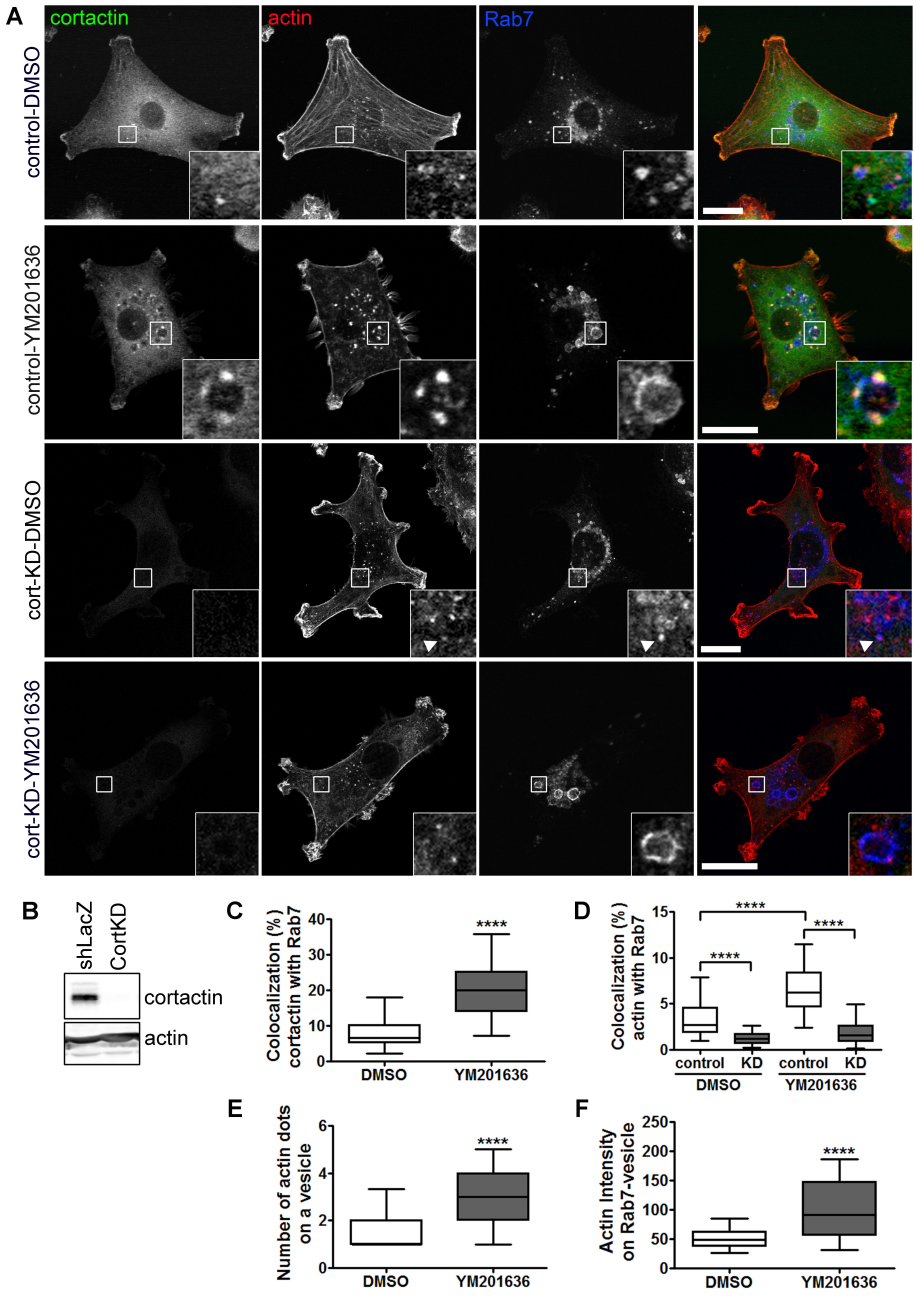

Figure 21. Inhibition of PI(3,5)P_2 production leads to accumulation of cortactin and actin at LE membranes. (A) Representative images showing cortactin (green) and actin (red) localization on Rab7-positive endosomes (blue) after 2 h treatment with 800 nM YM201636 or DMS0 diluent control in control and cortactin-KD MDA-MB-231 cells. Scale bars = 20 μm. (B) Immunoblot of cortactin expression and beta-actin loading control in MDA-MB-231 cells. (C, D) Images were analyzed for % colocalization of cortactin or actin with Rab7, and average number and intensity of actin dots on Rab7-positive endosomes. Three independent experiemnts, n≥ 55 cells in each condition. (E, F) The average number and intensity of actin dots on Rab7-positive endosomes were analyzed. Total > 170 vesicles from 12-19 cells were analyzed. **** *P<0.0001.*

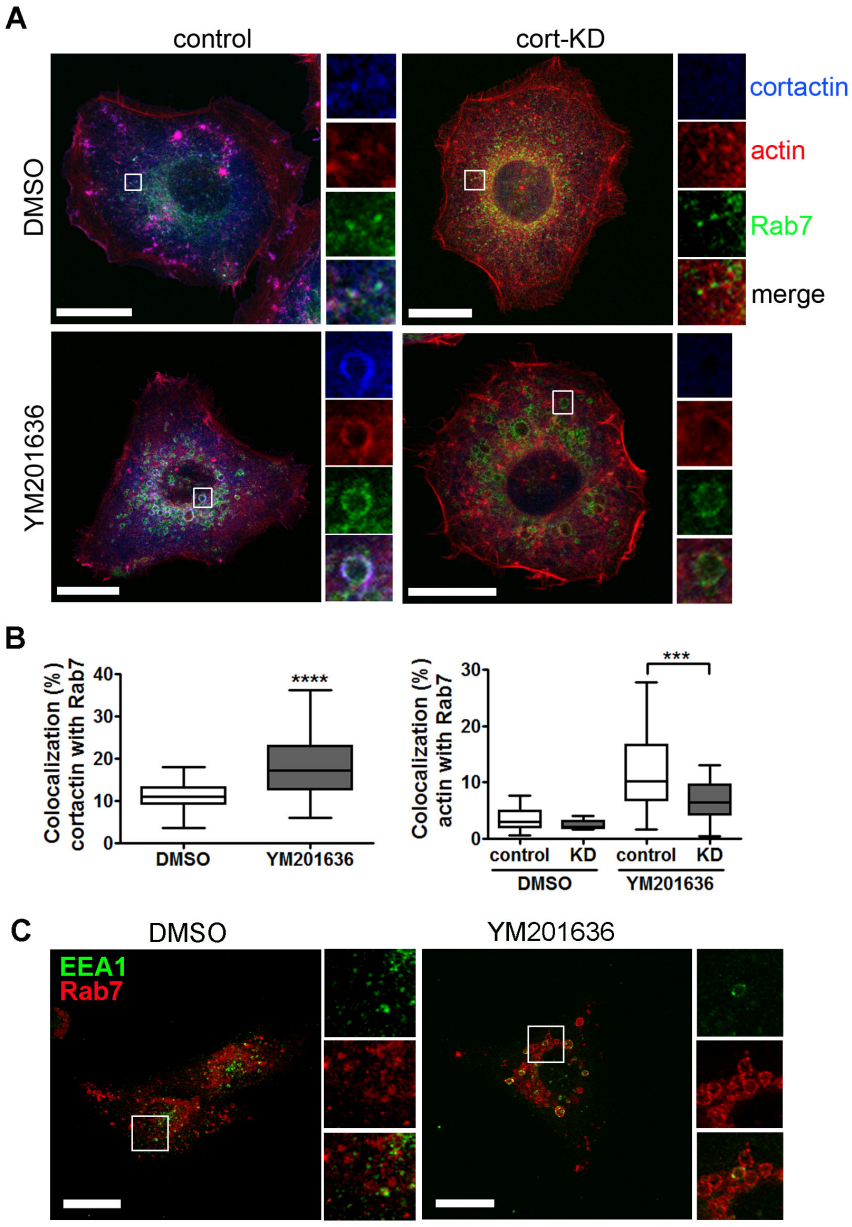

Figure 22. Inhibition of PI(3,5)P_2 production leads to accumulation of cortactin and actin at LE membrane in SCC61 cells. (A) Immunolocalization of Rab7 (green), actin (red), and cortactin (blue) in DMSO or YM201636-treated SCC61 cells. Scale bars indicate 20 µm. (B) Quantitation of % colocalization of cortactin or actin with Rab7. Note decrease in actin localization to late endosomes in cortactin-KD (KD) cells. 3 independent experiments, n≥ 45 in each condition. ***$P\leq 0.001$ and ****$P\leq 0.0001$. (C) Representative images from MDA-MB-231 cells showing localization of early (EEA1, green) and late (Rab7, red) endosome markers upon 2 h treatment with 800 nM YM201636. Scale bars indicate 20 µm.

Cortactin localization to late endosomes depends on Arp2/3 complex activity

One mechanism by which cortactin could promote accumulation of actin on endosomes is by regulating branched actin network assembly by the Arp2/3 complex (Uruno et al., 2001; Weaver et al., 2001). To determine whether Arp2/3-mediated branched actin nucleation is required for recruiting cortactin to endosomal membranes,we treated cells with the the Arp2/3 complex inhibitor CK-666 (Hetrick et al., 2013; Nolen et al., 2009). Treatment with CK-666 resulted in significantly reduced cortactin localization on Rab7-positive endosomes (Figure 23, A and B). Moreover, the accumulation of cortactin that occurs with inhibition of $PI(3,5)P_2$ synthesis by YM201636 was abolished in CK-666 treated cells. Likewise, Arp2/3 inhibition with CK-666 treatment inhibited actin accumulation on Rab7-positive late endosomes in both control and YM201636-treated cells (Figure 23, A and C). These data suggest a model in which cortactin is recruited to late endosomes by interactions with branched actin networks and removed by interaction with $PI(3,5)P_2$.

The 4^{th} repeat region of cortactin is necessary for $PI(3,5)P_2$ binding

Cortactin does not contain canonical phosphoinositide-binding motifs, such as PH (pleckstin homology) or FYVE domains. However, it has been predicted that a series of basic residues within the N-terminal 4^{th} repeat domain of cortactin may bind phosphoinositides (He et al., 1998). To map the $PI(3,5)P_2$ binding site of cortactin, we tested the ability of the purified cortactin N-terminus and 4^{th} repeat deletion mutant to bind $PI(3,5)P_2$-containing liposomes (Figure 24 A). Consistent with the prediction, we found that the N-terminus of cortactin is sufficient to bind $PI(3,5)P_2$ (Figure 24 B) while the 4^{th} repeat deletion mutant of cortactin cannot bind $PI(3,5)P_2$-liposomes (Figure 24 C).

$PI(3,5)P_2$ competes with actin filaments for binding to cortactin

The 4^{th} repeat region of cortactin is a critical F-actin binding site (Weed et al., 2000) and

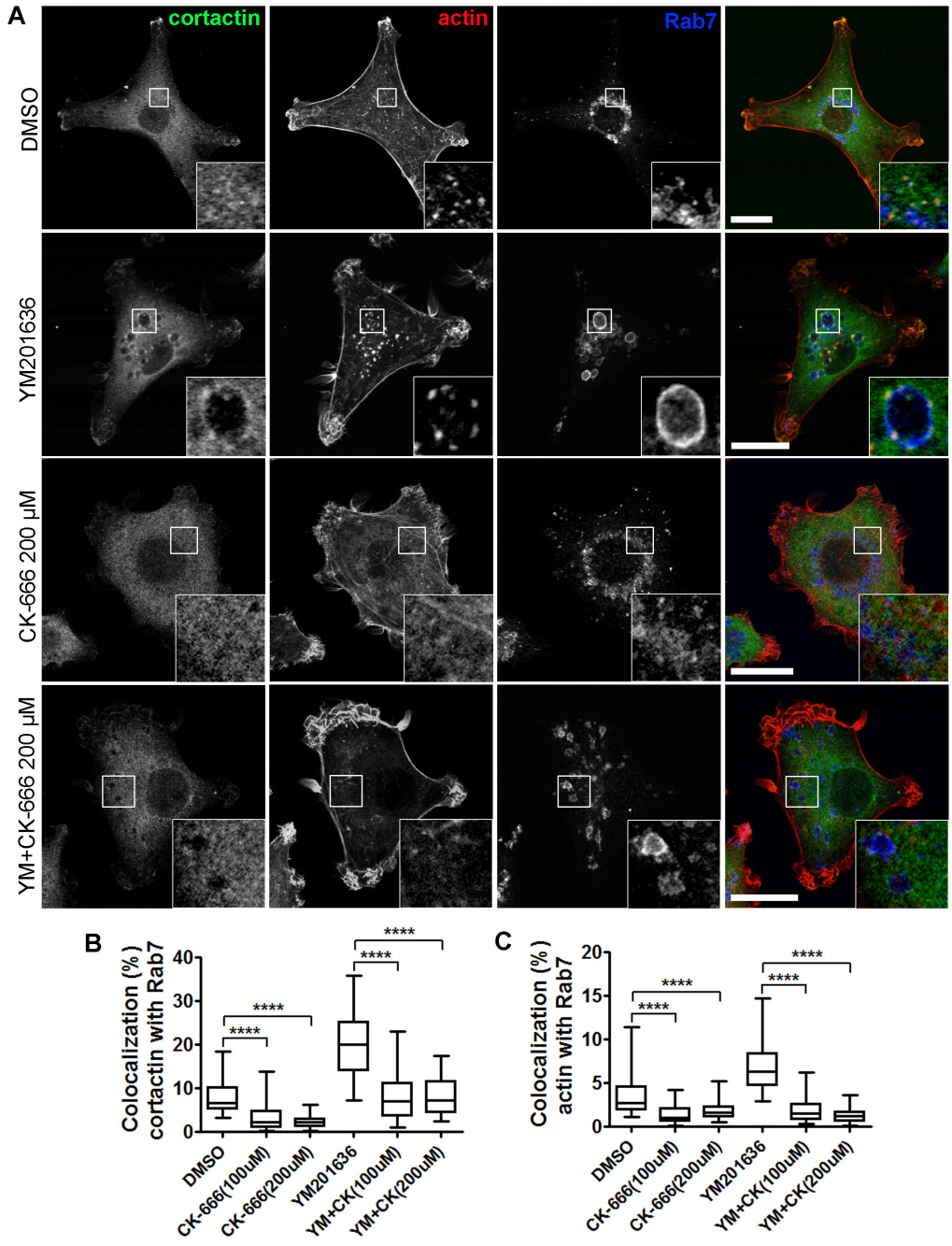

Figure 23. Recruitment of cortactin to late endosomes depends on Arp2/3 complex activity. (A) Representative images showing cortactin (green), actin (red), and Rab7 (blue) localization after 2 h treatment of MDA-MB-231 cells with 800 nM YM201636 alone in combination with 200 µM CK-666. Scale bars = 20 µm. (B) Images from cells treated with YM201636 and various concentrations of CK-666 were analyzed for % colocalization of cortactin or actin with Rab7. 3 independent experiments, n≥ 50 cells from each condition. **** *P<0.0001*.

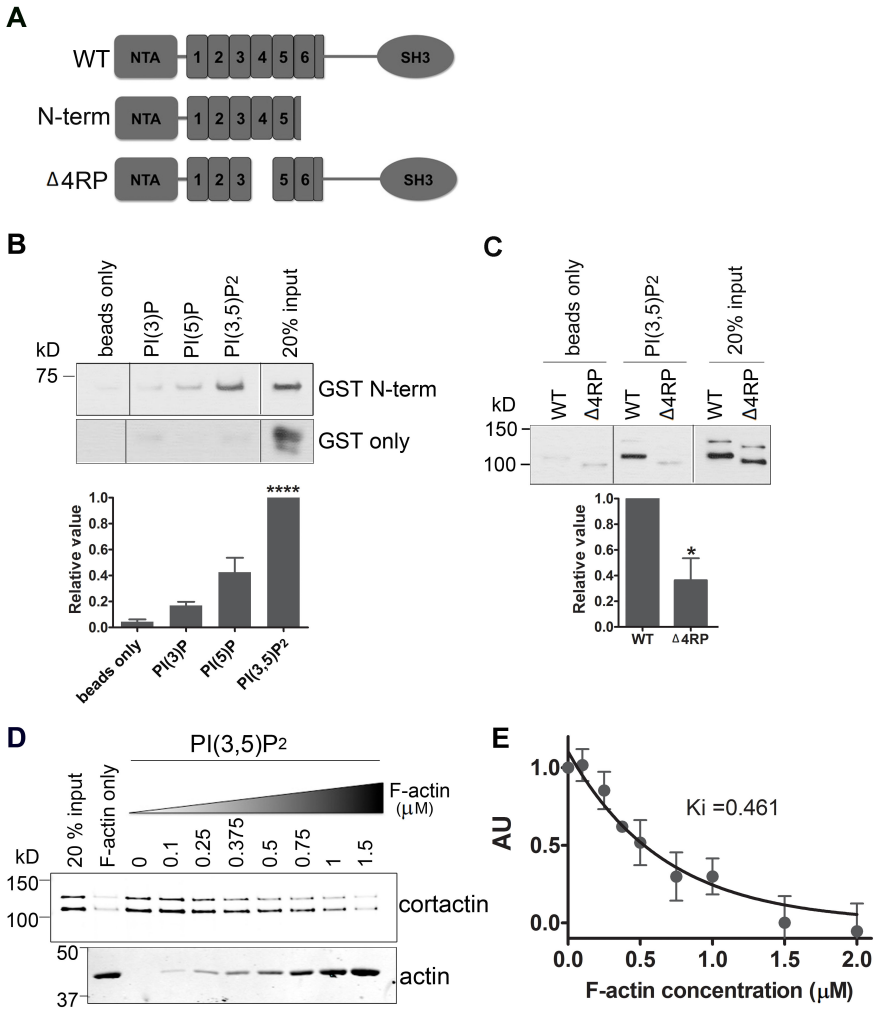

Figure 24. PI(3,5)P_2 regulates the interaction of cortactin with actin filaments. (A) Schematic cartoon of wildtype (WT) and mutant cortactin constructs. (B, C) Representative Western blots from (B) GST-N-term and (C) GST-Δ4RP cortactin-pull-down experiments. Cortactin proteins bound to PI(3,5)P_2-liposome were identified with an anti-GST antibody. Relative binding affinity was quantified by densitometric analysis of Western blot data from three independent experiments. Mean+/-SE plotted. * *P<0.05* and **** *P<0.0001* (D, E) F-actin competes with PI(3,5)P_2 for binding to cortactin. (D) Increasing concentrations of actin filaments were incubated with 70 nM cortactin and 250 nM PI(3,5)P_2-containing liposomes. In the presence of F-actin, cortactin binding to liposomes was significantly reduced. (E) Data points show average binding from four independent experiments. Fit to hyperbolic decay model yields a Ki value of 0.461 μM.

binding to F-actin is required for cortactin to regulate Arp2/3-mediated branched actin assembly and stability (Uruno et al., 2001; Weaver et al., 2001). Thus, we hypothesized that PI(3,5)P_2 may compete with actin filaments for binding to cortactin. To test whether this competition occurs, we performed *in vitro* binding assays using purified proteins and tested if the interaction between cortactin and PI(3,5)P_2 is altered by actin filaments. As shown in Figure 24, D and E, the addition of increasingconcentrations of actin filaments to samples containing cortactin and PI(3,5)P_2-liposomes led to a dose-dependent decrease in the amount of cortactin bound to the liposomes. The Ki of 0.461 μM is consistent with the lower published affinity of cortactin for F-actin (K_d = 0.250 μM, (Bryce et al., 2005)) than for PI(3,5)P_2 (K_d = 30 nM, Figure 19).

PI(3,5)P_2 affects *in vitro* activity of cortactin

The finding that PI(3,5)P_2 prevents cortactin from binding to actin filaments suggests that PI(3,5)P_2 may inhibit the activity of cortactin in controlling branched actin dynamics. To directly test the role of cortactin in branched actin nucleation, we used total internal reflection microscopy (TIRF) to monitor formation of branched actin filaments from purified proteins in real time (Videos 2-5). Consistent with previous reports (Helgeson and Nolen, 2013; Helgeson et al., 2014; Siton et al., 2011; Uruno et al., 2003; Weaver et al., 2001; 2002), addition of cortactin to reactions containing Arp2/3 complex, the active VCA domain of N-WASp (GST-VCA), and G-actin increased the rate of actin branch formation (Figure 25, A and B). Addition of 200 nM PI(3,5)P_2-liposomes significantly reduced the cortactin-induced enhancement of branched actin assembly, although it did not totally ablate it. At higher concentrations of liposomes there was a greater inhibition of cortactin-mediated enhanced branched actin assembly; however there was also an effect on control reactions (data not shown). By contrast, at concentrations ≤ 200 nM PI(3,5)P_2-liposomes had no effect on branching induced by

GST-VCA+Arp2/3 complex in the absence of cortactin, indicating a selective effect on cortactin. Since cortactin is also known to stabilize actin branches (Weaver et al., 2001), we tested whether PI(3,5)P_2 prevents branch stabilization by cortactin. Actin filaments were pre-polymerized in the presence of Arp2/3 complex and GST-VCA and then cortactin, PI(3,5)P_2-liposomes, both cortactin and PI(3,5)P_2-liposomes, or buffer were added to individual reactions. At various time points, rhodamine-phalloidin was added to visualize and stabilize the filaments and images were obtained. The number of branched actin filaments at each timepoint was quantitated. Consistent with previous observations (Weaver et al., 2001), the presence of cortactin inhibited debranching (Figure 25, C and D). In contrast, the addition of PI(3,5)P_2-liposomes reversed branch stabilization by cortactin but had no effect on control networks (Figure 25, C and D). Together, these data indicate that PI(3,5)P_2 can remodel branched networks by regulating interaction of cortactin with actin filaments.

PI(3,5)P_2 regulates actin stability on late endosomes

The finding that PI(3,5)P_2 competes with F-actin for binding to cortactin (Figure 25, D and E) suggests that synthesis of PI(3,5)P_2 may regulate cortactin cycling on and off of branched actin networks on late endosomal membranes. Consistent with that model, we found that inhibition of PI(3,5)P_2 synthesis leads to accumulation of cortactin on Rab7-positive endosomes (Figure 20 B-D; Figure 21; and Figure 22, A and B). In addition, PI(3,5)P_2-mediated removal of cortactin from actin branchpoints could lead to decreased actin assembly and/or destabilization of branched actin networks associated with the endosomal surface. Indeed, in fixed cell analyses, we found that inhibition of PI(3,5)P_2 synthesis led to cortactin-dependent accumulation of actin on Rab7-positive endosomes (Figure 21; and Figure 22, A and B). To test whether endosomal actin turnover is regulated by cortactin and PI(3,5)P_2, live imaging was performed on control

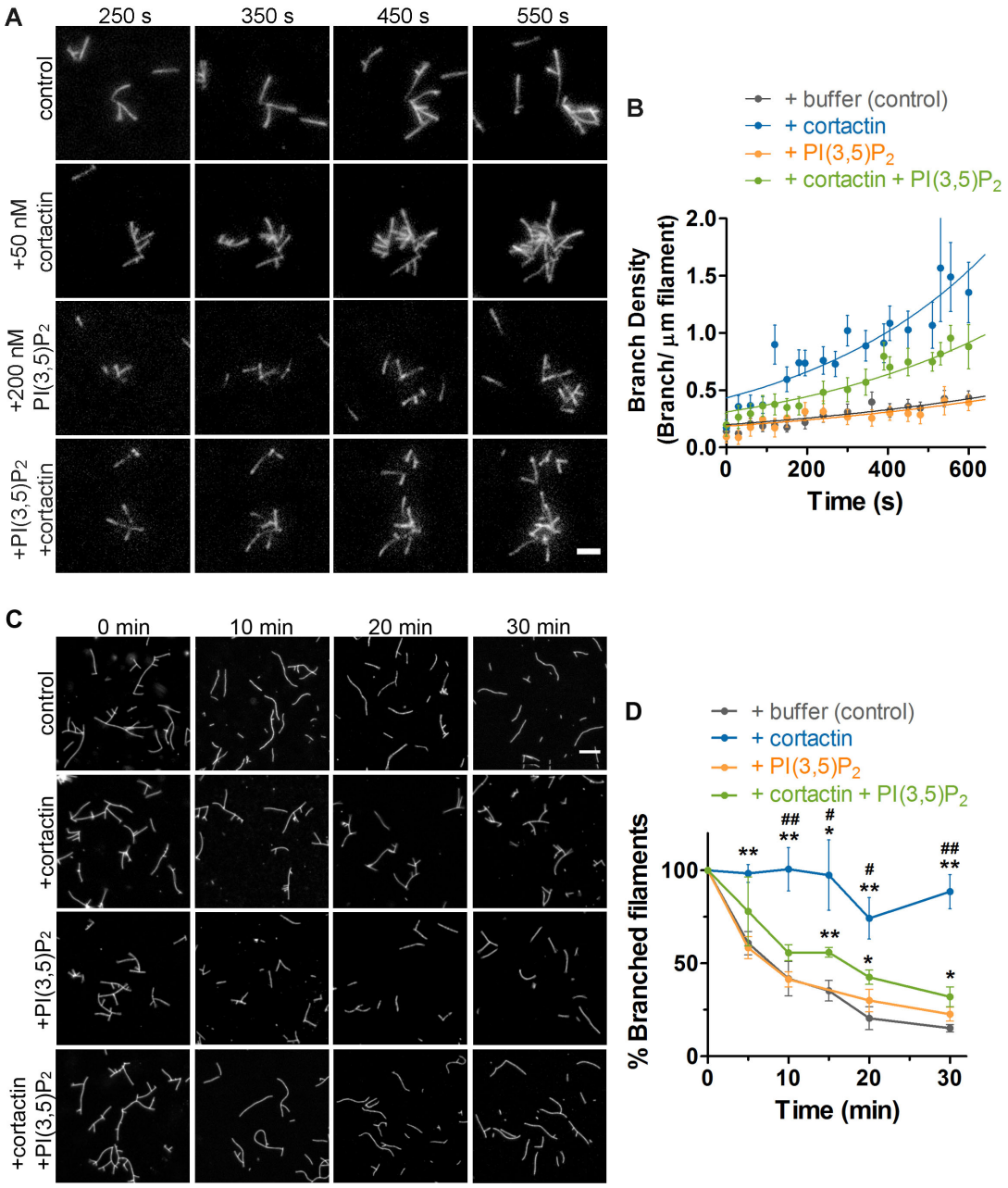

Figure 25. Figure legend on next page.

Figure 25. $PI(3,5)P_2$ antagonizes the activity of cortactin in branched actin regulation. (A) and (B) Synergistic activation of actin branching. (A) TIRF microscopy images of reactions containing actin (0.75 μM 33% Oregon-Green labeled), 10 nM Arp2/3 complex, 50 nM GST-VCA and the indicated amounts of cortactin and $PI(3,5)P_2$-liposomes. Scale bar = 3 μm (B) Branch density was plotted as a function of time. Error bars represent SEM for at least three independent experiments. Branch density of cortactin + $PI(3,5)P_2$-liposome were significantly decreased ($p<0.05$) as compared to that of + cortactin only condition for each time point after 150 sec, except for the 390 and 450 sec timepoints. (C) and (D) Debranching. (C) Representative images of actin debranching over time. 3 μM G-actin was polymerized in the presence of 100 nM Arp2/3 and 600 nM GST-VCA for 8 min. At that time, buffer, 500 nM cortactin, 500 nM $PI(3,5)P_2$, or 500 nM cortactin + 500 nM $PI(3,5)P_2$-liposome were added to individual reactions. Samples were incubated for additional min as indicated before the debranching reactions were stopped with equimolar rhodamine-phalloidin and visualized. Scale bar = 3 μm. (D) Data points represent the percentage of branched filaments per field from each condition, calculated from three or four independent experiments. Error bars represent SEM. *($^{\#}$) *P<0.05*, **($^{\#\#}$) *P<0.01.* * compares cortactin vs. + buffer control and $^{\#}$ compares +cortactin vs. +cortactin+$PI(3,5)P_2$ condition.

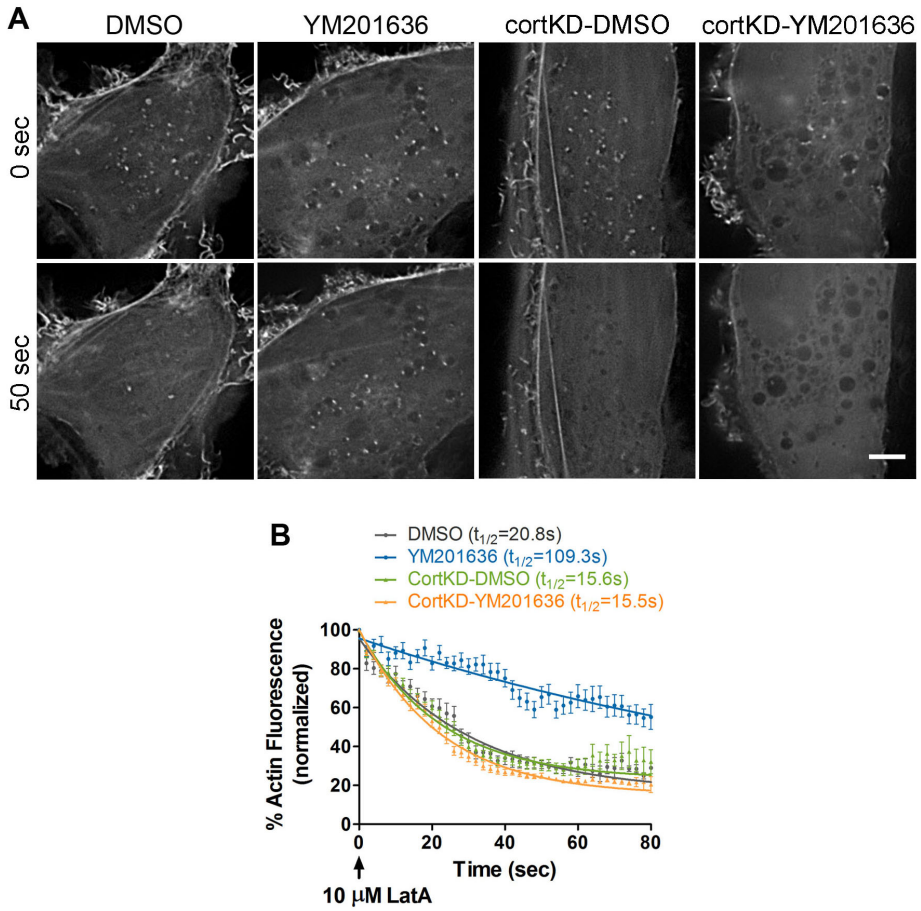

Figure 26. Actin stability on endosomal membranes is controlled by PI(3,5)P_2. (A) MDA-MB-231 cells stably expressing mEGFP-F-tractin were treated with DMSO or YM201636 for 2 h, then imaged live after treatment with 10 µM latrunculin A for the indicated times. Scale bar = 5 µm (B) The change in endosomal actin fluorescence over time after latrunculin A was normalized to initial endosomal actin fluorescence (n= 10-15 cells from three independent experiments of each condition). Data were fitted with one-phase decay equation model using GraphPad Prism software to determine half-life ($t_{1/2}$) of endosomal actin.

or cortactin-KD cells expressing the dynamic actin probe mEGFP-F-tractin in the presence or absence of the PI(3,5)P_2 synthesis inhibitor YM201636 (Figure 26, Video 6). In order to specifically analyze actin turnover, cells were treated with 10 μM latrunculin A, a drug that prevents actin polymerization by sequestering monomeric actin (Morton et al., 2000). In control cells treated with DMSO as the diluent control for YM201636, endosomal actin fluorescence became undetectable within 40-50 s after Latrunculin A. When quantified across cells, endosomal actin fluorescence showed an exponential loss after latrunculin exposure in control cells, with a $t_{1/2}$ of 20.8 s. However, endosomal actin fluorescence in YM201636-treated cells decreased more slowly, yielding a $t_{1/2}$ of 109.3 s, indicating that PI(3,5)P_2 is important for dynamic turnover of late endosomal actin assemblies. DMSO-treated cortactin knockdown cells showed similar exponential loss of actin fluorescence ($t_{1/2}$ = 15.6 s) compared to DMSO-treated control cells. Importantly, the delayed actin turnover observed in YM201636-treated control cells was not observed in cortactin knockdown cells with curve fits yielding $t_{1/2}$ of 15.5 s. These data indicate that PI(3,5)P_2 controls endosomal actin turnover in a cortactin-dependent manner.

WASH localization is regulated by PI(3,5)P_2.

Activation of Arp2/3 complex occurs upon binding of an activator in the WASP family of proteins (Millard et al., 2004). At endosomes, the WASP family member WASH appears to be the main activator of Arp2/3 complex (Derivery et al., 2009; Duleh and Welch, 2010; Gomez and Billadeau, 2009) and should act in concert with cortactin to promote endosomal branched actin assembly. Consistent with those reports, WASH, cortactin and actin show strong colocalization on endosomal membranes (Figure 27). By dot blot, the FAM21 component of WASH has been found to bind multiple phosphoinositides, including the major endosomal lipids PI(3)P and PI(3,5)P_2 (Jia et al., 2010). However, the consequence of that interaction is unclear. To assess the effect of

$PI(3,5)P_2$ on WASH localization, MDA-MB-231 and SCC61 cells were treated with YM201636 and immunostained for WASH and cortactin and colocalized with either actin (Figure 27 A) or mRFP-Rab7 (Figure 27 B). Inhibition of $PI(3,5)P_2$ synthesis led to an increase in the localization of WASH to cortactin- and actin-positive structures at Rab7-positive endosomes, suggesting that similarly to cortactin, $PI(3,5)P_2$ does not recruit WASH to endosomal membranes but instead may promote its removal. However, the increase in WASH localization was small compared to the increase in cortactin localization in YM201636-treated cells (40% increase in WASH vs. 300% increase in cortactin colocalization with Rab7, compare Figures 28 C and 3 C). Overall, $PI(3,5)P_2$ plays a concerted role to remove branched actin regulators from late endosomes and promote disassembly of endosome-associated actin assemblies (see model in Figure 28).

Discussion

Dynamic actin assembly plays an important role in controlling cellular membrane trafficking. Here we identify a specific molecular mechanism that regulates actin dynamics on endosomes: $PI(3,5)P_2$-mediated removal of cortactin from actin filament arrays. In vitro biochemical studies revealed that cortactin preferentially and specifically binds to $PI(3,5)P_2$ via its F-actin binding region. Furthermore, $PI(3,5)P_2$ inhibits binding of actin filaments to cortactin as well as the activity of cortactin in branched actin assembly and stabilization. In cells, inhibition of $PI(3,5)P_2$ synthesis leads to accumulation of stable WASH-cortactin-actin assemblies on Rab7-positive endosomes. Finally, the accumulation of actin that occurs in the absence of $PI(3,5)P_2$ depends on the presence of cortactin, indicating a key role for the $PI(3,5)P_2$-cortactin interactions in promoting turnover of late endosomal branched actin assemblies. These findings suggest a model in which actin dynamics on late endosomes are regulated by

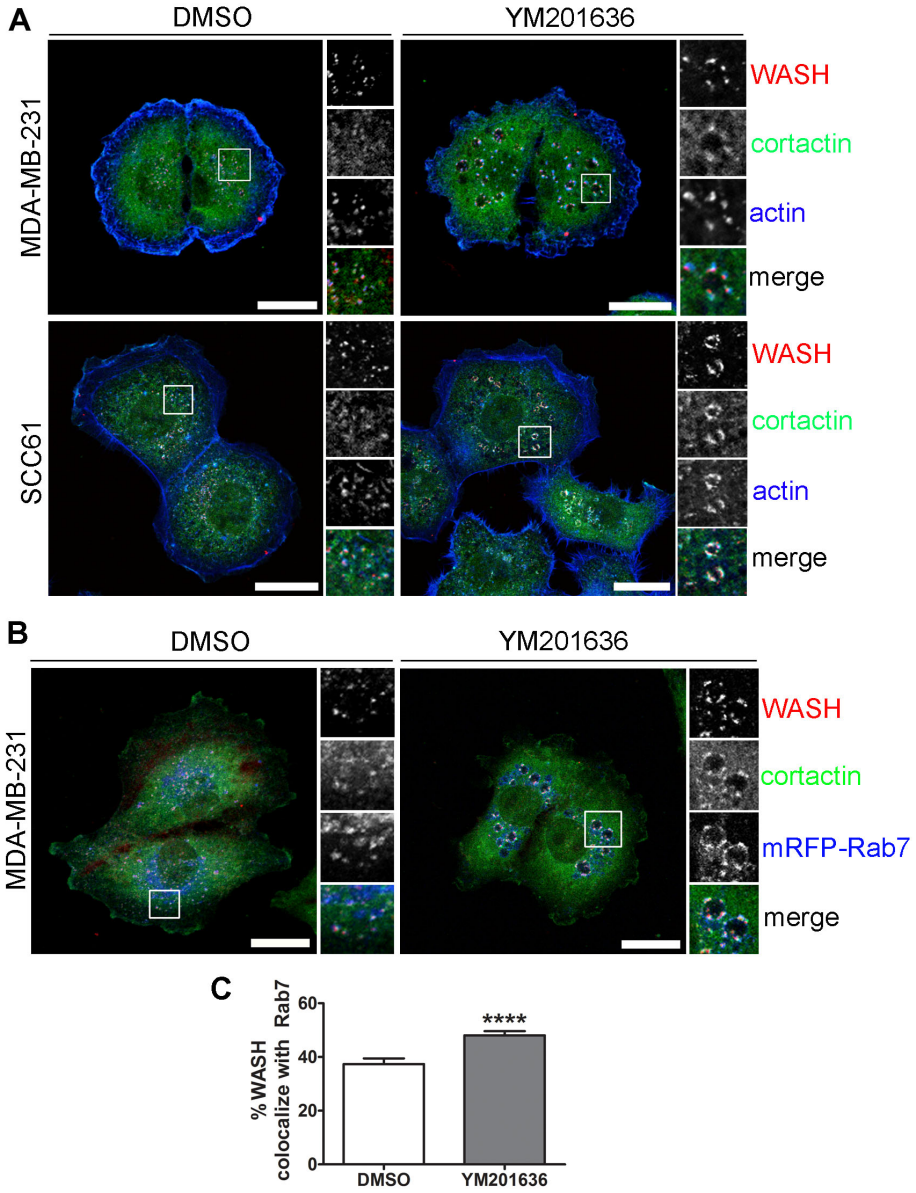

Figure 27. WASH localization is controlled by PI(3,5)P_2 levels. (A) Representative images from MDA-MB-231 (upper) and SCC61 (bottom) showing localization of WASH (red), cortactin (green), and actin (blue) after 2 h treatment with 800 nM YM201636 or DMSO diluent control. Scale bars = 20 μm. (B) Representative images of MDA-MB-231 cells stably expressing mRFP-Rab7 (pseudocolored blue) immunostained by WASH (red) and cortactin (green) after 2 h treatment with 800 nM YM201636 or DMS0 diluent control. Scale bars indicate 20 μm. (C) Images were analyzed for % colocalization of WASH with Rab7. Mean +/- SE. 2 independent experiments, n≥ 62 cells in each condition. **** *P<0.0001*.

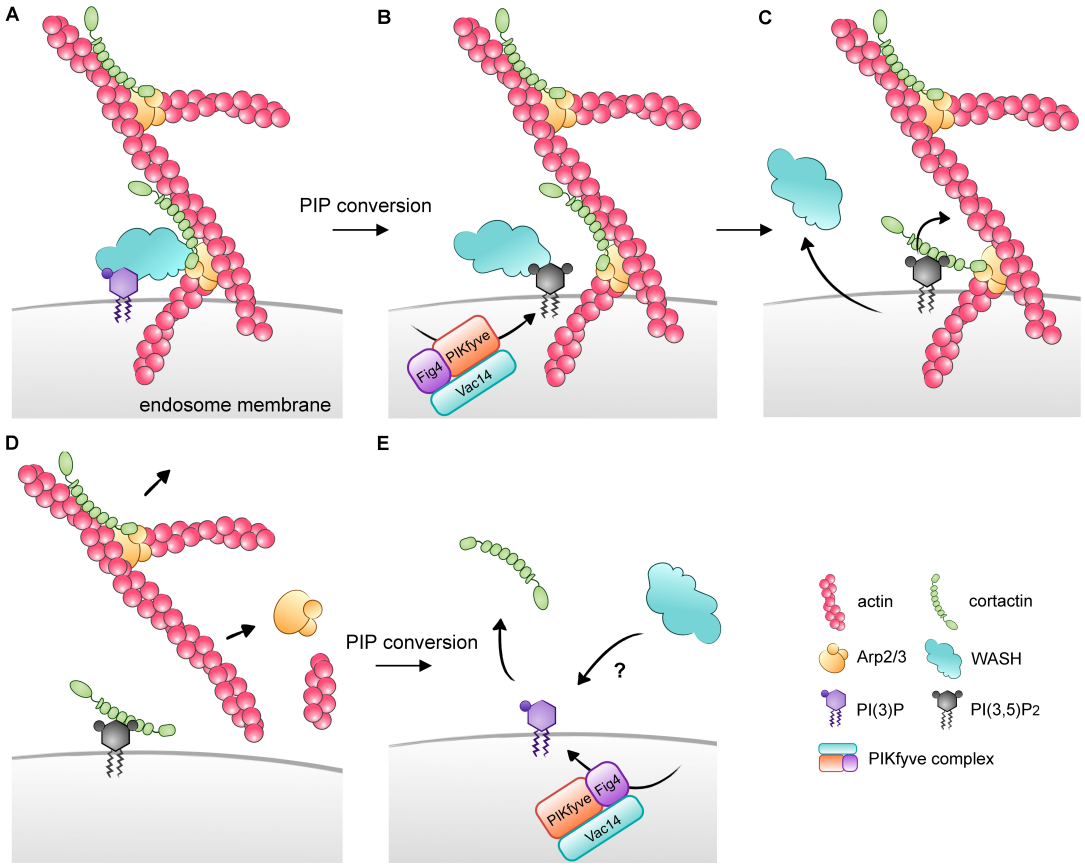

Figure 28. Model of endosomal branched actin network regulation by PI(3,5)P_2. (A) Branched actin nucleation is initiated by the WASH complex which is bound to the surface of late endosomes by signaling molecules that likely include PI(3)P (Jia et al., 2010). WASH-induced activation of the Arp2/3 complex recruits cortactin to nascent branch points (Figure 23) where it synergistically promotes actin assembly. (B) Conversion of PI(3)P to PI(3,5)P_2 is accomplished by the enzymatic activity of PIKfyve within the 3-member PIKfyve complex that includes the scaffold protein Vac14 and the opposing 5' phosphatase Fig4 (Dove et al., 2009; Shisheva, 2008). (C) PI(3,5)P_2 binds to cortactin, releasing actin filaments (Figure 24) and potentially the WASH complex from endosomes (Figure 27). (D) Without cortactin binding to the branchpoint, Arp2/3 complex loses affinity for the mother filament (Uruno et al., 2001) causing debranching ((Weaver et al., 2001) and Figure 25). Disassembly of branched actin networks leads to diminished recruitment of cortactin. (E) Conversion of PI(3,5)P_2 back to PI(3)P should release cortactin from the endosome surface unless new branched actin networks are available for rebinding. Interconversion of PI(3)P and PI(3,5)P_2 by the PIKfyve complex may facilitate dynamic cycling of actin assembly and disassembly through control of cortactin–actin interactions.

$PI(3,5)P_2$-induced cycling of cortactin on and off of actin filaments (see Model Figure 28).

In cells, branched actin is very dynamic and controls rapid membrane events, including plasma membrane protrusions and membrane trafficking events. Our data indicate that the $PI(3,5)P_2$-cortactin interaction we described is a major regulator of actin dynamics at the late endosome and provide a unique example of coordination of endosomal actin dynamics. Since we did not detect significant binding of cortactin to other PIs, it is possible that this specific mechanism of PI-cortactin interactions may be unique to the late endosome. At the plasma membrane, other mechanisms may control branched actin dynamics including control of WAVE2-mediated actin polymerization by $PI(3,4,5)P_3$ (Oikawa et al., 2004). Conversely, disassembly of lamellipodial branched actin networks may occur by antagonism of cortactin by coronin and of antagonism of Arp2/3 complex by glial maturation factor (Cai et al., 2008; Gandhi et al., 2010; Luan and Nolen, 2013; Ydenberg et al., 2013).

Cortactin can promote actin assembly by both enhancing the ability of WASP family members to activate Arp2/3 complex and by stabilizing actin branches after they are formed (Weaver et al., 2001). Both of those activities require binding of cortactin to actin filaments and were inhibited by $PI(3,5)P_2$ binding *in vitro*. Since access to $PI(3,5)P_2$ is intrinsically limited to the membrane surface where WASH also is localized, a possible consequence of $PI(3,5)P_2$ binding to cortactin could be to limit co-activation of Arp2/3 complex. This mechanism would be consistent with the strong colocalization of WASH and cortactin on the endosome surface (Figure 27) and is supported by *in vitro* evidence that cortactin and WASP family members uniquely act together to promote Arp2/3 complex activation (Helgeson and Nolen, 2013; Siton et al., 2011; Uruno et al., 2003; Weaver et al., 2001). However, our finding that $PI(3,5)P_2$-cortactin interactions specifically promote turnover of endosomal actin in the absence of new actin polymerization (Figure 26) suggests that inhibition of debranching is a key cortactin

activity that is controlled by PI(3,5)P_2. Furthermore, inhibition of Arp2/3 complex but not PI(3,5)P_2 synthesis (Figure 23) inhibited accumulation of cortactin at late endosomes. These data suggest a model in which activation of Arp2/3 complex leads to recruitment of cortactin to actin nucleation sites at the late endosome surface. Local synthesis of PI(3,5)P_2 promotes removal of cortactin and net disassembly of endosomal actin (Figure 28).

PI(3,5)P_2 regulates maturation and trafficking from late endosomes. Interestingly, our previous studies with cortactin-knockdown cells identified a number of strong phenotypes that are similar to those in cells with defective PI(3,5)P_2 formation, including enlargement of immature LE/Lys compartments and defects in retrograde trafficking from endosomes to the Golgi apparatus (Kirkbride et al., 2012; Sung et al., 2011). Moreover, cortactin-mediated actin remodeling is also known to regulate EGFR trafficking (Lladó et al., 2008; Timpson et al., 2005) and autophagosome-lysosome fusion (Lee et al., 2010), both phenotypes controlled by PI(3,5)P_2 (de Lartigue et al., 2009). Our data suggest that control of branched actin dynamics through cortactin is at least one important mechanism by which PI(3,5)P_2 controls endosomal function.

In summary, we described a unique molecular mechanism that controls branched actin dynamics at late endosomes via PI(3,5)P_2-mediated removal of cortactin from actin filament networks. Dynamic cycling of phosphoinositides to orchestrate both assembly and disassembly of filament networks may be a powerful mechanism to control actin-membrane interactions and downstream membrane trafficking events.

Acknowledgements

I thank Nelson Alexander for pilot data that launched the project as well as critical reading of the manuscript. I thank David Kovar and Jon Winkelman for advice on TIRF imaging of actin assembly as well as for some purified components for the assay. I

thank Matt Tyska for use of the TIRF microscope and plasma cleaner and scientific feedback. I thank members of the Weaver laboratory for scientific feedback. I thank Jessica Mazerik for advice on liposome assays. Funding was provided by NIH grants R01 CA163592 and R01GM075126 to AMW, CTSA grants UL1 RR024975 and TR000445-06, NCI Cancer Center Support Grant P30 CA068485, and VUMC Cell Imaging Shared Resource (CISR) grants CA68485, DK20593, DK58404, HD15052, DK59637 and EY08126.

CHAPTER V

CONCLUSION AND SIGNIFICANCE

Conclusion

Cortactin has emerged as a central element connecting signaling pathways with the actin cytoskeleton. Our laboratory, especially, has played a central role in understanding the role of cortactin-regulated actin assembly in the aggressiveness of cancer cells, including motility, invasiveness and tumor growth. My study focusing on cortactin function in membrane trafficking stemmed from our previous findings demonstrating that cortactin is essential for secretion of invadopodia-localized proteinases, MMP2, MMP9, and MT1-MMP (Clark and Weaver, 2008; Clark et al., 2007). Since the Golgi complex serves as the major protein-packaging hub for secreted proteins, a likely mechanism for regulation of MMP secretion by cortactin was control of Golgi-mediated secretion (Kienzle and Blume, 2014). Furthermore, actin had been implicated in Golgi trafficking and the maintenance of Golgi morphology (Dippold et al., 2009; Egea et al., 2006; Lázaro-Diéguez et al., 2007). In addition, we found that cortactin knockdown cells displayed a collapsed (compact) Golgi morphology and previous studies from other groups had implicated cortactin in Golgi trafficking (Cao et al., 2005; Salvarezza et al., 2009). Thus, we initially hypothesized that cortactin controls anterograde trafficking of MMPs to the plasma membrane. However, our study revealed that cortactin does not affect anterograde trafficking of the model protein VSVG. In addition, we found that the morphological alteration of the Golgi complex observed in cortactin-depleted cells occurs secondary to defective accumulation of cholesterol in late endosomes. Thus late endosomes appeared to be the major membrane compartment sensitive to cortactin levels.

Recent studies have shown that the majority of internalized the key invadopodia proteinase MT1-MMP is located in a late endocytic compartment and recycled from there back to the plasma membrane invadopodia (Steffen et al., 2008; Williams and Coppolino, 2011), Based on these data, we hypothesized that cortactin controls MMP secretion by regulating late endosomal trafficking. Indeed, we found that cortactin localizes to late endosome and regulates LE/Lys maturation and trafficking. Thus, cortactin-depleted cells accumulate enlarged LE/Lys hybrid organelles that are filled with undegraded organelles and membrane. Furthermore, retrograde trafficking of CI-M6PR is defective in cortactin-depleted cells. Moreover, our laboratory has found that the ECM component fibronectin is recycled from a LE/Lys compartment in a cortactin-dependent way to promote cell motility (Sung et al., 2011). Taken together, these data suggest that regulation of late endosomal trafficking by cortactin is important not only for Golgi homeostasis but also for cell motility and invasiveness by regulating protein secretion.

Cortactin bridges branched actin networks to various cellular processes including vesicular trafficking, likely functions through promotion of branched actin assembly. Importantly, we found that the cortactin knockdown phenotypes depend on interaction with the branched actin nucleator Arp2/3 complex, suggesting that regulation of branched actin networks is critical. Intriguingly, studies have suggested the importance of regulation of actin dynamics in endosome function (Carnell et al., 2011; Derivery et al., 2009; Gomez and Billadeau, 2009; Harrington et al., 2011; Puthenveedu et al., 2010). These studies support a model that Arp2/3-mediated actin assembly organizes endosomal membrane into functional subdomains and contributes to cargo sorting and formation of tubular transport intermediates. Therefore, we speculate that cortactin plays a key role in MMP sorting and secretion by regulating LE/Lys maturation and trafficking through the regulation of Arp2/3-mediated branched actin assembly on endosomes.

Consistent with our finding of cortactin-mediated regulation of LE/Lys compartment maturation and trafficking, other studies indicated cortactin as a key regulator of actin dependent endosomal processes (Lee et al., 2010; Monteiro et al., 2013; Ohashi et al., 2011; Puthenveedu et al., 2010). Although these studies emphasize the importance of cortactin-mediated actin dynamics in regulating endosomal processes the upstream inputs and the mechanisms how cortactin itself is controlled on endosomes still remain poorly understood. Phosphoinositide (PIP) conversion is known to control membrane trafficking and is frequently involved in recruitment of cytoskeletal proteins to membranes. Hence PIPs were attractive candidates for us that might connect cortactin to endosomal membrane and provide a molecular mechanism that regulates endosomal actin dynamics. In fact, cortactin was previously shown to interact with $PI(4,5)P_2$ resulting in dissociation from actomyosin II complex (He et al., 1998), yet interaction with other PIPs on intracellular membrane were not tested. In this study, we identified a novel interaction between cortactin and $PI(3,5)P_2$. Our data suggest a unique mechanism for disassembly of actin networks on membranes in which removal of cortactin by $PI(3,5)P_2$ destabilizes actin assemblies at late endosomes.

The endosome phenotype observed in cortactin depleted cells, enlarged endosomes with no tubule, suggests that cortactin may be necessary for endosomal tubulation at late endosomes. In fact, endosomal actin has shown to be concentrated at tubular domains of endosomes and to stabilize the tubules. This may allow sufficient time for tubules to serve as scaffolding platforms for other molecules that are involved in cargo sorting (Puthenveedu et al., 2010). However, it has not been tested whether this tubular structure formation and/or stability is affected by cortactin-$PI(3,5)P_2$ interaction. Thus, a future study should include live imaging movies at a sufficient frame speed to examine whether $PI(3,5)P_2$-mediated regulation of actin dynamics participate in tubule formation and thus cargo sorting.

In addition, the enlarged endosomal phenotype of cortactin-KD cells is reminiscent of an endosomal fusion defect (Coen et al., 2012; Huotari and Helenius, 2011; Rosenfeld et al., 2001). Endosomal fusion is an essential step in vesicle trafficking that allows the efficient exchange of contents between compartments. Indeed, actin assembly has been previously implicated in promoting membrane fusion whereas disruption of actin dynamics has been shown to cause the formation of a greatly enlarged endocytic compartment that has been attributed to uncontrolled fusion between compartments (Gomez et al., 2012; Kjeken et al., 2004; Ohashi et al., 2011). Enlarged endosomes are also the hallmark of $PI(3,5)P_2$-deficiency (Ho et al., 2011), suggesting a possible fusion defect in $PI(3,5)P_2$-deficient cells that could be caused by the defective regulation of actin dynamics. To investigate whether vesicle fusion is modulated by $PI(3,5)P_2$-mediated regulation of actin dynamics, future study should examine the effect of cortactin and $PI(3,5)P_2$ on fusion between endosomes. Fluorescence microscopy based *in vitro* fusion assay using fluorescently labeled endosomes will address this question.

Interestingly, the actin filaments have been shown to bind proteins involved in membrane fusion, including SNAREs (Band et al., 2002; Thurmond et al., 2003). Dynamic assembly and disassembly of SNARE proteins is required for preventing inappropriate fusion, and aberrant disassembly of SNARE proteins has been shown to result in the accumulation of vesicle in clusters (Fraldi et al., 2010; Shin et al., 2012). Since we frequently observe enlarged endosomes studded with small vesicles in cortactin-KD cells, it is possible that cortactin-regulated branched actin assembly is important for proper SNARE disasembly. Since the actin cytoskeleton also has been proposed to organize membrane domains via protein-protein or lipid-protein interactions (Liu and Fletcher, 2006; Winter et al., 2012), it is possible that spatial regulation of actin dynamics on membrane controls local assembly and/or disassembly of SNAREs.

Therefore, an important future direction is to determine whether $PI(3,5)P_2$-mediated regulation of actin dynamics controls SNARE-mediated vesicle fusion by regulating SNARE assembly and/or disassembly. Pairing of target SNARE (t-SNARE) and vesicle SNARE (v-SNARE) and subsequent assembly of functional SNARE complex enables fusion of opposing vesicle and target membrane (Chen and Scheller, 2001). Hence, we could examine the late endosome associated SNARE pairing such as syntaxin 7 with its partner VAMP7 or VAMP8 (Pryor et al., 2004) by immunofluorescence or coimmunoprecipitation. In addition, biochemical fractionation assay will address whether $PI(3,5)P_2$-regulated actin dynamics controls SNARE association with endolysosomal membrane domain.

$PI(3,5)P_2$ is known to regulate acidification of endolysosomes in yeast, *C. elegans*, *Droshophila* , and *Arabidopsis* (Bak et al., 2013; Nicot et al., 2006; Rusten et al., 2006; Gary et al., 1998) by unknown mechanisms. The vacuolar H+-ATPase (V-ATPase) has been suggested as a likely candidate of $PI(3,5)P_2$ effector, as V-ATPase is best known for pumping protons across membrane to acidify intracellular compartment. Interestingly, it was shown that V-ATPase binds F-actin and that WASH-mediated actin assembly on endosomal surface leads to sorting of the V-ATPase, which in turn regulates membrane fusion and exocytosis, in *Dictyostelium discoides* (Carnell et al., 2011; Holliday et al., 2000; Park et al., 2013). Our data showing $PI(3,5)P_2$-mediated regulation of actin dynamics thus suggests the possibility that $PI(3,5)P_2$ may regulate endosomal acidification by controlling V-ATPase recycling through the regulation of actin assembly on endosomal surface. In addition to direct binding to F-actin, V-ATPase directly interacts with SNARE proteins, consequently affecting SNARE pairing between membranes that promotes membrane fusion and/or exocytosis (Vavassori and Mayer, 2014).

Membrane fusion is one of the important steps in exosome secretion. Exosomes are small vesicles derived from endosomal MVB, which has been studied extensively in recent as they participate in intercellular communication by carrying ligands, receptors, signaling molecules, lipids, and nucleic acid, thereby supporting or perturbing (in the case of cancer) different physiological processes (Azmi et al., 2013; Colombo et al., 2014; Schorey and Bhatnagar, 2008). Fusion between endosomal MVBs carrying exosomes and the plasma membrane is critical step in the release of exosomes. In deed, V-ATPase has been proposed to regulate exosome secretion containing hedgehog related protein in *C. elegans* (Liégeois et al., 2006). Furthermore, our laboratory observed that treatment of HNSCC cells with selective V-ATPase inhibitor, bafilomycin A, inhibits exosomes secretion (data not shown). Based on these, my study also suggest the possible functional connection between localized endosomal actin assembly regulated by cortactin-PI(3,5)P_2 interaction and late endosome/MVB-mediated secretion. Therefore, it will be interesting to investigate whether PI(3,5)P_2 and cortactin work together to promote endolysosomal acidification and exosome secretion.

Another important observation from our study is that cortactin deficient cells accumulate cholesterol in LE/Lys compartment. As an essential structural component in the cell membranes membrane cholesterol can facilitate protein-protein interactions and modulate the function of membrane proteins critical to cellular function (Maxfield and Tabas, 2005). Cholesterol transport between intracellular organelles is important since key cholesterol processing steps take place in different subcellular localization. Thus, the accurate delivery of cholesterol to appropriate membrane domains is vital for cholesterol homeostasis, and normal cellular function. Consequently, aberrant cholesterol trafficking has been linked to several human diseases, mostly neurodegenerative disorder (Ikonen, 2006; Maxfield and Tabas, 2005). Interestingly, it has shown that multivesicular late endosomes serve as important regulators of cholesterol transport (Kobayashi et al.,

1999). Since cortactin is an actin regulator that is known to regulate endosomal dynamics, we speculate that cholesterol accumulation in cortactin knockdown cells occurs secondary to LE/Lys maturation and/or trafficking defects. Importantly, it has been shown that the secretion of cholesterol by exosomes contributes to maintain cellular cholesterol homeostasis (Strauss et al., 2010). Given that cortactin regulates exosome secretion (data not shown, Sinha et al., submitted), it is plausible that defective secretion of exosomes that carry cholesterol may cause the accumulation of cholesterol in cortactin-KD cells. However, further investigations are required to determine molecular mechanism by which actin dynamics regulated by cortactin controls cholesterol homeostasis.

Significance

Cortactin has been shown to control tumor aggressiveness by regulation of protein secretion. However, it has been difficult to identify the specific molecular mechanism by which cortactin controls trafficking. My current study provides important insight into that mechanism. The major finding in the first part of my study is that LE/Lys maturation and trafficking is highly sensitive to cortactin-regulated branched actin assembly and the cytoskeletal-induced Golgi morphology changes can be a consequence of altered trafficking at late endosomes. This work is important for the following reasons: 1) I delineated fundamental cytoskeletal mechanisms that regulate Golgi size; 2) we identified retrograde trafficking from late endosome regulated by cortactin as a major regulation point for Golgi size homeostasis; and 3) we identified a novel mechanism for cortactin-mediated regulation of Golgi morphology which likely explains the findings of many previous reports.

In the second part of my studies, I identified a key part of the mechanism by which phosphoinositides and the actin cytoskeleton interact on endosomal membranes

to control LE/Lys trafficking. I identified a unique mechanism to promote rapid disassembly of branched actin networks at membranes. I also identified cortactin as an effector of $PI(3,5)P_2$, an understudied lipid with disease associations. These findings advance our understanding of Arp2/3-mediated regulation of endosomal actin dynamics and specifically assign a function for a relatively uncharacterized PIP, $PI(3,5)P_2$.

Overall, my studies give mechanistic insight to an important but poorly understood area of cell biology, how actin and membranes interface to control membrane trafficking and secretion. By understanding the underlying molecular mechanisms that promote secretion by aggressive cancer cells, this study may also point towards future targets for novel cancer therapies.

REFERENCES

Akervall, J.A., Jin, Y., Wennerberg, J.P., Zätterström, U.K., Kjellén, E., Mertens, F., Willén, R., Mandahl, N., Heim, S., and Mitelman, F. (1995). Chromosomal abnormalities involving 11q13 are associated with poor prognosis in patients with squamous cell carcinoma of the head and neck. Cancer *76*, 853–859.

Anitei, M., and Hoflack, B. (2012). Bridging membrane and cytoskeleton dynamics in the secretory and endocytic pathways. Nat. Cell Biol. *14*, 11–19.

Aridor, M., and Hannan, L.A. (2002). Traffic jams II: an update of diseases of intracellular transport. Traffic *3*, 781–790.

Ayala, I., Babià, T., Baldassarre, M., Pompeo, A., Fabra, A., Kok, J.W., Luini, A., Buccione, R., and Egea, G. (1999). Morphological and biochemical analysis of the secretory pathway in melanoma cells with distinct metastatic potential. FEBS Letters *451*, 315–320.

Ayala, I., Baldassarre, M., Giacchetti, G., Caldieri, G., Tetè, S., Luini, A., and Buccione, R. (2008). Multiple regulatory inputs converge on cortactin to control invadopodia biogenesis and extracellular matrix degradation. J. Cell Sci. *121*, 369–378.

Azmi, A.S., Bao, B., and Sarkar, F.H. (2013). Exosomes in cancer development, metastasis, and drug resistance: a comprehensive review. Cancer Metastasis Rev. *32*, 623–642.

Bak, G., Lee, E.-J., Lee, Y., Kato, M., Segami, S., Sze, H., Maeshima, M., Hwang, J.-U., and Lee, Y. (2013). Rapid structural changes and acidification of guard cell vacuoles during stomatal closure require phosphatidylinositol 3,5-bisphosphate. Plant Cell *25*, 2202–2216.

Band, A.M., Ali, H., Vartiainen, M.K., Welti, S., Lappalainen, P., Olkkonen, V.M., and Kuismanen, E. (2002). Endogenous plasma membrane t-SNARE syntaxin 4 is present in rab11 positive endosomal membranes and associates with cortical actin cytoskeleton. FEBS Letters *531*, 513–519.

Bard, F., Mazelin, L., Péchoux-Longin, C., Malhotra, V., and Jurdic, P. (2003). Src regulates Golgi structure and KDEL receptor-dependent retrograde transport to the endoplasmic reticulum. J. Biol. Chem. *278*, 46601–46606.

Behnia, R., and Munro, S. (2005). Organelle identity and the signposts for membrane traffic. Nature *438*, 597–604.

Blok, J., Mulder-Stapel, A.A., Daems, W.T., and Ginsel, L.A. (1981a). The effect of chloroquine on the intralysosomal degradation of cell-coat glycoproteins in the absorptive cells of cultured human small-intestinal tissue as shown by silver proteinate staining. Histochemistry *73*, 429–438.

Blok, J., Mulder-Stapel, A.A., Ginsel, L.A., and Daems, W.T. (1981b). The effect

of chloroquine on lysosomal function and cell-coat glycoprotein transport in the absorptive cells of cultured human small-intestinal tissue. Cell Tissue Res. *218*, 227–251.

Blume, von, J., Duran, J.M., Forlanelli, E., Alleaume, A.-M., Egorov, M., Polishchuk, R., Molina, H., and Malhotra, V. (2009). Actin remodeling by ADF/cofilin is required for cargo sorting at the trans-Golgi network. J. Cell Biol. *187*, 1055–1069.

Bolino, A., Muglia, M., Conforti, F.L., LeGuern, E., Salih, M.A., Georgiou, D.M., Christodoulou, K., Hausmanowa-Petrusewicz, I., Mandich, P., Schenone, A., et al. (2000). Charcot-Marie-Tooth type 4B is caused by mutations in the gene encoding myotubularin-related protein-2. Nat. Genet. *25*, 17–19.

Bonifacino, J.S., and Rojas, R. (2006). Retrograde transport from endosomes to the trans-Golgi network. Nat. Rev. Mol. Cell Biol. *7*, 568–579.

Brown, W.J., Constantinescu, E., and Farquhar, M.G. (1984). Redistribution of mannose-6-phosphate receptors induced by tunicamycin and chloroquine. J. Cell Biol. *99*, 320–326.

Bryce, N.S., Clark, E.S., Leysath, J.L., Currie, J.D., Webb, D.J., and Weaver, A.M. (2005). Cortactin Promotes Cell Motility by Enhancing Lamellipodial Persistence. Curr. Biol. *15*, 1276–1285.

Buday, L., and Downward, J. (2007). Roles of cortactin in tumor pathogenesis. Biochim. Biophys. Acta *1775*, 263–273.

Burman, J.L., Hamlin, J.N.R., and McPherson, P.S. (2010). Scyl1 Regulates Golgi Morphology. PLoS ONE *5*, e9537.

Burn, P., Rotman, A., Meyer, R.K., and Burger, M.M. (1985). Diacylglycerol in large alpha-actinin/actin complexes and in the cytoskeleton of activated platelets. Nature *314*, 469–472.

Cai, L., Makhov, A.M., Schafer, D.A., and Bear, J.E. (2008). Coronin 1B antagonizes cortactin and remodels Arp2/3-containing actin branches in lamellipodia. Cell *134*, 828–842.

Campellone, K.G., Webb, N.J., Znameroski, E.A., and Welch, M.D. (2008). WHAMM Is an Arp2/3 Complex Activator That Binds Microtubules and Functions in ER to Golgi Transport. Cell *134*, 148–161.

Cao, H., Chen, J., Krueger, E.W., and McNiven, M.A. (2010). SRC-mediated phosphorylation of dynamin and cortactin regulates the “constitutive” endocytosis of transferrin. Mol. Cell. Biol. *30*, 781–792.

Cao, H., Orth, J.D., Chen, J., Weller, S.G., Heuser, J.E., and McNiven, M.A. (2003). Cortactin is a component of clathrin-coated pits and participates in receptor-mediated endocytosis. Mol. Cell. Biol. *23*, 2162–2170.

Cao, H., Weller, S., Orth, J.D., Chen, J., Huang, B., Chen, J.-L., Stamnes, M.,

and McNiven, M.A. (2005). Actin and Arf1-dependent recruitment of a cortactin–dynamin complex to the Golgi regulates post-Golgi transport. Nat. Cell Biol. *7*, 483–492.

Carnell, M., Zech, T., Calaminus, S.D., Ura, S., Hagedorn, M., Johnston, S.A., May, R.C., Soldati, T., Machesky, L.M., and Insall, R.H. (2011). Actin polymerization driven by WASH causes V-ATPase retrieval and vesicle neutralization before exocytosis. J. Cell Biol. *193*, 831–839.

Castro-Castro, A., Janke, C., Montagnac, G., Paul-Gilloteaux, P., and Chavrier, P. (2012). ATAT1/MEC-17 acetyltransferase and HDAC6 deacetylase control a balance of acetylation of alpha-tubulin and cortactin and regulate MT1-MMP trafficking and breast tumor cell invasion. Eur. J. Cell Biol. *91*, 950–960.

Chen, Y.A., and Scheller, R.H. (2001) SNARE-mediated membrane fusion. Nat. Rev. Mol. Cell Biol. *2*, 98-106.

Chesarone, M.A., and Goode, B.L. (2009). Actin nucleation and elongation factors: mechanisms and interplay. Curr. Opin. Cell Biol. *21*, 28–37.

Choudhury, A., Dominguez, M., Puri, V., Sharma, D.K., Narita, K., Wheatley, C.L., Marks, D.L., and Pagano, R.E. (2002). Rab proteins mediate Golgi transport of caveola-internalized glycosphingolipids and correct lipid trafficking in Niemann-Pick C cells. J. Clin. Invest. *109*, 1541–1550.

Chow, C.Y., Zhang, Y., Dowling, J.J., Jin, N., Adamska, M., Shiga, K., Szigeti, K., Shy, M.E., Li, J., Zhang, X., et al. (2007). Mutation of FIG4 causes neurodegeneration in the pale tremor mouse and patients with CMT4J. Nature *448*, 68–72.

Chuma, M., Sakamoto, M., Yasuda, J., Fujii, G., Nakanishi, K., Tsuchiya, A., Ohta, T., Asaka, M., and Hirohashi, S. (2004). Overexpression of cortactin is involved in motility and metastasis of hepatocellular carcinoma. J. Hepatol. *41*, 629–636.

Clark, E., and Weaver, A. (2008). A new role for cortactin in invadopodia: Regulation of protease secretion. Eur. J. Cell Biol. *87*, 581–590.

Clark, E.S., Brown, B., Whigham, A.S., Kochaishvili, A., Yarbrough, W.G., and Weaver, A.M. (2009). Aggressiveness of HNSCC tumors depends on expression levels of cortactin, a gene in the 11q13 amplicon. Oncogene *28*, 431–444.

Clark, E.S., Whigham, A.S., Yarbrough, W.G., and Weaver, A.M. (2007). Cortactin is an essential regulator of matrix metalloproteinase secretion and extracellular matrix degradation in invadopodia. Cancer Research *67*, 4227–4235.

Coen, K., Flannagan, R.S., Baron, S., Carraro-Lacroix, L.R., Wang, D., Vermeire, W., Michiels, C., Munck, S., Baert, V., Sugita, S., et al. (2012). Lysosomal calcium homeostasis defects, not proton pump defects, cause endo-lysosomal dysfunction in PSEN-deficient cells. J. Cell Biol. *198*, 23–35.

Colombo, M., Raposo, G., and Thery, C. (2014). Biogenesis, secretion, and intercellular interactions of exosomes and other extracellular vesicles. Annu. Rev. Cell Dev. Biol. *30*, 255–289.

Connolly, C.N., Futter, C.E., Gibson, A., Hopkins, C.R., and Cutler, D.F. (1994). Transport into and out of the Golgi complex studied by transfecting cells with cDNAs encoding horseradish peroxidase. J. Cell Biol. *127*, 641–652.

Cooper, J.A., and Sept, D. (2008). New insights into mechanism and regulation of actin capping protein. Int. Rev. Cell Mol. Biol. *267*, 183–206.

Cudmore, S., Cossart, P., Griffiths, G., and Way, M. (1995). Actin-based motility of vaccinia virus. Nature *378*, 636–638.

de Lartigue, J., Polson, H., Feldman, M., Shokat, K., Tooze, S.A., Urbé, S., and Clague, M.J. (2009). PIKfyve Regulation of Endosome-Linked Pathways. Traffic *10*, 883–893.

Derby, M.C., Lieu, Z.Z., Brown, D., Stow, J.L., Goud, B., and Gleeson, P.A. (2007). The trans-Golgi network golgin, GCC185, is required for endosome-to-Golgi transport and maintenance of Golgi structure. Traffic *8*, 758–773.

Derivery, E., Helfer, E., Henriot, V., and Gautreau, A. (2012). Actin Polymerization Controls the Organization of WASH Domains at the Surface of Endosomes. PLoS ONE *7*, e39774.

Derivery, E., Sousa, C., Gautier, J.J., Lombard, B., Loew, D., and Gautreau, A. (2009). The Arp2/3 Activator WASH Controls the Fission of Endosomes through a Large Multiprotein Complex. Dev. Cell *17*, 712–723.

di Campli, A., Valderrama, F., Babià, T., De Matteis, M.A., Luini, A., and Egea, G. (1999). Morphological changes in the Golgi complex correlate with actin cytoskeleton rearrangements. Cell Motil. Cytoskeleton *43*, 334–348.

Di Paolo, G., and De Camilli, P. (2006). Phosphoinositides in cell regulation and membrane dynamics. Nature *443*, 651–657.

Dippold, H.C., Ng, M.M., Farber-Katz, S.E., Lee, S.-K., Kerr, M.L., Peterman, M.C., Sim, R., Wiharto, P.A., Galbraith, K.A., Madhavarapu, S., et al. (2009). GOLPH3 bridges phosphatidylinositol-4- phosphate and actomyosin to stretch and shape the Golgi to promote budding. Cell *139*, 337–351.

Dong, B., Kakihara, K., Otani, T., Wada, H., and Hayashi, S. (2013). Rab9 and retromer regulate retrograde trafficking of luminal protein required for epithelial tube length control. Nat. Comms. *4*, 1358.

Dong, X.-P., Shen, D., Wang, X., Dawson, T., Li, X., Zhang, Q., Cheng, X., Zhang, Y., Weisman, L.S., Delling, M., et al. (2010). PI(3,5)P2 controls membrane trafficking by direct activation of mucolipin Ca2+ release channels in the endolysosome. Nat. Comms. *1*, 1–11.

Dove, S.K., Dong, K., Kobayashi, T., Williams, F.K., and Michell, R.H. (2009). Phosphatidylinositol 3,5-bisphosphate and Fab1p/PIKfyve underPPIn endo-lysosome function. Biochem. J. *419*, 1.

Dove, S.K., Piper, R.C., McEwen, R.K., Yu, J.W., King, M.C., Hughes, D.C., Thuring, J., Holmes, A.B., Cooke, F.T., Michell, R.H., et al. (2004). Svp1p defines a family of phosphatidylinositol 3,5-bisphosphate effectors. EMBO J. *23*, 1922–1933.

Drengk, A., Fritsch, J., Schmauch, C., Rühling, H., and Maniak, M. (2003). A Coat of Filamentous Actin Prevents Clustering of Late-Endosomal Vacuoles in Vivo. Curr. Biol. *13*, 1814–1819.

Du, Y., Weed, S.A., Xiong, W.C., Marshall, T.D., and Parsons, J.T. (1998). Identification of a novel cortactin SH3 domain-binding protein and its localization to growth cones of cultured neurons. Mol. Cell. Biol. *18*, 5838–5851.

Dudek, S.M., Birukov, K.G., Zhan, X., and Garcia, J.G.N. (2002). Novel interaction of cortactin with endothelial cell myosin light chain kinase. Biochem. Biophys. Res. Commun. *298*, 511–519.

Duleh, S.N., and Welch, M.D. (2010). WASH and the Arp2/3 complex regulate endosome shape and trafficking. Cytoskeleton (Hoboken) *67*, 193–206.

Egea, G., Lázaro-Diéguez, F., and Vilella, M. (2006). Actin dynamics at the Golgi complex in mammalian cells. Curr. Opin. Cell Biol. *18*, 168–178.

Egorov, M.V., Capestrano, M., Vorontsova, O.A., Di Pentima, A., Egorova, A.V., Mariggiò, S., Ayala, M.I., Tetè, S., Gorski, J.L., Luini, A., et al. (2009). Faciogenital dysplasia protein (FGD1) regulates export of cargo proteins from the golgi complex via Cdc42 activation. Mol. Biol. Cell *20*, 2413–2427.

Engqvist-Goldstein, A.E.Y., Zhang, C.X., Carreno, S., Barroso, C., Heuser, J.E., and Drubin, D.G. (2004). RNAi-mediated Hip1R silencing results in stable association between the endocytic machinery and the actin assembly machinery. Mol. Biol. Cell *15*, 1666–1679.

Feinstein, T.N., and Linstedt, A.D. (2008). GRASP55 regulates Golgi ribbon formation. Mol. Biol. Cell *19*, 2696–2707.

Ferguson, C.J., Lenk, G.M., and Meisler, M.H. (2009). Defective autophagy in neurons and astrocytes from mice deficient in PI(3,5)P2. Hum. Mol. Genet. *18*, 4868–4878.

Fletcher, S.J., and Rappoport, J.Z. (2009). The role of vesicle trafficking in epithelial cell motility. Biochem. Soc. Trans. *37*, 1072–1076.

Fraldi, A., Annunziata, F., Lombardi, A., Kaiser, H.-J., Medina, D.L., Spampanato, C., Fedele, A.O., Polishchuk, R., Sorrentino, N.C., Simons, K., et al. (2010). Lysosomal fusion and SNARE function are impaired by cholesterol accumulation in lysosomal storage disorders. EMBO J. *29*, 3607–3620.

Fraley, T.S., Pereira, C.B., Tran, T.C., Singleton, C., and Greenwood, J.A. (2005). Phosphoinositide binding regulates alpha-actinin dynamics: mechanism for modulating cytoskeletal remodeling. J. Biol. Chem. *280*, 15479–15482.

Fucini, R.V., Chen, J.-L., Sharma, C., Kessels, M.M., and Stamnes, M. (2002). Golgi vesicle proteins are linked to the assembly of an actin complex defined by mAbp1. Mol. Biol. Cell *13*, 621–631.

Gandhi, M., Smith, B.A., Bovellan, M., Paavilainen, V., Daugherty-Clarke, K., Gelles, J., Lappalainen, P., and Goode, B.L. (2010). GMF is a cofilin homolog that binds Arp2/3 complex to stimulate filament debranching and inhibit actin nucleation. Curr. Biol. *20*, 861–867.

Ganley, I.G., and Pfeffer, S.R. (2006). Cholesterol accumulation sequesters Rab9 and disrupts late endosome function in NPC1-deficient cells. J. Biol. Chem. *281*, 17890–17899.

Gary, J.D., Wurmser, A.E., Bonangelino, C.J., Weisman, L.S., Emr, S.D.(1998). Fab1p is essential for PtdIns(3)P 5-kinase activity and the maintenance of vacuolar size and membrane homeostasis. J. Cell Biol. *143*, 65–79.

Goley, E.D., and Welch, M.D. (2006). The ARP2/3 complex: an actin nucleator comes of age. Nat. Rev. Mol. Cell Biol. *7*, 713–726.

Gomez, T.S., and Billadeau, D.D. (2009). A FAM21-Containing WASH Complex Regulates Retromer-Dependent Sorting. Dev. Cell *17*, 699–711.

Gomez, T.S., Gorman, J.A., de Narvajas, A.A.-M., Koenig, A.O., and Billadeau, D.D. (2012). Trafficking defects in WASH-knockout fibroblasts originate from collapsed endosomal and lysosomal networks. Mol. Biol. Cell *23*, 3215–3228.

Grassart, A., Meas-Yedid, V., Dufour, A., Olivo-Marin, J.-C., Dautry-Varsat, A., and Sauvonnet, N. (2010). Pak1 phosphorylation enhances cortactin-N-WASP interaction in clathrin-caveolin-independent endocytosis. Traffic *11*, 1079–1091.

Guo, Y., and Linstedt, A.D. (2006). COPII-Golgi protein interactions regulate COPII coat assembly and Golgi size. J. Cell Biol. *174*, 53–63.

Harrington, A.W., St Hillaire, C., Zweifel, L.S., Glebova, N.O., Philippidou, P., Halegoua, S., and Ginty, D.D. (2011). Recruitment of actin modifiers to TrkA endosomes governs retrograde NGF signaling and survival. Cell *146*, 421–434.

Hayes, G.L., and Pfeffer, S.R. (2008). WHAMMing into the Golgi. Developmental Cell *15*, 171–172.

He, H., Watanabe, T., Zhan, X., Huang, C., Schuuring, E., Fukami, K., Takenawa, T., Kumar, C.C., Simpson, R.J., and Maruta, H. (1998). Role of phosphatidylinositol 4,5-bisphosphate in Ras/Rac-induced disruption of the cortactin-actomyosin II complex and malignant transformation. Mole. Cell. Biol. *18*, 3829–3837.

Heard, J.M., Bruyère, J., Roy, E., Bigou, S., Ausseil, J., and Vitry, S. (2010). Storage problems in lysosomal diseases. Biochem. Soc. Trans. *38*, 1442–1447.

Hehnly, H., Xu, W., Chen, J.-L., and Stamnes, M. (2010). Cdc42 regulates microtubule-dependent Golgi positioning. Traffic *11*, 1067–1078.

Helgeson, L.A., and Nolen, B.J. (2013). Mechanism of synergistic activation of Arp2/3 complex by cortactin and N-WASP. eLife *2*, e00884–e00884.

Helgeson, L.A., Prendergast, J.G., Wagner, A.R., Rodnick-Smith, M., and Nolen, B.J. (2014). Interactions with Actin Monomers, Actin Filaments and Arp2/3 Complex Define the Roles of WASP Family Proteins and Cortactin in Coordinately Regulating Branched Actin Networks. J. Biol. Chem. 289, 28856-28869.

Hetrick, B., Han, M.S., Helgeson, L.A., and Nolen, B.J. (2013). Small Molecules CK-666 and CK-869 Inhibit Actin-Related Protein 2/3 Complex by Blocking an Activating Conformational Change. Chem. Biol. *20*, 701–712.

Higgs, H.N., and Pollard, T.D. (2001). Regulation of actin filament network formation through ARP2/3 complex: activation by a diverse array of proteins. Annu. Rev. Biochem. *70*, 649–676.

Hirschberg, K., Miller, C.M., Ellenberg, J., Presley, J.F., Siggia, E.D., Phair, R.D., and Lippincott-Schwartz, J. (1998). Kinetic analysis of secretory protein traffic and characterization of golgi to plasma membrane transport intermediates in living cells. J. Cell Biol. *143*, 1485–1503.

Ho, C.Y., Alghamdi, T.A., and Botelho, R.J. (2011). Phosphatidylinositol-3,5-Bisphosphate: No Longer the Poor PIP2. Traffic *13*, 1–8.

Holliday, L.S., Lu, M., Lee, B.S., Nelson, R.D., Solivan, S., Zhang, L., and Gluck, S.L. (2000). The amino-terminal domain of the B subunit of vacuolar H+-ATPase contains a filamentous actin binding site. J. Biol. Chem. *275*, 32331–32337.

Hou, P., Estrada, L., Kinley, A.W., Parsons, J.T., Vojtek, A.B., and Gorski, J.L. (2003). Fgd1, the Cdc42 GEF responsible for Faciogenital Dysplasia, directly interacts with cortactin and mAbp1 to modulate cell shape. Hum. Mol. Genet. *12*, 1981–1993.

Howell, G.J., Holloway, Z.G., Cobbold, C., Monaco, A.P., and Ponnambalam, S. (2006). Cell biology of membrane trafficking in human disease. Int. Rev. Cytol. *252*, 1–69.

Hölttä-Vuori, M., Alpy, F., Tanhuanpää, K., Jokitalo, E., Mutka, A.-L., and Ikonen, E. (2005). MLN64 is involved in actin-mediated dynamics of late endocytic organelles. Mol. Biol. Cell *16*, 3873–3886.

Huang, C., Tandon, N.N., Greco, N.J., Ni, Y., Wang, T., and Zhan, X. (1997). Proteolysis of platelet cortactin by calpain. J. Biol.Chem. *272*, 19248–19252.

Huotari, J., and Helenius, A. (2011). Focus Review Endosome maturation. EMBO J. *30*, 3481–3500.

Ikonen, E. (2006). Mechanisms for cellular cholesterol transport: defects and human disease. Physiol. Rev. *86*, 1237–1261.

Ikonomov, O.C., Sbrissa, D., and Shisheva, A. (2001). Mammalian cell morphology and endocytic membrane homeostasis require enzymatically active

phosphoinositide 5-kinase PIKfyve. J. Biol. Chem. *276*, 26141–26147.

Ikonomov, O.C., Sbrissa, D., and Shisheva, A. (2006). Localized PtdIns 3,5-P2 synthesis to regulate early endosome dynamics and fusion. Am. J. Cell Physiol. *291*, C393–C404.

Ikonomov, O.C., Sbrissa, D., and Shisheva, A. (2009a). YM201636, an inhibitor of retroviral budding and PIKfyve-catalyzed PtdIns(3,5)P2 synthesis, halts glucose entry by insulin in adipocytes. Biochem. Biophys. Res. Commun. *382*, 566–570.

Ikonomov, O.C., Sbrissa, D., Delvecchio, K., Feng, H.-Z., Cartee, G.D., Jin, J.-P., and Shisheva, A. (2013). Muscle-specific Pikfyve gene disruption causes glucose intolerance, insulin resistance, adiposity, and hyperinsulinemia but not muscle fiber-type switching. Am. J. Physiol. Endocrinol. Metab. *305*, E119–E131.

Ikonomov, O.C., Sbrissa, D., Delvecchio, K., Xie, Y., Jin, J.-P., Rappolee, D., and Shisheva, A. (2011). The phosphoinositide kinase PIKfyve is vital in early embryonic development: preimplantation lethality of PIKfyve-/- embryos but normality of PIKfyve+/- mice. J. Biol. Chem. *286*, 13404–13413.

Ikonomov, O.C., Sbrissa, D., Fenner, H., and Shisheva, A. (2009b). PIKfyve-ArPIKfyve-Sac3 core complex: contact sites and their consequence for Sac3 phosphatase activity and endocytic membrane homeostasis. J. Biol. Chem. *284*, 35794–35806.

Itoh, Y., and Seiki, M. (2006). MT1-MMP: a potent modifier of pericellular microenvironment. J. Cell. Physiol. *206*, 1–8.

Janmey, P.A., and Stossel, T.P. (1987). Modulation of gelsolin function by phosphatidylinositol 4,5-bisphosphate. Nature *325*, 362–364.

Janmey, P.A., and Lindberg, U. (2004). Cytoskeletal regulation: rich in lipids. Nat. Rev. Mol. Cell Biol. *5*, 658–666.

Jefferies, H.B.J., Cooke, F.T., Jat, P., Boucheron, C., Koizumi, T., Hayakawa, M., Kaizawa, H., Ohishi, T., Workman, P., Waterfield, M.D., et al. (2008). A selective PIKfyve inhibitor blocks PtdIns(3,5)P2 production and disrupts endomembrane transport and retroviral budding. EMBO Rep. *9*, 164–170.

Jerome, W.G., Cash, C., Webber, R., Horton, R., and Yancey, P.G. (1998). Lysosomal lipid accumulation from oxidized low density lipoprotein is correlated with hypertrophy of the Golgi apparatus and trans-Golgi network. J. Lipid Res. *39*, 1362–1371.

Jia, D., Gomez, T.S., Metlagel, Z., Umetani, J., Otwinowski, Z., Rosen, M.K., and Billadeau, D.D. (2010). WASH and WAVE actin regulators of the Wiskott-Aldrich syndrome protein (WASP) family are controlled by analogous structurally related complexes. Proc. Natl. Acad. Sci. U.S.A. *107*, 10442–10447.

Jin, N., Chow, C.Y., Liu, L., Zolov, S.N., Bronson, R., Davisson, M., Petersen, J.L., Zhang, Y., Park, S., Duex, J.E., et al. (2008). VAC14 nucleates a protein complex

essential for the acute interconversion of PI3P and PI(3,5)P(2) in yeast and mouse. EMBO J. *27*, 3221–3234.

Kaksonen, M., Toret, C.P., and Drubin, D.G. (2006). Harnessing actin dynamics for clathrin-mediated endocytosis. Nat. Rev. Mol. Cell Biol. *7*, 404–414.

Kanner, S.B., Reynolds, A.B., Vines, R.R., and Parsons, J.T. (1990). Monoclonal antibodies to individual tyrosine-phosphorylated protein substrates of oncogene-encoded tyrosine kinases. Proc. Natl. Acad. Sci. U.S.A. *87*, 3328–3332.

Katsube, T., Takahisa, M., Ueda, R., Hashimoto, N., Kobayashi, M., and Togashi, S. (1998). Cortactin associates with the cell-cell junction protein ZO-1 in both Drosophila and mouse. J. Biol. Chem. *273*, 29672–29677.

Katsube, T., Togashi, S., Hashimoto, N., Ogiu, T., and Tsuji, H. (2004). Filamentous actin binding ability of cortactin isoforms is responsible for their cell-cell junctional localization in epithelial cells. Arch. Biochem. Biophys. *427*, 79–90.

Kessels, M.M., Engqvist-Goldstein, A.E., Drubin, D.G., and Qualmann, B. (2001). Mammalian Abp1, a signal-responsive F-actin-binding protein, links the actin cytoskeleton to endocytosis via the GTPase dynamin. J. Cell Biol. *153*, 351–366.

Kessels, M.M., and Qualmann, B. (2004). The syndapin protein family: linking membrane trafficking with the cytoskeleton. J. Cell Sci. *117*, 3077–3086.

Kienzle, C., and Blume, von, J. (2014). Secretory cargo sorting at the trans-Golgi network. Trends Cell Biol. *24*, 584–593.

Kinley, A.W., Weed, S.A., Weaver, A.M., Karginov, A.V., Bissonette, E., Cooper, J.A., and Parsons, J.T. (2003). Cortactin interacts with WIP in regulating Arp2/3 activation and membrane protrusion. Curr. Biol. *13*, 384–393.

Kirkbride, K.C., Hong, N.H., French, C.L., Clark, E.S., Jerome, W.G., and Weaver, A.M. (2012). Regulation of late endosomal/lysosomal maturation and trafficking by cortactin affects Golgi morphology. Cytoskeleton *69*, 625–643.

Kirkbride, K.C., Sung, B.H., Sinha, S., and Weaver, A.M. (2011). Cortactin: A multifunctional regulator of cellular invasiveness. Celladhesion *5*, 187–198.

Kjeken, R., Egeberg, M., Habermann, A., Kuehnel, M., Peyron, P., Floetenmeyer, M., Walther, P., Jahraus, A., Defacque, H., Kuznetsov, S.A., et al. (2004). Fusion between phagosomes, early and late endosomes: a role for actin in fusion between late, but not early endocytic organelles. Mol. Biol. Cell *15*, 345–358.

Klausner, R.D., Donaldson, J.G., and Lippincott-Schwartz, J. (1992). Brefeldin A: insights into the control of membrane traffic and organelle structure. J. Cell Biol. *116*, 1071–1080.

Kobayashi, T., Beuchat, M.H., Lindsay, M., Frias, S., Palmiter, R.D., Sakuraba, H., Parton, R.G., and Gruenberg, J. (1999). Late endosomal membranes rich in lysobisphosphatidic acid regulate cholesterol transport. Nat. Cell Biol. *1*, 113–118.

Kokkonen, N., Rivinoja, A., Kauppila, A., Suokas, M., Kellokumpu, I., and Kellokumpu, S. (2004). Defective acidification of intracellular organelles results in aberrant secretion of cathepsin D in cancer cells. J.Biol. Chemi. *279*, 39982–39988.

Kotoulas, A., Kokotas, H., Kopsidas, K., Droutsas, K., Grigoriadou, M., Bajrami, H., Schorderet, D.F., and Petersen, M.B. (2011). A novel PIKFYVE mutation in fleck corneal dystrophy. Mol. Vis. *17*, 2776–2781.

Kowalski, J.R., Egile, C., Gil, S., Snapper, S.B., Li, R., and Thomas, S.M. (2005). Cortactin regulates cell migration through activation of N-WASP. J. Cell Sci. *118*, 79–87.

Kutateladze, T.G. (2010). Translation of the phosphoinositide code by PI effectors. Nat. Chem. Biol. *6*, 507–513.

Lai, F.P.L., Szczodrak, M., Block, J., Faix, J., Breitsprecher, D., Mannherz, H.G., Stradal, T.E.B., Dunn, G.A., Small, J.V., and Rottner, K. (2008). Arp2/3 complex interactions and actin network turnover in lamellipodia. EMBO J. *27*, 982–992.

Lanzetti, L. (2007). Actin in membrane trafficking. Curr. Opin. Cell Biol. *19*, 453–458.

Lázaro-Diéguez, F., Colonna, C., Cortegano, M., Calvo, M., Martínez, S.E., and Egea, G. (2007). Variable actin dynamics requirement for the exit of different cargo from the trans-Golgi network. FEBS Letters *581*, 3875–3881.

Lázaro-Diéguez, F., Jiménez, N., Barth, H., Koster, A.J., Renau-Piqueras, J., Llopis, J.L., Burger, K.N.J., and Egea, G. (2006). Actin filaments are involved in the maintenance of Golgi cisternae morphology and intra-Golgi pH. Cell Motil. Cytoskeleton *63*, 778–791.

Lee, J.-Y., Koga, H., Kawaguchi, Y., Tang, W., Wong, E., Gao, Y.-S., Pandey, U.B., Kaushik, S., Tresse, E., Lu, J., et al. (2010). HDAC6 controls autophagosome maturation essential for ubiquitin-selective quality-control autophagy. EMBO J. *29*, 969–980.

Lemmon, M.A. (2008). Membrane recognition by phospholipid-binding domains. Nat. Rev. Mol. Cell Biol. *9*, 99–111.

Li, X.-Y., Ota, I., Yana, I., Sabeh, F., and Weiss, S.J. (2008). Molecular dissection of the structural machinery underlying the tissue-invasive activity of membrane type-1 matrix metalloproteinase. Mol. Biol. Cell *19*, 3221–3233.

Li, X., Wang, X., Zhang, X., Zhao, M., Tsang, W.L., Zhang, Y., Yau, R.G.W., Weisman, L.S., and Xu, H. (2013). Genetically encoded fluorescent probe to visualize intracellular phosphatidylinositol 3,5-bisphosphate localization and dynamics. Proc. Natl. Acad. Sci. U.S.A. *110*, 21165–21170.

Liégeois, S., Benedetto, A., Garnier, J.-M., Schwab, Y., and Labouesse, M. (2006). The V0-ATPase mediates apical secretion of exosomes containing Hedgehog-related proteins in Caenorhabditis elegans. J. Cell Biol. *173*, 949–961.

Liu, A.P., and Fletcher, D.A. (2006). Actin Polymerization Serves as a Membrane Domain Switch in Model Lipid Bilayers. Biophys. J. *91*, 4064–4070.

Lladó, A., Timpson, P., Vilà de Muga, S., Moretó, J., Pol, A., Grewal, T., Daly, R.J., Enrich, C., and Tebar, F. (2008). Protein kinase Cdelta and calmodulin regulate epidermal growth factor receptor recycling from early endosomes through Arp2/3 complex and cortactin. Mol. Biol. Cell *19*, 17–29.

Lowe, M. (2002). Golgi complex: biogenesis de novo? Curr. Biol. *12*, R166–R167.

Luan, Q., and Nolen, B.J. (2013). Structural basis for regulation of Arp2/3 complex by GMF. Nat. Struct. Mol. Biol. *20*, 1062–1068.

Lynch, D.K., Winata, S.C., Lyons, R.J., Hughes, W.E., Lehrbach, G.M., Wasinger, V., Corthals, G., Cordwell, S., and Daly, R.J. (2003). A Cortactin-CD2-associated protein (CD2AP) complex provides a novel link between epidermal growth factor receptor endocytosis and the actin cytoskeleton. J. Biol. Chem. *278*, 21805–21813.

Martin, S., Harper, C.B., May, L.M., Coulson, E.J., Meunier, F.A., and Osborne, S.L. (2013). Inhibition of PIKfyve by YM-201636 dysregulates autophagy and leads to apoptosis-independent neuronal cell death. PLoS ONE *8*, e60152.

Martinez-Quiles, N., Ho, H.-Y.H., Kirschner, M.W., Ramesh, N., and Geha, R.S. (2004). Erk/Src phosphorylation of cortactin acts as a switch on-switch off mechanism that controls its ability to activate N-WASP. Mol. Cell. Biol. *24*, 5269–5280.

Matas, O.B., Martínez-Menárguez, J.A., and Egea, G. (2004). Association of Cdc42/N-WASP/Arp2/3 signaling pathway with Golgi membranes. Traffic *5*, 838–846.

Maxfield, F.R., and Tabas, I. (2005). Role of cholesterol and lipid organization in disease. Nature *438*, 612–621.

McCrea, H.J., and De Camilli, P. (2009). Mutations in phosphoinositide metabolizing enzymes and human disease. Physiology *24*, 8–16.

McNiven, M.A., Kim, L., Krueger, E.W., Orth, J.D., Cao, H., and Wong, T.W. (2000). Regulated interactions between dynamin and the actin-binding protein cortactin modulate cell shape. J. Cell Biol. *151*, 187–198.

Merrifield, C.J., Moss, S.E., Ballestrem, C., Imhof, B.A., Giese, G., Wunderlich, I., and Almers, W. (1999). Endocytic vesicles move at the tips of actin tails in cultured mast cells. Nat. Cell. Biol. *1*, 72–74.

Merrifield, C.J., Perrais, D., and Zenisek, D. (2005). Coupling between clathrin-coated-pit invagination, cortactin recruitment, and membrane scission observed in live cells. Cell *121*, 593–606.

Merrifield, C.J., Qualmann, B., Kessels, M.M., and Almers, W. (2004). Neural Wiskott Aldrich Syndrome Protein (N-WASP) and the Arp2/3 complex are recruited to

sites of clathrin-mediated endocytosis in cultured fibroblasts. Eur. J. Cell Biol. *83*, 13–18.

Michell, R.H., Heath, V.L., Lemmon, M.A., and Dove, S.K. (2006). Phosphatidylinositol 3,5-bisphosphate: metabolism and cellular functions. Trends Biochem. Sci. *31*, 52–63.

Miki, H., Miura, K., and Takenawa, T. (1996). N-WASP, a novel actin-depolymerizing protein, regulates the cortical cytoskeletal rearrangement in a PIP2-dependent manner downstream of tyrosine kinases. EMBO J. *15*, 5326–5335.

Millard, T.H., Sharp, S.J., and Machesky, L.M. (2004). Signalling to actin assembly via the WASP (Wiskott-Aldrich syndrome protein)-family proteins and the Arp2/3 complex. Biochem. J. *380*, 1–17.

Monteiro, P., Rossé, C., Castro-Castro, A., Irondelle, M., Lagoutte, E., Paul-Gilloteaux, P., Desnos, C., Formstecher, E., Darchen, F., Perrais, D., et al. (2013). Endosomal WASH and exocyst complexes control exocytosis of MT1-MMP at invadopodia. J.Cell Biol. *203*, 1063–1079.

Morton, W.M., Ayscough, K.R., and McLaughlin, P.J. (2000). Latrunculin alters the actin-monomer subunit interface to prevent polymerization. Nat. Cell Biol. *2*, 376–378.

Mukherjee, S., and Maxfield, F.R. (2004). Lipid and cholesterol trafficking in NPC. Biochim. Biophys. Acta *1685*, 28–37.

Mullins, R.D., Heuser, J.A., and Pollard, T.D. (1998). The interaction of Arp2/3 complex with actin: nucleation, high affinity pointed end capping, and formation of branching networks of filaments. Proc. Natl. Acad. Sci. U.S.A. *95*, 6181–6186.

Nakayama, Y., Hisano, T., Okimoto, T., Tanaka, Y., Ishikawa, T., Himeno, M., Ono, M., and Kuwano, M. (1994). Microtubule reorganization and lysosome redistribution by a viral v-src oncogene, in mouse Balb/3T3 cells expressing human EGF receptor. Cell Struct. Funct. *19*, 397–409.

Narita, M., Young, A.R.J., Arakawa, S., Samarajiwa, S.A., Nakashima, T., Yoshida, S., Hong, S., Berry, L.S., Reichelt, S., Ferreira, M., et al. (2011). Spatial coupling of mTOR and autophagy augments secretory phenotypes. Science *332*, 966–970.

Nicot, A.-S., Fares, H., Payrastre, B., Chisholm, A.D., Labouesse, M., and Laporte, J. (2006). The phosphoinositide kinase PIKfyve/Fab1p regulates terminal lysosome maturation in Caenorhabditis elegans. Mol. Biol. Cell *17*, 3062–3074.

Nolen, B.J., Tomasevic, N., Russell, A., Pierce, D.W., Jia, Z., McCormick, C.D., Hartman, J., Sakowicz, R., and Pollard, T.D. (2009). Characterization of two classes of small molecule inhibitors of Arp2/3 complex. Nature *460*, 1031–1034.

Novikoff, A.B., Essner, E., and Quintana, N. (1964). Golgi Apparatus and Lysosomes. Fed. Proc. *23*, 1010–1022.

Ohashi, E., Tanabe, K., Henmi, Y., Mesaki, K., Kobayashi, Y., and Takei, K. (2011). Receptor sorting within endosomal trafficking pathway is facilitated by dynamic actin filaments. PLoS ONE *6*, e19942–e19942.

Oikawa, T., Yamaguchi, H., Itoh, T., Kato, M., Ijuin, T., Yamazaki, D., Suetsugu, S., and Takenawa, T. (2004). PtdIns(3,4,5)P3 binding is necessary for WAVE2-induced formation of lamellipodia. Nat. Cell Biol. *6*, 420–426.

Onabajo, O.O., Seeley, M.K., Kale, A., Qualmann, B., Kessels, M., Han, J., Tan, T.-H., and Song, W. (2008). Actin-binding protein 1 regulates B cell receptor-mediated antigen processing and presentation in response to B cell receptor activation. J. Immunol. *180*, 6685–6695.

Ono, S. (2007). Mechanism of depolymerization and severing of actin filaments and its significance in cytoskeletal dynamics. Int. Rev. Cytol. *258*, 1–82.

Ormandy, C.J., Musgrove, E.A., Hui, R., Daly, R.J., and Sutherland, R.L. (2003). Cyclin D1, EMS1 and 11q13 amplification in breast cancer. Breast Cancer Res. Treat. *78*, 323–335.

Oser, M., Yamaguchi, H., Mader, C.C., Bravo-Cordero, J.J., Arias, M., Chen, X., Desmarais, V., van Rheenen, J., Koleske, A.J., and Condeelis, J. (2009). Cortactin regulates cofilin and N-WASp activities to control the stages of invadopodium assembly and maturation. J. Cell Biol. *186*, 571–587.

Otomo, A., Pan, L., and Hadano, S. (2012). Dysregulation of the autophagy-endolysosomal system in amyotrophic lateral sclerosis and related motor neuron diseases. Neurol. Res. Int. *2012*, 498428–12.

Paavilainen, V.O., Bertling, E., Falck, S., and Lappalainen, P. (2004). Regulation of cytoskeletal dynamics by actin-monomer-binding proteins. Trends Cell Biol. *14*, 386–394.

Panaretou, C., and Tooze, S.A. (2002). Regulation and recruitment of phosphatidylinositol 4-kinase on immature secretory granules is independent of ADP-ribosylation factor 1. Biochem. J. *363*, 289–295.

Papayannopoulos, V., Co, C., Prehoda, K.E., Snapper, S., Taunton, J., and Lim, W.A. (2005). A Polybasic Motif Allows N-WASP to Act as a Sensor of PIP2 Density. Mol. Cell *17*, 181–191.

Park, L., Thomason, P.A., Zech, T., King, J.S., Veltman, D.M., Carnell, M., Ura, S., Machesky, L.M., and Insall, R.H. (2013). Cyclical Action of the WASH Complex: FAM21 and Capping Protein Drive WASH Recycling, Not Initial Recruitment. Dev. Cell *24*, 169–181.

Patel, A.M., Incognito, L.S., Schechter, G.L., Wasilenko, W.J., and Somers, K.D. (1996). Amplification and expression of EMS-1 (cortactin) in head and neck squamous cell carcinoma cell lines. Oncogene *12*, 31–35.

Patel, A.S., Schechter, G.L., Wasilenko, W.J., and Somers, K.D. (1998).

Overexpression of EMS1/cortactin in NIH3T3 fibroblasts causes increased cell motility and invasion in vitro. Oncogene *16*, 3227–3232.

Perrin, B.J., Amann, K.J., and Huttenlocher, A. (2006). Proteolysis of cortactin by calpain regulates membrane protrusion during cell migration. Mol. Biol. Cell *17*, 239–250.

Pfeffer, S.R. (2009). Multiple routes of protein transport from endosomes to the trans Golgi network. FEBS Letters *583*, 3811–3816.

Pollard, T.D., and Cooper, J.A. (2009). Actin, a central player in cell shape and movement. Science *326*, 1208–1212.

Ponnambalam, S., and Baldwin, S.A. (2003). Constitutive protein secretion from the trans-Golgi network to the plasma membrane. Mol. Membr. Biol. *20*, 129–139.

Presley, J.F., Cole, N.B., Schroer, T.A., Hirschberg, K., Zaal, K.J., and Lippincott-Schwartz, J. (1997). ER-to-Golgi transport visualized in living cells. Nature *389*, 81–85.

Press, B., Feng, Y., Hoflack, B., and Wandinger-Ness, A. (1998). Mutant Rab7 causes the accumulation of cathepsin D and cation-independent mannose 6-phosphate receptor in an early endocytic compartment. J. Cell Biol. *140*, 1075–1089.

Pryor, P.R., Mullock, B.M., Bright, N.A., Lindsay, M.R., Gray, S.R., Richardson, S.C., Stewart, A., James, D.E., Piper, R.C., Luzio, J.P. (2004) Combinatorial SNARE complex with VAMP7 or VAMP8 define different late endocytic fusion events. EMBO Rep. *5*, 590-595.

Pulvirenti, T., Giannotta, M., Capestrano, M., Capitani, M., Pisanu, A., Polishchuk, R.S., Pietro, E.S., Beznoussenko, G.V., Mironov, A.A., Turacchio, G., et al. (2008). A traffic-activated Golgi-based signalling circuit coordinates the secretory pathway. Nat. Cell Biol. *10*, 912–922.

Puthenveedu, M.A., Lauffer, B., Temkin, P., Vistein, R., Carlton, P., Thorn, K., Taunton, J., Weiner, O.D., Parton, R.G., and Zastrow, von, M. (2010). Sequence-Dependent Sorting of Recycling Proteins by Actin-Stabilized Endosomal Microdomains. Cell *143*, 761–773.

Quinn, P., Griffiths, G., and Warren, G. (1983). Dissection of the Golgi complex. II. Density separation of specific Golgi functions in virally infected cells treated with monensin. J. Cell Biol. *96*, 851–856.

Reddy, J.V., Burguete, A.S., Sridevi, K., Ganley, I.G., Nottingham, R.M., and Pfeffer, S.R. (2006). A functional role for the GCC185 golgin in mannose 6-phosphate receptor recycling. Mol. Biol. Cell *17*, 4353–4363.

Roberts, C.T., and Kurre, P. (2013). Vesicle trafficking and RNA transfer add complexity and connectivity to cell-cell communication. Cancer Res. *73*, 3200–3205.

Roepstorff, K., Grøvdal, L., Grandal, M., Lerdrup, M., and van Deurs, B. (2008). Endocytic downregulation of ErbB receptors: mechanisms and relevance in cancer.

Histochem. Cell Biol. *129*, 563–578.

Rohatgi, R., Ho, H.Y., and Kirschner, M.W. (2000). Mechanism of N-WASP activation by CDC42 and phosphatidylinositol 4, 5-bisphosphate. J. Cell Biol. *150*, 1299–1310.

Rosenfeld, J.L., Moore, R.H., Zimmer, K.P., Alpizar-Foster, E., Dai, W., Zarka, M.N., and Knoll, B.J. (2001). Lysosome proteins are redistributed during expression of a GTP-hydrolysis-defective rab5a. J. Cell Sci. *114*, 4499–4508.

Rossé, C., Lodillinsky, C., Fuhrmann, L., Nourieh, M., Monteiro, P., Irondelle, M., Lagoutte, E., Vacher, S., Waharte, F., Paul-Gilloteaux, P., et al. (2014a). Control of MT1-MMP transport by atypical PKC during breast-cancer progression. Proc. Natl. Acad. Sci. U.S.A. *111*, E1872–E1879.

Roth, M.G. (2004). Phosphoinositides in constitutive membrane traffic. Physiol. Rev. *84*, 699–730.

Rotty, J.D., Wu, C., and Bear, J.E. (2013). New insights into the regulation and cellular functions of the ARP2/3 complex. Nat. Rev. Mol. Cell Biol. *14*, 7–12.

Rudge, S.A., Anderson, D.M., and Emr, S.D. (2004). Vacuole size control: regulation of PtdIns(3,5)P2 levels by the vacuole-associated Vac14-Fig4 complex, a PtdIns(3,5)P2-specific phosphatase. Mol. Biol. Cell *15*, 24–36.

Rusten, T.E., Rodahl, L.M.W., Pattni, K., Englund, C., Samakovlis, C., Dove, S., Brech, A., and Stenmark, H. (2006). Fab1 phosphatidylinositol 3-phosphate 5-kinase controls trafficking but not silencing of endocytosed receptors. Mol. Biol. Cell *17*, 3989–4001.

Rutherford, A.C., Traer, C., Wassmer, T., Pattni, K., Bujny, M.V., Carlton, J.G., Stenmark, H., and Cullen, P.J. (2006). The mammalian phosphatidylinositol 3-phosphate 5-kinase (PIKfyve) regulates endosome-to-TGN retrograde transport. J. Cell Sci. *119*, 3944–3957.

Saarikangas, J., Zhao, H., and Lappalainen, P. (2010). Regulation of the Actin Cytoskeleton-Plasma Membrane Interplay by Phosphoinositides. Physiol. Rev. *90*, 259–289.

Salvarezza, S.B., Deborde, S., Schreiner, R., Campagne, F., Kessels, M.M., Qualmann, B., Caceres, A., Kreitzer, G., and Rodriguez-Boulan, E. (2009). LIM kinase 1 and cofilin regulate actin filament population required for dynamin-dependent apical carrier fission from the trans-Golgi network. Mol. Biol. Cell *20*, 438–451.

Sandilands, E., and Frame, M.C. (2008). Endosomal trafficking of Src tyrosine kinase. Trends Cell Biol. *18*, 322–329.

Sauvonnet, N., Dujeancourt, A., and Dautry-Varsat, A. (2005). Cortactin and dynamin are required for the clathrin-independent endocytosis of gammac cytokine receptor. J. Cell Biol. *168*, 155–163.

Sbai, O., Ould Yahoui, A., Ferhat, L., Gueye, Y., Bernard, A., Charrat, E., Mehanna, A., Risso, J.J., Chauvin, J.P., Fenouillet, E., et al. (2010). Differential vesicular distribution and trafficking of MMP-2, MMP-9, and their inhibitors in astrocytes. Glia *58*, 344–366.

Sbrissa, D., Ikonomov, O.C., Fenner, H., and Shisheva, A. (2008). ArPIKfyve Homomeric and Heteromeric Interactions Scaffold PIKfyve and Sac3 in a Complex to Promote PIKfyve Activity and Functionality. J. Mol. Biol. *384*, 766–779.

Sbrissa, D., Ikonomov, O.C., Fu, Z., Ijuin, T., Gruenberg, J., Takenawa, T., and Shisheva, A. (2007). Core protein machinery for mammalian phosphatidylinositol 3,5-bisphosphate synthesis and turnover that regulates the progression of endosomal transport. Novel Sac phosphatase joins the ArPIKfyve-PIKfyve complex. J. Biol. Chem. *282*, 23878–23891.

Schorey, J.S., and Bhatnagar, S. (2008). Exosome function: from tumor immunology to pathogen biology. Traffic *9*, 871–881.

Schuuring, E. (1995). The involvement of the chromosome 11q13 region in human malignancies: cyclin D1 and EMS1 are two new candidate oncogenes-a review. Gene *159*, 83–96.

Schuuring, E., Verhoeven, E., Litvinov, S., and Michalides, R.J. (1993). The product of the EMS1 gene, amplified and overexpressed in human carcinomas, is homologous to a v-src substrate and is located in cell-substratum contact sites. Mol. Cell. Biol. *13*, 2891–2898.

Seebohm, G., Neumann, S., Theiss, C., Novkovic, T., Hill, E.V., Tavaré, J.M., Lang, F., Hollmann, M., Manahan-Vaughan, D., and Strutz-Seebohm, N. (2012). Identification of a novel signaling pathway and its relevance for GluA1 recycling. PLoS ONE *7*, e33889.

Shin, L., Wang, S., Lee, J.S., Flack, A., Mao, G., and Jena, B.P. (2012). Lysophosphatidylcholine inhibits membrane-associated SNARE complex disassembly. J. Cell. Mol. Med. *16*, 1701–1708.

Shisheva, A. (2008). PIKfyve: Partners, significance, debates and paradoxes. Cell Biol. Int. *32*, 591–604.

Siton, O., Ideses, Y., Albeck, S., Unger, T., Bershadsky, A.D., Gov, N.S., and Bernheim-Groswasser, A. (2011). Cortactin releases the brakes in actin- based motility by enhancing WASP-VCA detachment from Arp2/3 branches. Curr. Biol. *21*, 2092–2097.

Sorkin, A., and Zastrow, von, M. (2009). Endocytosis and signalling: intertwining molecular networks. Nat. Rev. Mol. Cell Biol. *10*, 609–622.

Steffen, A., Le Dez, G., Poincloux, R., Recchi, C., Nassoy, P., Rottner, K., Galli, T., and Chavrier, P. (2008). MT1-MMP-dependent invasion is regulated by TI-VAMP/VAMP7. Curr. Biol. *18*, 926–931.

Strauss, K., Goebel, C., Runz, H., Möbius, W., Weiss, S., Feussner, I., Simons,

M., and Schneider, A. (2010). Exosome secretion ameliorates lysosomal storage of cholesterol in Niemann-Pick type C disease. J. Biol. Chem. *285*, 26279–26288.

Suetsugu, S., Kurisu, S., Oikawa, T., Yamazaki, D., Oda, A., and Takenawa, T. (2006). Optimization of WAVE2 complex-induced actin polymerization by membrane-bound IRSp53, PIP(3), and Rac. J. Cell Biol. *173*, 571–585.

Sung, B.H., Zhu, X., Kaverina, I., and Weaver, A.M. (2011). Cortactin Controls Cell Motility and Lamellipodial Dynamics by Regulating ECM Secretion. Curr. Biol. *21*, 1460–1469.

Tanabe, K., Ohashi, E., Henmi, Y., and Takei, K. (2011). Receptor sorting and actin dynamics at early endosomes. Commun. Integr Biol. *4*, 742-744.

Taunton, J., Rowning, B.A., Coughlin, M.L., Wu, M., Moon, R.T., Mitchison, T.J., and Larabell, C.A. (2000). Actin-dependent propulsion of endosomes and lysosomes by recruitment of N-WASP. J. Cell Biol. *148*, 519–530.

Theriot, J.A., Mitchison, T.J., Tilney, L.G., and Portnoy, D.A. (1992). The rate of actin-based motility of intracellular Listeria monocytogenes equals the rate of actin polymerization. Nature *357*, 257–260.

Thurmond, D.C., Gonelle-Gispert, C., Furukawa, M., Halban, P.A., and Pessin, J.E. (2003). Glucose-stimulated insulin secretion is coupled to the interaction of actin with the t-SNARE (target membrane soluble N-ethylmaleimide-sensitive factor attachment protein receptor protein) complex. Mol. Endocrinol. *17*, 732–742.

Timpson, P., Lynch, D.K., Schramek, D., Walker, F., and Daly, R.J. (2005). Cortactin overexpression inhibits ligand-induced down-regulation of the epidermal growth factor receptor. Cancer Res. *65*, 3273–3280.

Tojkander, S., Gateva, G., and Lappalainen, P. (2012). Actin stress fibers--assembly, dynamics and biological roles. J. Cell Sci. *125*, 1855–1864.

Tsai, C.-H., Cheng, H.-C., Wang, Y.-S., Lin, P., Jen, J., Kuo, I.-Y., Chang, Y.-H., Liao, P.-C., Chen, R.-H., Yuan, W.-C., et al. (2014). Small GTPase Rab37 targets tissue inhibitor of metalloproteinase 1 for exocytosis and thus suppresses tumour metastasis. Nat. Comms. *5*, 4804.

Uruno, T., Liu, J., Li, Y., Smith, N., and Zhan, X. (2003). Sequential interaction of actin-related proteins 2 and 3 (Arp2/3) complex with neural Wiscott-Aldrich syndrome protein (N-WASP) and cortactin during branched actin filament network formation. J. Biol. Chem. *278*, 26086–26093.

Uruno, T., Liu, J., Zhang, P., Fan, Y.-X., Egile, C., Li, R., Mueller, S.C., and Zhan, X. (2001). Activation of Arp2/3 complex-mediated actin polymerization by cortactin. Nat. Cell Biol. *3*, 259-266

Valderrama, F., Babià, T., Ayala, I., Kok, J.W., Renau-Piqueras, J., and Egea, G. (1998). Actin microfilaments are essential for the cytological positioning and morphology of the Golgi complex. Eur. J. Cell Biol. *76*, 9–17.

Valderrama, F., Duran, J.M., Babià, T., Barth, H., Renau-Piqueras, J., and Egea, G. (2001). Actin microfilaments facilitate the retrograde transport from the Golgi complex to the endoplasmic reticulum in mammalian cells. Traffic *2*, 717–726.

Valderrama, F., Luna, A., Babià, T., Martinez-Menárguez, J.A., Ballesta, J., Barth, H., Chaponnier, C., Renau-Piqueras, J., and Egea, G. (2000). The golgi-associated COPI-coated buds and vesicles contain beta/gamma -actin. Proc. Natl. Acad. Sci. U.S.A. *97*, 1560–1565.

van Meer, G., Voelker, D.R., and Feigenson, G.W. (2008). Membrane lipids: where they are and how they behave. Nat. Rev. Mol. Cell Biol. *9*, 112–124.

van Rheenen, J., Song, X., van Roosmalen, W., Cammer, M., Chen, X., Desmarais, V., Yip, S.-C., Backer, J.M., Eddy, R.J., and Condeelis, J.S. (2007). EGF-induced PIP2 hydrolysis releases and activates cofilin locally in carcinoma cells. The J. Cell Biol. *179*, 1247–1259.

Vanlandingham, P.A., and Ceresa, B.P. (2009). Rab7 regulates late endocytic trafficking downstream of multivesicular body biogenesis and cargo sequestration. J. Biol. Chem. *284*, 12110–12124.

Vavassori, S., and Mayer, A. (2014). A new life for an old pump: V-ATPase and neurotransmitter release. J. Cell Biol. *205*, 7–9.

Vincent, C., Maridonneau-Parini, I., Le Clainche, C., Gounon, P., and Labrousse, A. (2007). Activation of p61Hck triggers WASp- and Arp2/3-dependent actin-comet tail biogenesis and accelerates lysosomes. J. Biol. Chem. *282*, 19565–19574.

Vitry, S., Bruyère, J., Hocquemiller, M., Bigou, S., Ausseil, J., Colle, M.-A., Prévost, M.-C., and Heard, J.M. (2010). Storage vesicles in neurons are related to Golgi complex alterations in mucopolysaccharidosis IIIB. Am. J. Pathol. *177*, 2984–2999.

Wang, Y.J., Wang, J., Sun, H.Q., Martinez, M., Sun, Y.X., Macia, E., Kirchhausen, T., Albanesi, J.P., Roth, M.G., and Yin, H.L. (2003). Phosphatidylinositol 4 phosphate regulates targeting of clathrin adaptor AP-1 complexes to the Golgi. Cell *114*, 299–310.

Warner, C.L., Stewart, A., Luzio, J.P., Steel, K.P., Libby, R.T., Kendrick-Jones, J., and Buss, F. (2003). Loss of myosin VI reduces secretion and the size of the Golgi in fibroblasts from Snell's waltzer mice. EMBO J. *22*, 569–579.

Weaver, A.M., Karginov, A.V., Kinley, A.W., Weed, S.A., Li, Y., Parsons, J.T., and Cooper, J.A. (2001). Cortactin promotes and stabilizes Arp2/3-induced actin filament network formation. Curr. Biol. *11*, 370–374.

Weaver, A.M. (2006). Invadopodia: Specialized Cell Structures for Cancer Invasion. Clin. Exp. Metastasis *23*, 97–105.

Weaver, A.M. (2008). Cortactin in tumor invasiveness. Cancer Letters *265*, 157–166.

Weaver, A.M., Heuser, J.E., Karginov, A.V., Lee, W.-L., Parsons, J.T., and Cooper, J.A. (2002). Interaction of cortactin and N-WASp with Arp2/3 complex. Curr. Biol. *12*, 1270–1278.

Weed, S.A., and Parsons, J.T. (2001). Cortactin: coupling membrane dynamics to cortical actin assembly. Oncogene *20*, 6418–6434.

Weed, S.A., Karginov, A.V., Schafer, D.A., Weaver, A.M., Kinley, A.W., Cooper, J.A., and Parsons, J.T. (2000). Cortactin localization to sites of actin assembly in lamellipodia requires interactions with F-actin and the Arp2/3 complex. J. Cell Biol. *151*, 29–40.

Weibel, E.R. (1979). Practical methods for biological morphometry. Stereological Methods. New York: Academic Press.

Weibel, E.R., Stäubli, W., Gnägi, H.R., and Hess, F.A. (1969). Correlated morphometric and biochemical studies on the liver cell. I. Morphometric model, stereologic methods, and normal morphometric data for rat liver. J. Cell Biol. *42*, 68–91.

Weller, S.G., Capitani, M., Cao, H., Micaroni, M., Luini, A., Sallese, M., and McNiven, M.A. (2010). Src kinase regulates the integrity and function of the Golgi apparatus via activation of dynamin 2. Proc. Natl. Acad. Sci. U.S.A. *107*, 5863–5868.

Williams, K.C., and Coppolino, M.G. (2011). Phosphorylation of membrane type 1-matrix metalloproteinase (MT1-MMP) and its vesicle-associated membrane protein 7 (VAMP7)-dependent trafficking facilitate cell invasion and migration. J. Biol. Chem. *286*, 43405–43416.

Winter, P.W., Van Orden, A.K., Roess, D.A., and Barisas, B.G. (2012). Actin-dependent clustering of insulin receptors in membrane microdomains. Biochimica Et Biophysica Acta (BBA) - Biomembranes *1818*, 467–473.

Wu, H., Reynolds, A.B., Kanner, S.B., Vines, R.R., and Parsons, J.T. (1991). Identification and characterization of a novel cytoskeleton-associated pp60src substrate. Mol. Cell. Biol. *11*, 5113–5124.

Xu, W., and Stamnes, M. (2006). The actin-depolymerizing factor homology and charged/helical domains of drebrin and mAbp1 direct membrane binding and localization via distinct interactions with actin. J. Biol. Chem. *281*, 11826–11833.

Yamaguchi, H., and Condeelis, J. (2007). Regulation of the actin cytoskeleton in cancer cell migration and invasion. Biochim. Biophys. Acta *1773*, 642–652.

Ydenberg, C.A., Padrick, S.B., Sweeney, M.O., Gandhi, M., Sokolova, O., and Goode, B.L. (2013). GMF severs actin-Arp2/3 complex branch junctions by a cofilin-like mechanism. Curr. Biol. *23*, 1037–1045.

Yin, H.L., and Janmey, P.A. (2003). Phosphoinositide regulation of the actin cytoskeleton. Annu. rev.Physiol. *65*, 761–789.

Yonezawa, N., Homma, Y., Yahara, I., Sakai, H., and Nishida, E. (1991). A short

sequence responsible for both phosphoinositide binding and actin binding activities of cofilin. J. Biol. Chem. *266*, 17218–17221.

Zech, T., Calaminus, S.D.J., Caswell, P., Spence, H.J., Carnell, M., Insall, R.H., Norman, J., and Machesky, L.M. (2011). The Arp2/3 activator WASH regulates α5β1-integrin-mediated invasive migration. J. Cell Sci. *124*, 3753–3759.

Zhang, M., Chen, L., Wang, S., and Wang, T. (2009). Rab7: roles in membrane trafficking and disease. Biosci. Rep. *29*, 193–209.

Zhang, Y., Zolov, S.N., Chow, C.Y., Slutsky, S.G., Richardson, S.C., Piper, R.C., Yang, B., Nau, J.J., Westrick, R.J., Morrison, S.J. (2007). Loss of Vac14, a regulator of the signaling lipid phosphatidylinositol 3,5-bisphosphate, results in neurodegeneration in mice. Proc. Natl. Acad. Sci. U.S.A. *104*, 17518–17523.

Zhu, J., Yu, D., Zeng, X.-C., Zhou, K., and Zhan, X. (2007). Receptor-mediated endocytosis involves tyrosine phosphorylation of cortactin. J. Biol. Chem. *282*, 16086–16094.

Zhu, J., Zhou, K., Hao, J.-J., Liu, J., Smith, N., and Zhan, X. (2005). Regulation of cortactin/dynamin interaction by actin polymerization during the fission of clathrin-coated pits. J. Cell Sci. *118*, 807–817.

Zolov, S.N., Bridges, D., Zhang, Y., Lee, W.-W., Riehle, E., Verma, R., Lenk, G.M., Converso-Baran, K., Weide, T., Albin, R.L., et al. (2012). In vivo, Pikfyve generates PI(3,5)P2, which serves as both a signaling lipid and the major precursor for PI5P. Proc. Natl. Acad. Sci. U.S.A. *109*, 17472–17477.